University of Alberta

Cracking and Heteroatom Removal from Hydrocarbons using Natural Zeolites

by

Vikas G. Gupta 

A thesis submitted to the Faculty of Graduate Studies and Research

in partial fulfillment of the requirements for the degree of **Master of Science**

in

Chemical Engineering

Department of Chemical and Materials Engineering

Edmonton, Alberta

Spring, 2008

Your file Votre référence
ISBN: 978-0-494-47633-8
Our file Notre référence
ISBN: 978-0-494-47633-8

Dedicated ....

To my wife,

Anju

Abstract

Hydroprocessing and hydrotreating are major processes in oil upgrading industry for heteroatoms removal. Hydroprocessing is highly expensive due to consumption of hydrogen. New developments in natural zeolites from clinoptilolite and chabazite, could result in development of low cost upgrading processes. The natural zeolites are effective in reducing the viscosity of heavy oil and removing sulphur and nitrogen. The study tested reactions with model compounds such as hexadecane, dibenzothiophene, quinoline and dihydroindole. Experiments were carried out at temperatures ranging from 300 to 425°C with clay catalysts such as commercial zeolite-Y, clinoptilolite and chabazite without hydrogen. Liquid samples were analyzed with gas chromatography and solid samples with XPS and elemental analysis. Natural zeolites were ineffective in reducing the concentration of dibenzothiophene or quinoline in 1-methylnaphthalene. They were highly effective in removing dihydroindole from 1-methylnaphthalene solution. The order of reaction and activation energy was calculated for various catalysts used in the study.

Acknowledgements

I deeply thank my supervisor Dr. William C. McCaffrey who always has been a great mentor and support to me. Thanks for everything Dr. McCaffrey.

I sincerely thanks Dr. M R. Gray for all his support, assistance and providing his laboratory and equipments for my research.

I express my gratitude and thanks to Dr. Steven M. Kuznicki and his group for supplying the required modified catalyst whenever required and providing valuable information to me during the research.

I wish to express my sincere gratitude to the sponsoror of my research and providing financial support.

My sincere thanks to the support staff especially Tuyet Le and Andree Koenig for providing necessary supplies and guiding me with various set-up and operations during my lab work. I also thank Dimitri in the surface chemistry laboratory for performing all my XPS analysis.

Thank you Brian and Hasan for your esteemed guidance.

Deepest appreciation to my friend Harikrishnan Ramamoorthy for all his support during my MSc.

Finally, I express deepest appreciation to my family specially my wife Anju, daughter Aishwarya and son Rohan. Thanks for all your support, patience, affection and love.

Vikas

Table of Contents

1 Introduction 1

1.1 Objective of study 4

1.2 Hypothesis of study 4

2 Literature review 5

2.1 Non-catalytic Residue Conversion Process 6

2.1.1 Thermal cracking of Hexadecane 7

2.2 Catalytic residue process 8

2.2.1 Residue Fluid Catalytic Cracking 8

2.2.2 Hydroprocessing of residue 9

2.2.2.1 Hydroprocessing Catalysts 9

2.2.2.2 Heteroatoms removal from oil 10

2.2.2.3 Nitrogen compounds 10

2.2.2.3.1 HDN 12

2.2.2.3.2 Polymer Formation during HDN 14

2.2.2.4 Sulfur Compounds 15

2.2.2.4.1 HDS 15

2.3 Low Cost Upgrading (Introduction to Natural Zeolites) 16

2.3.1 Clinoptilolite 17

2.3.2 Acid Catalysis 18

3.0 Methods and Materials 20

3.1 Chemicals 20

3.2 Equipments 21

3.2.1 Microbatch Reactor 21

3.2.2 Sand Bath 23

3.2.3 Vacuum Oven 25

3.2.4 Micro-centrifuge 25

3.2.5 Gas Chromatograph 25

3.3 Experimental Procedure 26

3.3.1 Reactor Loading and Leak Test 27

3.3.2 Reactions 29

3.3.3 Product Recovery 29

3.3.4 Bitumen Reaction 30

3.4 Product Analysis 31

3.4.1 Gas Chromatography 31

3.4.2 X-Ray Photo Electron Spectroscopy 31

3.4.3 Elemental Analysis 32

4.0 Results 33

4.1 Sand Bath Performance 33

4.2 Reproducibility of Results 37

4.3 Thermal and Catalytic Cracking of Hexadecane 41

4.4 Dibenzothiophene Reaction 44

4.5 Aromatic Nitrogen Conversion 45

4.5.1 Quinoline Cracking 45

4.5.2 Dihydroindole Reactions 47

5.0 Discussion 61

5.1 Cracking 63

5.2 Desulphurization 64

5.3 Denitrogenation 65

5.4 Analysis of Catalysts 67

6.0 Conclusions 70

7.0 Recommendations 71

8.0 References 72

Appendices

Appendix A	**Sample Preparation, Experimental Procedure and Mass Balance Data**	**76**
Appendix B	**Gas Chromatogram Results**	**85**
Appendix C	**Gas Chromatogram Integration Data And Elemental Analysis**	**108**
Appendix D	**Order of Reaction and Activation Energy Calculations**	**127**

List of Tables

Table 4.1	Sand Bath Zone Temperature	35
Table 4.2	Minimum Heating Time	36
Table 4.3	Retention Time of Model Compounds	38
Table 4.4	Dihydroindole Area Percent (Fresh Solution)	39
Table 4.5	Mass of solution	39
Table 4.6	Mass of Catalyst	40
Table 4.7	Mass of Gas	40
Table 4.8	Dihydroindole Area Percent (Reacted Solution)	40
Table 4.9	Hexadecane Conversion	41
Table 4.11	Dibenzothiophene Area Percent after Reaction	45
Table 4.12	Quinoline Conversion	46
Table 4.13	Dihydroindole Mass Percent after Reaction	47
Table 4.14	Elemental Analysis of Dihydroindole Reacted Clinoptilolite	54
Table 4.15	Mass Percent Dihydroindole at 425°C	56
Table 4.16	Activation Energy of Different Catalyst	60

List of Figures

Figure 2.1	Operating Cost of Some Processes	7
Figure 2.2	Non-Basic Nitrogen Compounds	11
Figure 2.3	Basic Nitrogen compounds	11
Figure 3.1	Microbatch Reactor	22
Figure 3.2	Sand Bath Setup	24
Figure 3.3	Nitrogen Cylinder Manifold Schematic	27
Figure 4.1	Sand Bath Heating Profile	33
Figure 4.2	Zones of Sand Bath	34
Figure 4.3	Reactor Heating Profile	37
Figure 4.4	Plot of Temperature vs n-Hexadecane Percent Conversion	42
Figure 4.5	Gas Chromatogram of Thermal Cracked n-Hexadecane	43
Figure 4.6	Gas Chromatogram of n-Hexadecane Cracking with Clinptilolite at 425°C	43
Figure 4.7	Gas Chromatogram of n-Hexadecane Cracking with Zeolite-Y at 425°C	44
Figure 4.8	Gas Chromatogram of Quinoline in 1-Methylnaphthalene solution reacted with Clinoptilolite at 425°C	47

Figure 4.9	Reduction in Dihydroindole Mass Percent after Reaction	48
Figure 4.10	Gas Chromatogram of Dihydroindole in 1-Methylnaphthalene solution reacted with Clinoptilolite at 425 °C	49
Figure 4.11	XPS of Uncalcined NH_4^+ Exchanged Clinoptilolite Catalyst	50
Figure 4.12	XPS of Dihydroindole Reacted Clinoptilolite	51
Figure 4.13	XPS of Bitumen Reacted Clinoptilolite	52
Figure 4.14(a)	XPS of Dihydroindole Reacted Clinoptilolite	53
Figure 4.14(b)	XPS of Bitumen Reacted Clinoptilolite	53
Figure 4.15	Gas Chromatogram of Dihydroindole in 1-Methylnaphthalene solution reacted with clinoptilolite at 425°C at 3rd recycle (Catalyst Saturation Test)	55
Figure 4.16	Plot for Half Order Reaction	57
Figure 4.17	Plot for First Order Reaction	57
Figure 4.18	One and Half Order Plot	58
Figure 4.19	Second Order Plot	58
Figure 4.20	Arrhenius Plot	59

Figure 4.21	**Ammonia TPD of Some Natural Zeolite Catalysts**	**60**
Figure 5.1	**Hypothetical Model Compound**	**63**

List of Abbreviations

CHNS	Carbon Hydrogen Nitrogen Sulphur
GC	Gas Chromatography
HDS	Hydrodesulphurization
HDN	Hydrodenitrogenation
TPD	Thermal programmed desorption
XPS	X-ray photoelectron spectroscopy

List of Nomenclature

Av.	Average
AR	Area Ratio
$\mathbf{A_{MC}}$	Area % of model compound
$\mathbf{A_{IS}}$	Area % of internal standard
AC_{Total}	Area count of total peaks
A	Constant in Arrhenius relationship
^{o}C	Degree centigrade
E_a	Activation energy of reaction (kcal/mol)
g	Grams
K	Rate constant
kJ/mol	Kilojoules/mol
kPag	Kilopascal guage
mm	Millimeter
min.	minutes
MPa	Megapascal
psi	pounds per square inch
R	Ideal gas constant (8.314 J. K^{-1}. mol^{-1}.)
t	Time in minutes
T	Temperature
wt%	Weight percent
µL	microliter

1 Introduction

Due to depletion in the resources of the crude oil, it has become very essential to meet the demand of the petroleum products through non-conventional oil sources. Petroleum products which are extracted from Tar, Coal Oil and Oil sands are non-conventional oil sources. Non-conventional sources pose considerably more problems to the refiner than conventional oil sources. Some of the problems that need to be addressed when processing non-conventional oil sources are extracting the petroleum from the ground deposit, separating the valuable resource from the surrounding material and difficulties in handling and transportation properties [16].

Non-conventional oils pose another major problem because they contain unwanted molecules or classes of molecules that are higher in concentration than in conventional oil. Heteroatom compounds fall in one of these major classes. Heteroatom compounds are the ones which contain atoms such as nitrogen, sulfur and oxygen in addition to the carbon and hydrogen backbone of the hydrocarbon. Non-conventional oils have been exposed to physical, chemical and biological degradation due to their shallow location in the ground as compared with conventional oil reservoirs

Oil sources contain two classes of nitrogen compounds: heterocyclic and non-heterocyclic. Heterocyclic nitrogen compounds have nitrogen bound in the molecule as part of an otherwise carbon ring structure. Non-heterocyclic compounds such as amines and nitriles are species where the nitrogen atom is not a part of a ring structure of a molecule [16].

Heterocyclic nitrogen is further divided into basic and non-basic nitrogen compounds. Basic nitrogen compounds have a free electron pair located locally around the nitrogen

atom and are available to participate in acid/base type reactions. Examples are quinoline, dihydroindole and pyridine, etc. Non-basic nitrogen compounds have a free pair of electrons on the nitrogen atom delocalized around the ring structure and are therefore not available to participate in acid/ base type reactions. Examples are indole and carbazole. [16].

Hydroprocessing involves the processing of feed oil at high hydrogen pressure and low temperature with or without the presence of catalyst and is a combination of hydrocracking and hydrotreating. Catalyst is an integral part of most of the hydroconversion processes. Sulfur and nitrogen removal, or hydrodesulphurization (HDS) and hydrodenitrogenation (HDN), are very important steps in the upgrading of the non-conventional oil for a number of reasons. Sulfur, due to its potential to form SO_2 during combustion, is a serious environmental concern [34]. Nitrogen compounds also pose serious problems in meeting the stringent emission specifications for fuels. Heteroatom content also affects the stability of oil during storage and plays major role in catalyst deactivation or catalyst poisoning in the downstream secondary processing [1]. Studies of the nitrogen poisoning effect on the catalytic cracking of gas oil shows that the basic nitrogen reduces the gas oil cracking conversion by 5 to10 wt%, depending on the catalyst to oil ratio. The main types of nitrogen compounds responsible for catalyst deactivation are basic nitrogen compounds [3]. Residue hydroprocessing involves a catalyst consisting of sulfides of Co, Ni, W and Mo dispersed on a porous support. Non-basic nitrogen compounds are the most difficult ones to remove, followed by the basic nitrogen compounds. The non-heterocyclic compounds are generally the easiest ones to eliminate [34].

The following reactions are involved in the HDN of heterocyclic nitrogen compounds

1) Hydrogenation of nitrogen heterorings. Other attached non-nitrogen containing rings may also be hydrogenated.
2) Hydrogenation of aromatic rings and
3) C-N bond cleavage

Due to the consumption of large amounts of hydrogen required for HDN and HDS, this process has very high capital and operating costs as compared to thermal processes [16, 19, 34]

Catalytic and adsorptive properties of modified mineral zeolites such as chabazite have been found to reduce the viscosity of heavy oils considerably. Experimentally at 400 °C without the use of hydrogen, nitrogen was reduced by 60% and sulfur by 30 %. Natural zeolites also have the potential to lower or eliminate metals. Natural zeolites mixed with raw oil sands and reacted at moderate temperatures have improved the extractability of the oil from the sand. Simple natural clay minerals such as clinoptilolite and chabazite are far more effective in bitumen cracking and upgrading than catalyst used for the FCC process i.e. Zeolite-Y which is far more expensive than the natural zeolites. These cheap natural minerals could represent a new revolution in the field of low cost upgrading [23]. This approach may provide for a route for waterless extraction of oil from sand. Removal of heteroatoms without the use of hydrogen would also result in a massive saving in operating costs. These improvements could define a low cost approach to upgrading of oil sands and heavy oil.

1.1 Objective of Study

The objective of the study was to determine the effect of natural zeolites and clay minerals such as chabazite and clinoptilolite on cracking, sulfur removal and nitrogen removal using model compounds. Hexadecane was used as a model compound to determine the conversion on cracking. Quinoline and dihydroindole were taken as model compounds for determining the potential of basic nitrogen removal with these modified clay minerals. Also, dibenzothiophene was taken as a model compound to determine the potential of sulfur removal by these modified clay minerals. It was also decided to carry out the reactions in the presence of commercial Zeolite-Y in some cases to compare the potential of the modified clay minerals such as clinoptilolite and chabazite with commercial Zeolite-Y. Another interest was to determine the order of reaction and the activation energy of the different catalysts.

1.2 Hypothesis of Study

The hypothesis of the work was that the modified clay minerals such as clinoptilolite and chabazite would:

1) largely affect cracking and would give excellent conversion of hexadecane
2) removes adequate amounts of sulfur from dibenzothiphene in absence of hydrogen, due to the adsorption properties and acidity strength
3) Would remove adequate amounts of basic nitrogen from quinoline and dihydroindole in absence of hydrogen, due to the adsorption properties and acidity strength
4) Perform better or at par with expensive commercial zeolite-Y in nitrogen removal

2 Literature Review

Advanced technologies for residue hydroprocessing are becoming increasingly important to meet the gradual changes in petroleum specifications required by refiners. Part of this interest is in finding new markets for old products that are not in high demand such as heavy fuel oil. To upgrade atmospheric or vacuum oil residues, they must be refined in the presence of catalysts and hydrogen at high pressure. There is a constant decrease in the demand for low value products such as fuel oil and residua based products and an increasingly high demand for high value petroleum products such as gasoline, middle distillates and lube oil. Therefore, maximizing of liquid products yield from various processes and residues is of immediate attention to refiners. When treating non-conventional feedstocks the refiner faces increased environmental concerns and more rigorous petroleum product specifications. These trends have emphasized the importance of processes that convert the heavier oil fractions into lighter and more valuable clean products. Numerous technologies for upgrading residual oil have been developed for the upgrading of residual heavy oil and include carbon rejection and hydrogen addition processes [34].

Residues are required to be converted into more valuable products. The processing of these residues using various technologies can be classified in two main streams Non-catalytic residue processes and catalytic residue processes. Non-catalytic residue processes include solvent deasphalting and thermal processes (carbon rejection process).

2.1 Non-catalytic residue conversion processes

Athabasca bitumen residue is highly rich in asphaltenes. A separation process known as solvent deasphaltation is one process for asphaltene removal. In this process, residue separation is done by solubility parameter or molecular weight instead of boiling points. The product of solvent deasphalting is a low content deasphalted oil which is relatively rich in paraffin type of molecules. Solvent deasphalting has the advantage of being a relatively low cost process although it is usually coupled with a delayed coker to reduce the amount of waste.

Another important alternative for residua conversion are the thermal conversion processes. Thermal processes include gasification, delayed coking, fluid coking, Flexi coking and Visbreaking. Coking is carried out at moderately low pressures and high temperatures. Hydrogen is transferred from the heavy molecules to the lighter molecules and results in the production of volatile liquids and a coke or carbon byproduct. The residue acts as hydrogen donors at high temperature and this process further decreases H/C ratio of the solid waste to values between 0.5–1, which significantly increase the coke formation [34]. Cracking reactions which are responsible for reduction in molecular weight and formation of lighter products include the cleavage of side chains, ring opening of napthenic and hydroaromatic compounds, and dealkylation of alkyl aromatics [17]. Delayed coking is carried out at a temperature of 480 to 515 °C and 0.61 MPa, Visbreaking is carried out at 450 to 510 °C and 0.34 to 2.0 MPa. Fluid coking is done at 480 to 565 °C at 0.07 MPa, Flexi coking is carried out at 830 to 1000 °C and gasification is carried out at temperatures greater than 1000 °C. As compared to hydroprocessing, these processes are more economical having low investment and operating costs but

yielding less condensible liquid products. Liquid products require further purification by hydrotreating involving processes like hydrodesulphurization and hydrodenitrogenation to eliminate heteroatom like sulphur, nitrogen and metals. A disadvantage of thermal based processes is the production of a large amount of low valued by-products requiring extensive further processing [34].

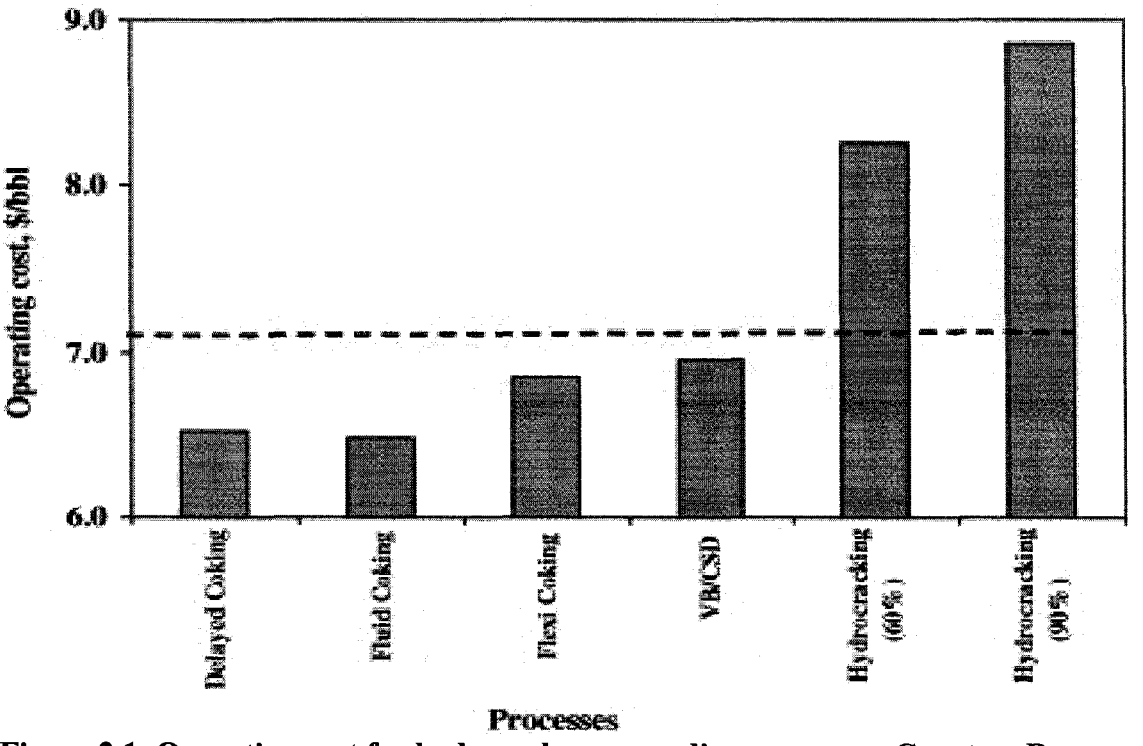

Figure 2.1: Operating cost for hydrocarbon upgrading processes, Courtesy Rana et.al (2007)

2.1.1 Thermal Cracking of Hexadecane

High pressure thermal cracking of n-hexadecane (n-C16) has been studied extensively [17]. In one study, the reaction was carried out in a tubular flow reactor at

380-450 °C, 13.9 MPa with residence times ranging from 0.06 to 2.0 h. Hexadecane conversion was reported to range from 1.5- 10%. Thermal cracking products of n-C16 fall in two categories; combination or polymerization products with higher molecular weights than n-C16 and the cracking products with molecular weights lower than n-C16. Products belonging to the lower molecular weight class were a complete series of n-alkanes from C1 to C14 and the corresponding α-olefins. n-C15 was present as a minor reaction product. These products were identified by their retention times when analyzed by gas chromatography. Isomeric products representing branched alkanes and internal olefins were also prominent in between the peaks of n-alkanes and α-olefins. Only a series of cis and trans-2-olefins were identified related to these isomeric products. Cis and trans-2-butene and cis and trans-2-pentene were present in the product gas [17].

2.2 Catalytic residue processes

2.2.1 Residue fluid catalytic cracking

A significant portion of the heavier fractions from crude oil is converted into a high-octane gasoline blending component by residue fluid catalytic cracking (RFCC). In RFCC, an acidic matrix such as crystalline aluminosilicate zeolite mixed with an inorganic matrix is used as a catalyst. RFCC is an extension of conventional fluid catalytic cracking (FCC) technology that was developed during the early 1980s, and offers better selectivity to high gasoline and lower gas yield than a combined hydroprocessing and thermal process. RFCC is less desirable than the hydroprocessing because it requires better feed quality i.e. high H/C ratio and low metal contents. FCC of Athabasca vacuum residue has a high coke yield, high catalyst consumption and poor unit

operability. Therefore, only atmospheric residues could be treated with RFCC which contains lower amounts of metals, sulfur and carbon [34].

2.2.2 Hydroprocessing of residue

In hydroprocessing, hydrocracking (molecular weight reduction), hydrodesulphurization (sulphur reduction), and hydrodenitrogenation (nitrogen reduction) all occur simultaneously. Selectivity for condensable liquid yields is much better with hydroprocessing as compared to any of the non-catalytic residue processes. Hydroprocessing also generates higher quality liquid products as compared to thermal processing. As a result, hydroprocessing not only offers better selectivity of the product but also cleaner fuel specifications [34]. Under hydroprocessing conditions NiMo sulphide on gamma alumina yields good HDN performance and CoMo sulphide on gamma alumina yields good HDS performance [16]. One of the most important properties for residue hydroconversion catalyst is the pore diameter due to the high molecular weight of the feed species. As can be expected, catalyst deactivation is a problem with this type of technology. Hydroprocessing also requires as relatively high initial investment and operating costs due to high consumption of hydrogen when compared to thermal processes. Selection of an upgrading process is also based on the combination of catalyst life, product yield and economics.

2.2.2.1 Hydroprocessing Catalysts

Other than the thermal conversion processes, such as visbreaking and coking, most of the hydroconversion processes require catalyst. In general a working

hydroprocessing catalyst is made of transition metal sulfides dispersed on high surface area support. Supply of hydrogen to large oil molecules is the main role of the catalyst in hydrocracking which otherwise becomes deficient in hydrogen [31]. Typical composition of the catalyst is 3–15 wt. % Group 6 metal oxide and 2–8 wt. % Group 8 metal oxide [34]. The catalyst has to be sulfided before its use. NiMo catalyst usually contain approximatley 3% Ni and the Mo ranges from 10 to 16% [4, 16, 19, 24], Hydrogen plays an important role in inhibiting coke formation over the catalyst by hydrogenation of coke precursor and removing hetero-atoms.

2.2.2.2 Heteroatom removal from oil

Liquids from thermal processes have high heteroatom content and must also be treated by hydrogen addition or hydrotreating process to meet product specifications. Heteroatom such as sulfur, nitrogen and oxygen are covalently bond to compounds in the heavy oil. To remove these heteroatoms, a hydrogenation catalyst is essential. Unlike in hydroprocessing and hydrocracking, hydrotreating does not involve significant molecular weight reduction via cracking but is primarily concerned with removing the heteroatom.

2.2.2.3 Nitrogen Compounds

Two major types of nitrogen species present in oils are heterocyclic and non-heterocyclic compounds. Non-heterocyclic compounds are attached to alkyl or aryl groups and are not part of aromatic or heterocycle compound. This class of nitrogen compounds are easily removed by the HDN process.

Heterocyclic nitrogen compounds occur when the nitrogen atom is part of a ring structure, including the aromatic ring structure. These heterocyclic compounds are further divided into basic and non-basic nitrogen compounds. Non-basic compounds are found to be harder to remove than the basic compounds during HDN process [16].

Indole **Carabazole**

Figure 2.2: Non- Basic Nitrogen Compounds

Quinoline **Dihydroindole**

Figure 2.3: Basic Nitrogen Compounds

Heavy gas oil (HGO) derived from the oil sands bitumen by Syncrude Canada typically contains approximately 3900 ppm of total nitrogen, with 1600 ppm reporting as basic and 2300 ppm reporting as non-basic nitrogen. Data for HDN reactions performed at different hydrogen to oil ratio, pressures, temperatures and sulfur concentrations has been reported in the literature [1]. The basic nitrogen compounds were always hydrogenated to a larger extent than the non-basic nitrogen compounds. The conversion of non-basic nitrogen

compounds was typically reported to be 15- 35% lower than the conversion of basic nitrogen compounds [1]. For example, at a reaction temperature of 385 °C, 88 bar, small liquid hourly space velocity of 1 h^{-1} , and a hydrogen gas to HGO ratio of 600 mL/mL, 78.5 % of the basic nitrogen was converted while only 51.1 % of the non-basic nitrogen was converted [1] Nitrogen conversion of typical basic (acridine) and non-basic (carbazole and 9-ethylcarbazole) compounds has also been studied using a trickle bed reactor filled with a commercial $NiMo/Al_2O_3$ catalyst. In this study, HDN was investigated by adjusting different variables such as H_2S concentration in the feed, butanethiol concentration, reaction pressure, temperature, liquid hourly space velocity (LHSV) and H_2 /feed ratio. It was found that the HDN conversion of basic compound was higher than that of the non- basic compounds at all of the butanethiol concentrations (0-4%) in the feed. High conversions, 98-99 wt%, of basic nitrogen at 355-400 °C was observed as compared to the conversion of non-basic nitrogen from 92 to 95%. Increase in pressure and LHSV had no significant impact on the conversion while a decrease in LHSV from 2 to 0.5 h-1 increased the conversion from 92 to 99%. Increase in the conversion of carbazole from 90 to 98% was observed with increase in the H_2/feed ratio from 200 to 800mL/mL [11].

2.2.2.3.1 HDN

The HDN mechanism has also been studied extensively [12, 33]. The first step is the diffusion of nitrogen containing molecule to the catalyst surface by both external bulk liquid diffusion and internal diffusion inside the pores. The molecule must then attach to the catalyst surface. The acidic nature of the hydrotreating sites explains why

basic compounds may be easier to hydrotreat. The acid/base reactions may aid in compound attachment to the catalyst and may promote subsequent HDN steps. In the hydrogenation step, heterocyclic rings must be saturated with hydrogen once the compound has attached to the catalyst site. Other rings that are attached to the heterocyclic ring may also become hydrogenated. Once the hydrogenation of the heterocyclic ring is completed, one of the carbon–nitrogen bonds can be broken, hence breaking the nitrogen containing ring. In the hydrogenolysis reaction, the carbon nitrogen bond is broken by replacement with hydrogen. The hydrogenation reactions up to the ring breaking step are generally reversible. Consequently hydrogen may be added to the ring and then subsequently removed from the ring in a step called dehydrogenation, yielding the original starting compound. Dehydrogenation of a partially hydrogenated reactant may result in a new less hydrogenated product. At this point, the nitrogen atom is no longer a part of a ring once the ring is broken (generally a non-reversible step), and can be removed quickly. An intermediate compound may form in the product oil as result of the compound detachment during any of the steps. Diffusion of the compound out of catalyst back to the bulk liquid must take place once the compound is detached from the catalyst [12, 33]. Nitrogen species in the heavier gas oil fractions are more resistant to HDN than the nitrogen species in the lighter fractions. It has been reported that with heavier fractions, there was decrease in HDN in the heavy gas oil derived from the Athabasca bitumen [38]. Similarly with shale oil, HDN is less effective with the heavier fractions [14]. Low HDN in the heavier fractions is possibly due to the lower reactivities of higher molecular weight nitrogen compounds, possible diffusion effects and possible inhibition of the catalyst by inhibitory nitrogen species. Some nitrogen compounds can

inhibit the HDN of other types. Pyridine has been found to inhibit the HDN of aniline (experiment carried out at 300°C and hydrogen partial pressure of 2.29 MPa). In this case, the operating parameters used in the experiments were much lower than typically used in the industrial applications. Reactions were found to be following (LHHW) predictions while determining the adsorption and rate constants of ammonia, aniline and pyridine. The adsorption constant of pyridine was 18 times larger than for aniline and the reaction rate constant for aniline was found to be 4 times greater than pyridine. Pyridine underwent HDN faster than aniline when a mixture of aniline and pyridine was reacted and acted as an inhibitor to aniline HDN. This indicated that compound which is difficult to hydrotreat inhibits the HDN of another compound which is easier to hydrotreat [16, 24].

2.2.2.3.2 Polymer Formation during HDN

In addition to HDN reactions, there is also evidence of polymer formation during HDN reactions of indole [30, 36]. During the studies carried in the HDN of indole over a NiMO/p-Al_2O_3 catalyst, it was found that depending upon the reaction conditions the material balance were often low. The low material balances were due to the failure of the GC analysis to detect the polymer in the product sample and possible loss of polymer by condensation [30]. Packed reactor plugging during HDN has also been reported. With only a material balance loss of 10%, the reactor pressure has been reported to gradually reduce and the reactor finally was completely plugged during the HDN of quinoline due to a trimer of partially hydrogenated quinoline [36].

2.2.2.4 Sulfur Compounds

Sulfur is present in the two main forms: aromatic ring bound sulphur compounds which are very sTable and alkyl sulphur compounds such as thioethers which are much easier to remove. Aromatic sulfur is the major class of sulphur found in heavy oils and account for approximately 60 % of the total sulfur.

2.2.2.4.1 Hydrodesulphurization (HDS)

CoMoS-loaded mesostructured clay supports have been used to determine the conversion of dibenzothiophene (DBT) to biphenyl by hydrodesulphurization (HDS) at 400 °C. There was no hydrogenation or hydrocracking observed with any of the clay supports. Ludox silica sol AS-30 was the most active clay derived having activity of 65% DBT conversion and 100% selectivity to biphenyl (BP) [5]. It was suggested that hydrodesulphurization and hydrodenitrogenation activities could be greatly improved by the addition of the zeolites in the catalysts. When 5 to 20 wt% beta zeolite containing catalysts were compared it was observed that the catalyst containing 10 wt% beta zeolite had the most hydrogenation activity. Further it was observed that hydrotreating activity was more effectively enhanced by Zeolite-Y as compared to beta zeolite [8].

It was observed that during hydrodesulphurization of dibenzothiophene over laboratory synthesized bulk MoS_2 catalysts using a batch microautoclave reactor, regardless of the catalyst used, H_2S was found to inhibit the direct desulphurization route that leads to biphenyl. Depending on the catalyst nature, the hydrogenation pathway, which mainly produces phenylcyclohexane, was inferred to be either uninhibited or even more interestingly highly promoted by the presence of H_2S depending on the catalyst

nature [10]. Inhibition and promotion were the two extremes indicated by H_2S on the catalytic activity. The effect of molecular weight on HDS has also been evaluated. Gas oil was fractioned into five separate 20°C fractions; the boiling range of the gas oil was from 227°C to 377°C with five fractions. These five fractions had boiling ranges of less than 280°C, from 280-300°C, 300-320°C, 320-340°C and greater than 340°C separated by atmospheric distillation. It was observed that the HDS was slowed down by the presence of the higher molecular weight and higher boiling fractions. The higher molecular weight compounds were less reactive than the lighter sulfur compounds by two or three orders of magnitude. It was also suggested that inhibition of HDS is caused by the presence of other heavy compounds such as polyaromatics. A third possibility was that the HDS activity was inhibited by the presence of a higher concentration of nitrogen compounds in the heavier fractions [16, 26]. The HDS of thiophene has also been found to be inhibited over a wide range of temperature from 250 to 400°C in the presence of the quinoline [25].

2.3 Low cost Upgrading (Introduction of Natural Zeolites)

Simple, economical and disposable in-field bitumen upgrading material such as modified natural zeolites could improve bitumen production. Natural materials such as modified clays are able to break down heavy oils at temperatures approaching the onset of thermal cracking. Viscosity of bitumen was found to be reduced considerably by virtue of the catalytic and adsorptive properties of the modified mineral zeolite, chabazite and remove much of the metals, nitrogen and sulphur at 400°C. Performance of visbreaking processes could be substantially improved by economical, single pass,

disposable cracking agents and potentially enhance the economics of field upgrading for bitumen. Such agents would need to be much less expensive than current commercial cracking catalysts while manifesting substantial cracking activity. If heteroatoms and metals such as sulfur, nitrogen, vanadium and nickel could be eliminated with these modified minerals during cracking, an additional benefit could be derived. Zeolites have well-known properties as catalysts and adsorbents and would seem to offer promise for such a multi-functional field upgrading approach [23].

Zeolites are crystalline aluminosilicates with the structural formula Mx/n(AlO2)x(SiO2)y, where n is the valence of cation M, x+y is the total number of tetrahedral pr unit cell and y/x is the Si/Al atomic ratio varying from a minimum value of 1 to infinity. During the catalytic process, diffusion of molecules into the zeolite pores takes place. Following is the classification of zeolites categories: small pore zeolites, with 8 MR apertures having free diameter of 0.30-0.450 nm, medium pore zeolites with 10 MR apertures having free diameter of 0.45-0.60 nm and large pore with 12 MR aperture with free diameter of 0.60-0.75 nm [37].

During the synthesis of the zeolites their catalytic properties can be modified and can vary considerably. These types of catalysts can roughly be classified into four groups: Acid catalyst, hydrogenation/acid bi-functional catalyst, base catalyst and redox catalyst

2.3.1 Clinoptilolite

Clinoptilolite being the most common natural zeolite belongs to heulandites family or structural variation of zeolite mineral group and has the following general chemical formula: $(Na, K, Ca)_4Al_6Si_{30}O_{72}\cdot 24H_2O$. A ratio between silicon and aluminum

(Si/Al) of the clinoptilolite varies from 4.0 to 5.3 with a high thermal stability (600–800 .C). Sodium and potassium dominate mainly among sorbed exchangeable cations of clinoptilolite. The crystal structure of clinoptilolite is presented by a 3-dimensional aluminosilicate framework, whose specific building causes the developed system of micro pores and channels occupied by water molecules and exchangeable cations (Na, K, Ca, Mg, Fe, Sr, Ba and others) [22].

2.3.2 Acid Catalysis

Numerous important acid catalyzed reactions involve zeolite catalysts. In general, zeolite synthesis yields a form that is neutralized by sodium ions. Neutralized zeolites are also formed if template molecules (structure directing agents) are used during synthesis. The template removal step takes place before removal of Na^+ by an ion exchange technique. Decomposition of the crystalline zeolites takes place when treated with strong acids. Therefore the method involved in converting the sodium form into the hydrogen forms involves exchange of the cation by ammonium from an aqueous solution of ammonium salt. Proton (acidic) form of the zeolite is formed and NH_3 is liberated due to subsequent thermal treatment of the ammonium exchanged zeolites [37].

$$NH_4^+ \{zeolite\} \rightarrow NH_3\,(g) + H^+ \{zeolite\}$$

Zeolite-Y is recognized as a high potential cracking catalyst but its low stability was a serious drawback. Depending on the preparation of the catalyst the surface of zeolite can display Bronsted or Lewis acid sites or a combination of the two. As the temperature is

increased above approximately 500°C and water is driven off, Bronsted acid sites are converted to Lewis acid sites. The overall catalytic activity of zeolites as solid acids depends upon the number and the properties of the acid sites. The strength of the acid site is directly related to the framework composition of the zeolite. Strong acidity is an indication of high Si/Al ratio and zeolites with low Si/Al ratios can have higher concentration of catalytic sites [37]. Zeolites with intermediate Si/Al ratio of 2-5 such as chabazite, clinoptilolite have the properties of both low and high Si/Al ratio zeolites. There are some other properties exemplified by the acid form zeolites is that the zeolites with high concentrations of H^+ are hydrophilic, having more affinities for polar molecules small enough to enter the pores. The zeolites with low H+ concentration are hydrophobic, taking up organic compounds from water organic mixtures.

3 Method and Materials

3.1 Chemicals

During the course of the experiments following chemicals were used as received. As solvents, n-pentane, HPCL grade with 99.77 % purity, from Fisher Scientific was used for gas chromatography injection syringe cleaning and to wash the recovered catalyst. Toluene, with 99.5 % purity, certified ACS from Fisher Scientific was used to clean the reactor, pipettes and vials, 1-methylnaphthalene, reagent grade, from Sigma-Aldrich, 95% pure was used as a solvent to dissolve various model compounds used during the experiments.

Model compounds for the research were n-hexadecane 99 % pure, from Fisher Scientific, was used to perform the cracking experiments, dibenzothiophene with 98 % purity, from Sigma-Aldrich was used to evaluate sulphur removal, quinoline and dihydroindole reagent grade 98 % and 99 % pure, respectievely, from Sigma-Aldrich, were used to perform experiments on the removal of nitrogen. Cold Lake dewatered bitumen was used to perform the confirmation test on the removal of nitrogen.

Gases used to carry out experiments were nitrogen from Praxair, PP 4.8, to pressurize the reactor, helium carrier gas from Praxair, PP 4.5, hydrogen from Praxair, PP 4.5 and air, extra dry from Praxair

Catalysts used during the experiments were supplied by Dr. S. Kuznicki, Chemical and Materials Engineering, University of Alberta. Raw clinoptilolite was procured from Werris Greek, Australia, and the raw chabazite was procured from GSA resources, Arizona, USA. These clay minerals were modified and exchanged to produce active

natural zeolite catalysts. A pre-commercial Zeolite-Y was also supplied by Dr. S. Kuznicki and was undiluted.

Clinoptilolite was ammonia exchanged directly while raw sodium chabazite was upgraded first to remove impurities and then ammonia exchanged. The ammonia exchange procedure was provided by Dr. Kuznicki's group and is attached in the Appendix A for reference. Zeolite-Y was calcined prior to use.

3.2 Equipments

The following equipments were used during the experiments

3.2.1 Micro-Batch Reactor

The micro-batch reactor used in the experiments was made by University Of Alberta, Chemical Engineering Machine Shop. Since the volume of the samples taken in all the experiments were small, these reactors were very convenient to use and easy to handle. Figure 3.1 shows a picture of the micro batch reactor. The reactor is divided into three parts the top cap which has a hole drilled through it and is connected to a long tubing with a stainless steel needle valve and a number of Swagelok fittings. The middle tube forms the main body of the reactor and in which the feed is placed and the bottom cap is just meant to seal the reactor from beneath and is usually not opened once sealed. The material used to construct the reactor is stainless steel. To fill the reactor, the top cap is opened and the feed poured in the main body and the top cap replaced and tightened. The long tubing is connected to a nitrogen cylinder and is used to purge and pressurize

the reactor. A needle valve is used to maintain the desired pressure in the reactor and for the release of the gases after the reaction.

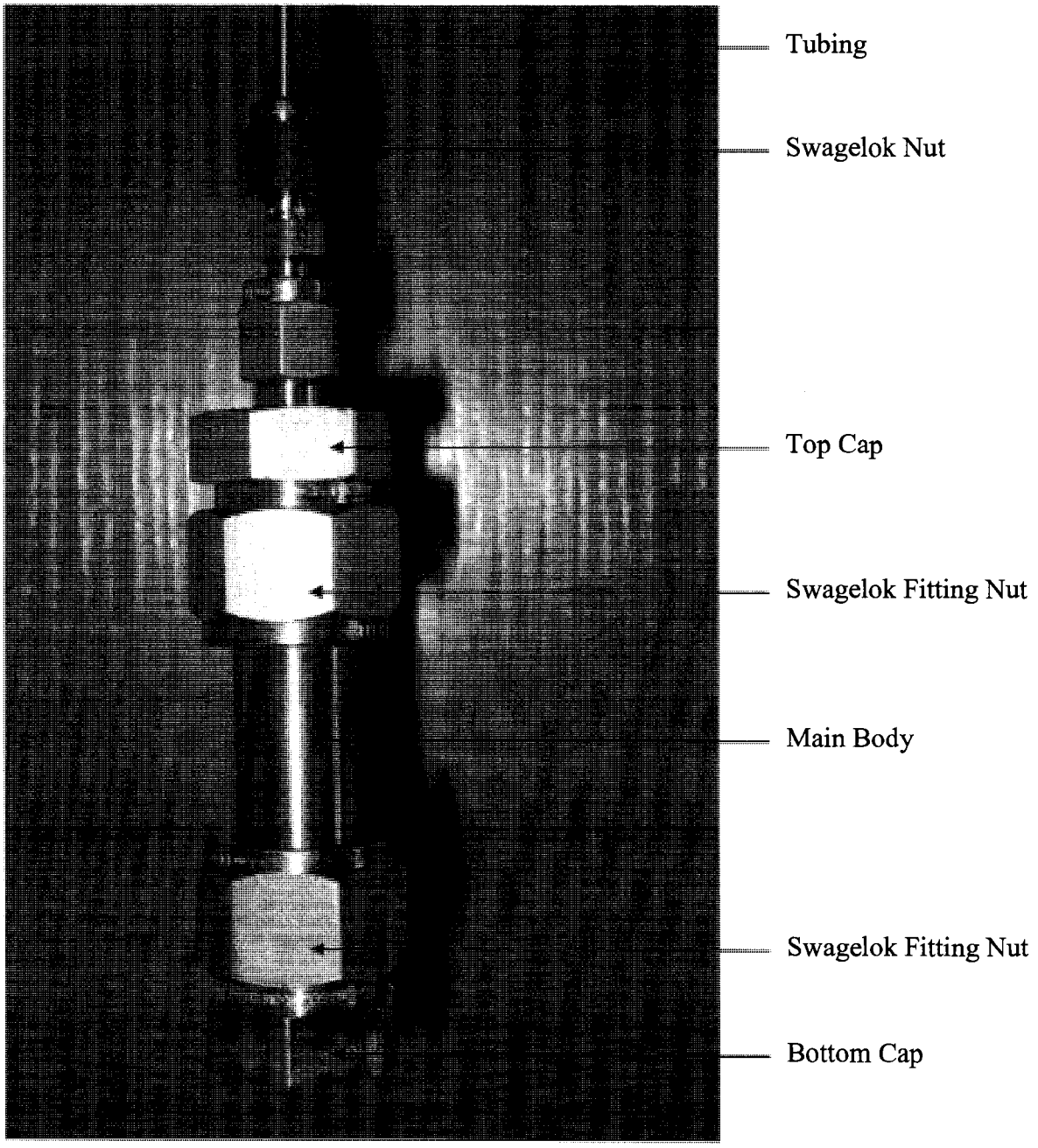

Figure 3.1 Microbatch Reactor

After the desired time of reaction, the reactors were cooled with dry air. Compared with cooling the reactors by quenching in liquid water, the air cooling enhanced the life of the reactor. Usually one reactor could be used 8-10 times before difficulties in sealing were encountered and the reactor had be taken out of service due to leaking. Once the reactor was taken out of service, the tubing connected to the top cap was removed by cutting the tube from the edge using a tube cutter and was filed to make appropriate opening and was fitted back on the top cap of the new reactor using the Swagelok fittings. Care was taken that all the joints are not over-tightened to avoid excessive wear and tear of the threads. All the joints were tightened ¼ turn after finger tightening.

3.2.2 Sand Bath

Figure 3.2 shows a picture of the sand bath set-up used to heat the reactors (Tecam Fluidized Sand Bath Model # SBS- 4). Sand used in the bath was brown aluminum oxide. Sand in the bath was kept in fluidized state with the air fed from the distributor provided at the bottom the unit. The air flow was maintained at 60 % of the scale on a Gilmont D1703 Rotameter and controlled with a needle valve. Fluidized sand provides for enhanced heat transfer when compared to a conventional oven and allows for easy immersion of the reactor into the sand bed. Temperature of the sand was measured by a thermocouple just above the distributor in the sand bath and the temperature of the heating element was controlled by OMRON E5CK controller. The temperature was maintained constantly at the desired set values with error of +/- 1°C. The micro-batch reactor was fixed on a vertical rod which was in turn was attached to a

horizontal arm. Agitation to the reactor was provided by placing the horizontal arm on a cam which was mounted on an electrically driven motor. Agitation of the reactor gave a better mixing of the solution and the catalyst.

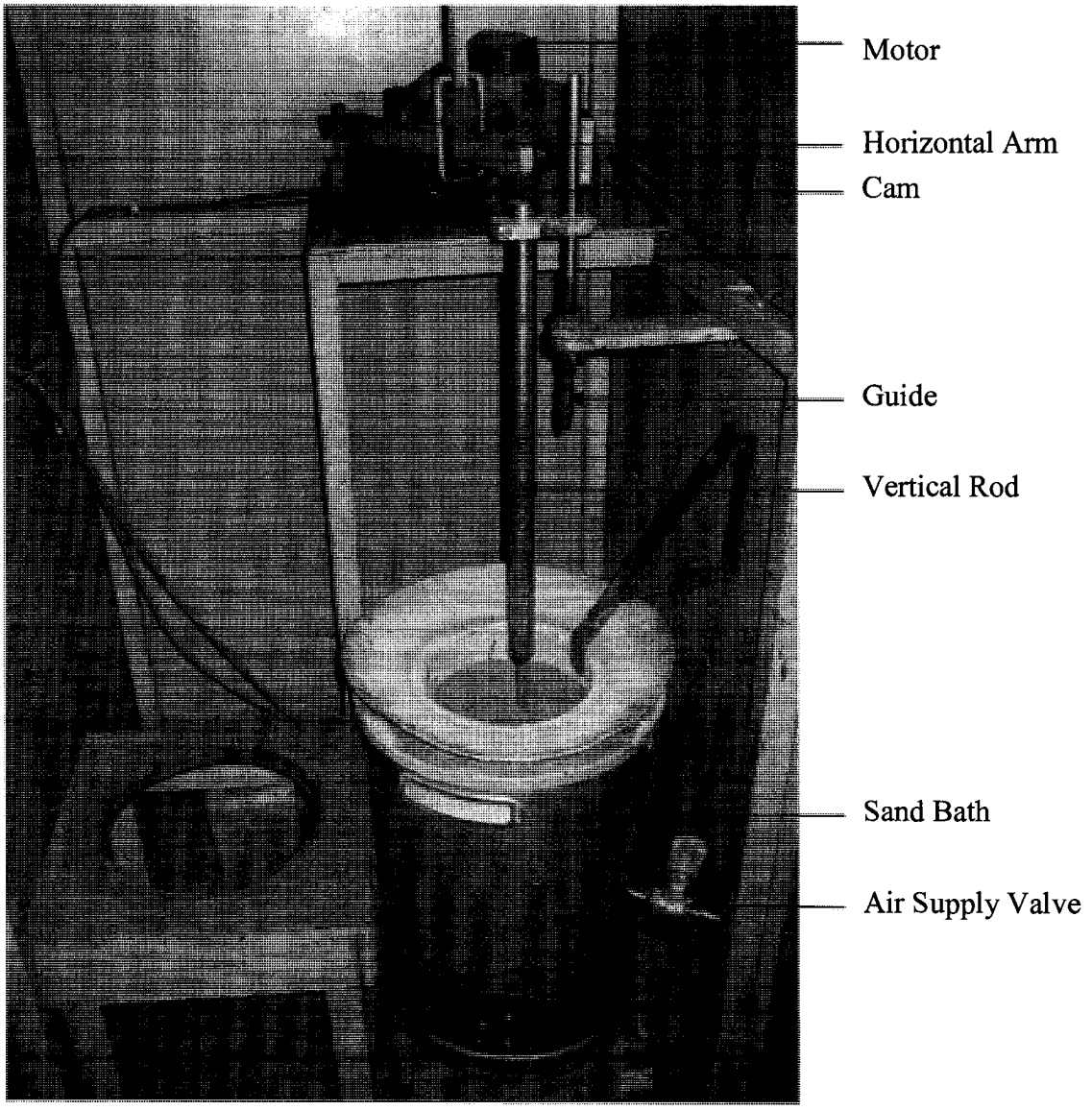

Figure 3.2 Sand Bath Setup

3.2.3 Vacuum Oven

The vacuum oven used was VWR Scientific, Model VWR 1410. Vacuum in the oven was created by a duo seal vacuum pump, Model 1400, and manufactured by The Welch Scientific Company, USA. The purpose of using this oven was to dry the catalyst completely prior to reuse in saturation tests. – 80 kPag of vacuum was created in the oven and the temperature of the oven maintained at 70°C. One hour of operation ensured complete drying of the catalyst.

3.2.4 Micro centrifuge

The micro-centrifuge used was Thermo IEC, USA, model Micromax. The purpose of using this centrifuge was separation of catalyst from the cracked solution so that the solution was free from solids prior to analysis. Two micro centrifuge tubes of 2.0 mL were used for this purpose and care was taken that the weights of the tubes were same and are placed exactly opposite to each other to maintain the balance. Solution was centrifuged at 5000 rpm for 3 minutes to ensure that the liquid product was solids free.

3.2.5 Gas Chromatograph

The cracked solutions with different catalyst were analyzed by gas chromatography. Two gas chromatographs were used for performing the analysis, a Varian 3800 and a Hewlett Packard 5890. The HP 5890 was fitted with a DB-1 column from J and W Scientific with a length of 20 meters and column internal diameter of 0.100 mm and film thickness of 0.40 micron. An auto sampler was used to inject the samples.

The detector was a flame ionizing detector (FID) using compressed hydrogen and air and was kept at a temperature higher than the maximum column temperature at 300 °C. The column used in the Varian 3800 Gas Chromatograph was Alltech Econo-CAP EC-1, which had a length of 30 meters, internal diameter of 0.32mm and film thickness of 0.25 microns. This gas chromatogram was capable of adjusting the gas flows according to the feed. The column was baked-out occasionally to ensure no traces from the previous samples remained in the column. The following settings were used for analysis of the liquid products.

Sample Volume	0.01 µl
Injector Temperature	300°C
Detector Temperature	300°C
Gas Pressure	10 psi
Initial temperature	35°C
Temperature Ramp	10°C/minute
Stabilization Time	0.5 minutes
Final Temperature	270°C
Total Time	23.5 minutes

3.3 Experimental Procedure

Experiments were carried out with hexadecane, dibenzothiophene, quinoline and dihydroindole. Hexadecane was cracked thermally, with ammonium exchanged clinoptilolite and with ammonium exchanged sodium chabazite. Dibenzothiophene was

thermally heated and also reacted in presence of modified chabazite. Quinoline reactions were done in presence of ammonium exchanged clinoptilolite only. Dihydroindole was heated thermally, reacted in presence of ammonium exchanged clinoptilolite with ammonium exchanged sodium chabazite and commercial Zeolite-Y. All of the reactions were carried out in the liquid phase by adjusting the nitrogen pressure inside the micro-batch reactor. Hexadecane was cracked in pure form. For dibenzothiophene reactions, a 10 % by mass solution of dibenzothiophene in 1-methylnaphthalene was used. For the reactions of quinoline and dihydroindole, a 0.25% concentration of nitrogen solution of both the compounds in 1-metylnaphthalene was prepared separately. This concentration was used because it represents the concentration of nitrogen actually present in the heavy oil. Procedures used for preparation of 0.25 % concentration of quinoline and dihydroindole in 1-methylnaphthalene are given in the appendix. For all the experiments, the micro-batch reactor was filled with 3 grams of solution and catalyst (10 % of the solution). The reactor was then sealed and leak tested.

3.3.1 Reactor Loading and Leak Test

Figure 3.3 shows the schematic of leak test set up. Fresh reactors, as received from the machine shop, were carefully tightened to ensure no leakage. Once sealed, the bottom cap was not opened again. The reactor was opened from the joint of main body and the top cap. Feed to the reactor is added at that position. The threads of both the main body and the top cap were cleaned with toluene to ensure no rust on the threads. Also the inside body of the reactor was cleaned with toluene and the reactor dried in the oven to remove any traces of oil. The reactor is dried with a jet of dry air to cool at room

temperature. A long stainless steel tube with a needle valve is attached to the top cap for pressurizing the reactor.

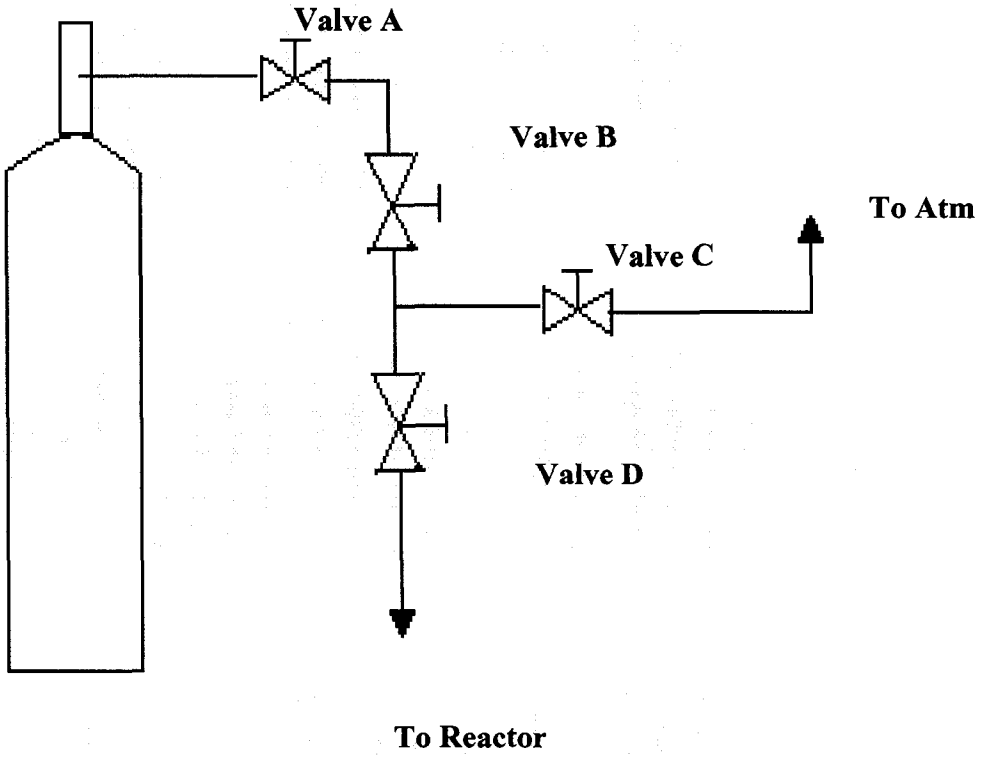

Figure 3.3 Nitrogen Cylinder Manifold Schematic

3 grams of solution is weighed in the reactor for thermal cracking and 0.3 grams of catalyst is added to the solution for catalytic cracking. A capped reactor is placed in a bench vice horizontally holding the top cap and nut of the main body tightened by turning ¼ turn. It is critical that all the joints are tightened properly.

The reactor is tested for leaks by applying adequate nitrogen pressure representative of the liquid phase cracking reactions. For this purpose, the vapor pressure of all the compounds being dealt with were calculated using Antoine equations from Yaws

handbook of Antoine coefficients for vapor pressure (electronic edition). Following were the vapor pressure of the different compounds at 425°C.

1-Methylnaphthalene	250 psi
Hexadecane	155 psi
Quinoline	296 psi
Dihydroindole	245 psi

3.3.2 Reactions

The reactions were carried out for 1 hour. Hexadecane was cracked at 410°C, 425°C and 435°C and 250 psi nitrogen. 0.25 % concentration of quinoline in 1-methylnaphthalene was reacted at 400°C, 410°C, 425°C and 0.25 % concentration of dihydroindole in 1-methylnaphthalene was reacted at 300°C, 325°C, 350°C, 375°C, 400°C, 410°C and 425°C. To quench the reaction, the reactor was detached from the vertical mixing arm and immediately cooled using an air jet. Cooling to room temperature was usually achieved within four minutes.

Once the reactor reached the room temperature, the gas was vented by opening the needle valve slowly.

3.3.3 Product Recovery

Once the reactor's top cap was removed, the product was decanted into micro centrifuge tubes. If the cracking reaction involved catalyst then the product was carefully decanted from the reactor into the vials. Once the catalyst settled in the vial, the clear

solution was carefully decanted into the reactor to wash the inside walls of the reactor. The process was repeated until all the catalyst from the reactor was decanted into the vial. The contents of the vials are carefully transferred to the centrifuge tubes. Usually two centrifuge tubes were sufficient to accommodate all of the products.

The centrifuge tubes were weighed and the liquids in both the tubes adjusted with a pipette to ensure that mass of both the centrifuge tubes containing the product were the same. An error of +/- 1 % was considered acceptable. The products were centrifuged at 5000 rpm for 3 minutes. The tubes were removed and the clear solution was decanted and stored. The samples were stored in a freezer prior to analysis.

Catalyst was recovered by filling the centrifuge tubes with toluene and agitating on a vortex mixer. Each of the centrifuge tubes was washed with toluene 5 times and the product decanted into a glass Petri dish. The catalyst was dried in a vacuum oven for 1 hour at -80 kPag and 70°C. The dried catalyst was washed again with heptane and dried. The catalyst was sent to the University of Alberta ACSES surface chemistry laboratory and the Department of Chemistry for analysis.

3.3.4 Bitumen Reaction

To compare the results of the surface analysis of dihydroindole reacted clinoptilolite with bitumen reacted clinoptilolite, a similar experiment under the same conditions was carried out with Cold Lake de-watered bitumen and catalyst. Three grams of Cold Lake de-watered bitumen was reacted in the presence of 0.3 grams clinoptilolite catalyst. Since the purpose was to characterize the catalyst only, the liquid product was

not recovered. The recovered bitumen reacted clinoptilolite catalyst was sent to the University of Alberta ACSES laboratory for XPS analysis.

3.4 Product Analysis

3.4.1 Gas Chromatography

The cracked liquid products were analyzed using gas chromatography. Toluene was used as solvent to clean the injection syringe. Before injecting the cracked sample, GC analysis of the fresh solutions were carried out to determine the retention time and the area percent of 1-methylnaphthalene dibenzothiphene, hexadecane, quinoline and dihydroindole. Reacted samples were injected in the GC and the results auto integrated. Initial area of hexadecane, dibenzothiophene, quinoline and dihydroindole in the fresh solution and the final area of hexadecane, dibenzothiophene, quinoline and dihydroindole in the cracked solution were used to calculate the conversion.

3.4.2 X-Ray Photo Electron Spectroscopy (XPS)

Surface analysis of the recovered catalyst was conducted with XPS. XPS was used to roughly identify the type of nitrogen adsorbed to the catalyst surface. Surface analysis of the catalyst surface was carried out in the University of Alberta ACSES laboratory in the Chemical and Materials Engineering building. Dihydroindole reacted clinoptilolite at 425°C was analyzed and uncalcined ammonia exchanged clinoptilolite was analyzed as a control. To compare the results of the model compound with actual

bitumen, an experiment was carried out where Cold Lake de-watered bitumen was reacted at 425°C in presence of calcined ammonia exchanged clinoptilolite and the sample of the recovered catalyst submitted XPS analysis.

3.4.3 Elemental Analysis

Part of the sample which was submitted to the University of Alberta ACSES laboratory for XPS was also sent for the elemental analysis to the Micro-analytical Laboratory in the Univeristy of Alberta Department of Chemistry. Carbon, hydrogen, nitrogen and sulfur (CHNS) analysis was carried out to determine the mass percent of the different elements in the catalyst.

4.0 Results

4.1 Sand Bath Performance

As mentioned earlier, a fluidized sand bath was used to heat the reactors used in this study. Prior to conducting experiments, the performance of the sand bath for both temperature stability and the rate of heating of the microbatch reactors was determined. The first parameter that was evaluated was the stability of the sand bath. The stability of sand bath at different temperatures is presented in Figure 4.1

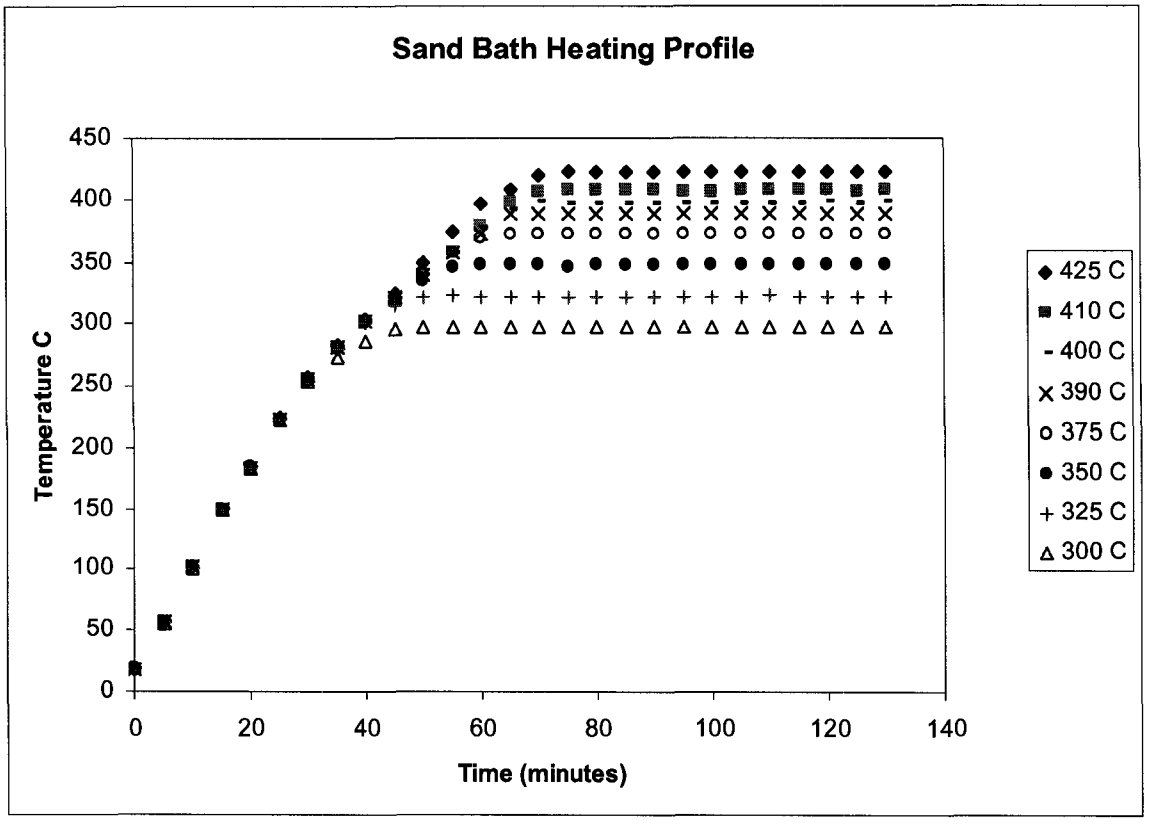

Figure 4.1 Sand Bath Heating Profile

Sand bath heating profile was measured at different temperatures at which the experiments were carried out. Sand bath temperature was measured from 0 to 130 minutes. At steady state temperature, profile is almost linear with very good control of the set point. Initial heating from 0 minutes to different steady state temperatures shows a linear increase of the sand bath temperature. Temperatures were also measured at five different zones of the sand bath at 425°C, with a thermocouple, so as to know the average temperature. Five different zones are shown in the Figure 4.2. Zone temperatures were generally consistent and are shown in the Table 4.1. Reactor was immersed in zone 5.

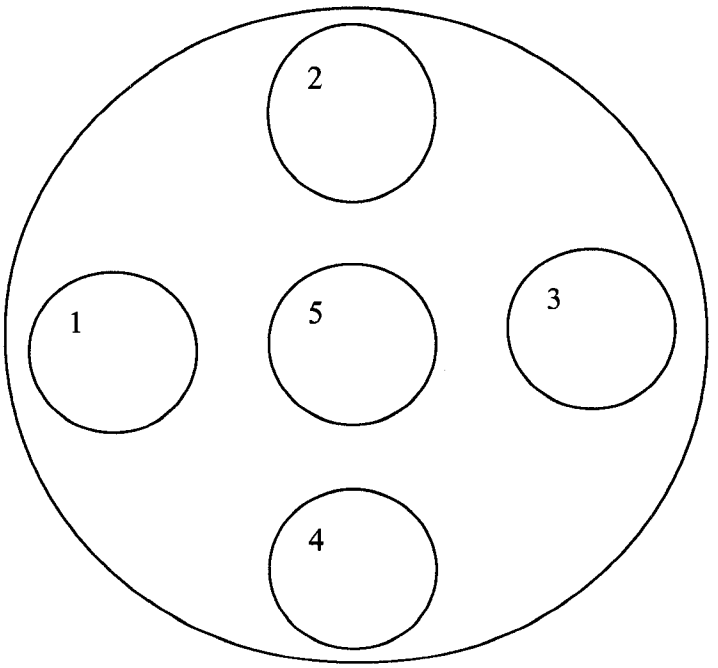

Figure 4.2 Zones of Sand Bath

Table 4.1 Sand Bath Zone Temperatures

Zone	Temperature °C
1	423.3
2	418.1
3	421.4
4	422.3
5	423.4
Average Temperature	421.7

As the reactions were carried out at temperature varying from 300 to 425 °C, the reactor temperature profile was determined at different temperatures ranging from 300 to 425 °C. To determine the temperature of the reactor when it was immersed in the sand bath, a thermocouple was inserted in the reactor ensuring it touched the inside bottom and then the reactor was immersed in the sand bath at a selected temperature. Pressurization of the reactor was not possible because the thermocouple was inserted from the space provided for nitrogen pressurization and the gas vent. Since the reactors were empty, the procedure gave a minimum estimate for the time required to heat the reactor. The reactor heating profile is shown in Figure 4.3 by plotting a graph of temperature versus time. Minimum heating time at different temperatures is tabulated in the Table 4.2. The time required for the reactor to reach 95% of the steady state temperature from the initial temperature is considered as the heat up time. From the plots it is observed that after reaching the steady state temperature the profile is relatively constant. There would be some small

temperature difference due to the fact that temperature of the heating element and the sand would oscillate due to control of the temperature set point controller but this variation was very minor as compared to the average temperature.

Table 4.2 Minimum Heating Time

Temperature (^{o} C)	Minimum Heating Time (Min.)
300	3.8
325	3.8
350	4.75
375	9.5
400	14.25
410	14.25
425	14.25

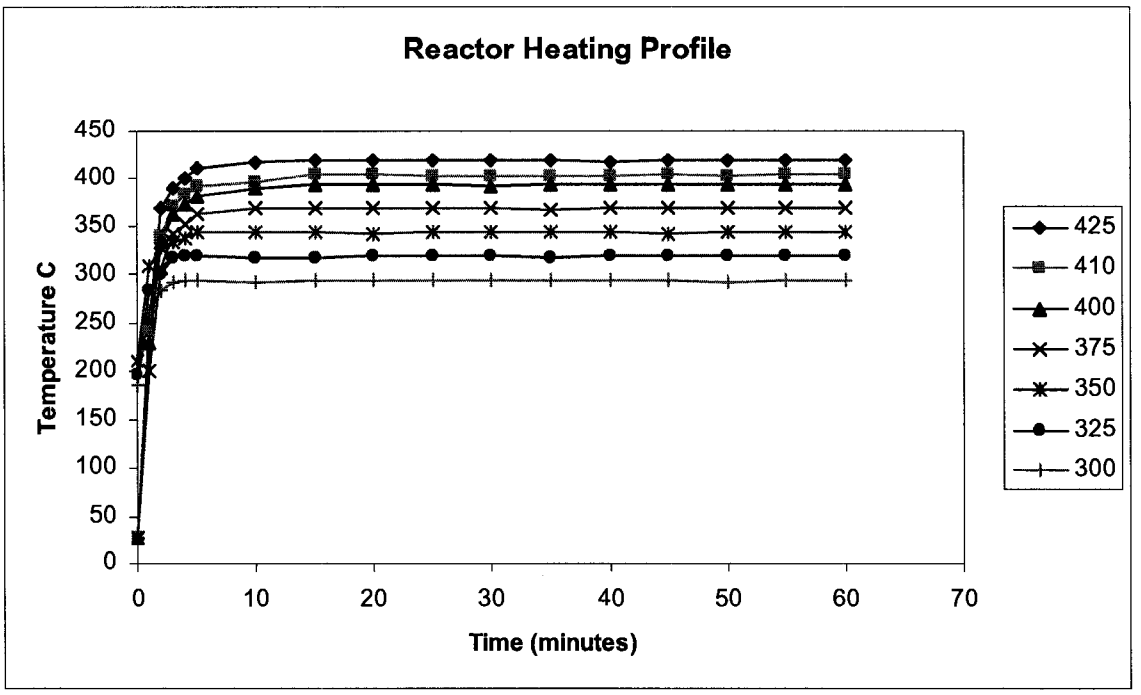

Figure 4.3 Reactor Heating Profile

4.2 Reproducibility of Results

The major areas which would affect the results are: sample preparation; experimental procedure; and compound analysis. The primary analytical tool for this study was gas chromatography. Residence times of the four model compounds used in this study (n-hexadecane, dibenzothiophene, quinoline and dihydroindole) as well as the solvent 1-methynaphthalene are presented in Table 4.3. Gas chromatograms of the pure compounds are presented in Appendix B.

Table 4.3 Retention Times of Model Compounds

Compound	Retention Time (minutes)	
	HP 5890	**Varian 3800**
n-Hexadecane	22.786	
Dibenzothiophene	24.392	
1methylnaphthalene	14.035	
Quinoline	11.680	
Dihydroindole	10.766	9.085

Analysis were carried out to examine the repeatability of the initial solutions of the above mentioned compounds.

To ensure the repeatability of the sample preparation, sample was prepared four times by making a 0.25% basic nitrogen concentration solution of 99% purity dihydroindole in 95% purity 1-methylnaphthalene. The sample was analyzed by gas chromatography. Table 4.4 shows dihydroindole area % as given by the GC analysis. The analysis was very reproducible with a standard deviation of 0.0102 area %.

Table 4.4 Dihydroindole Area Percent (fresh solution)

Nitrogen Concentration (wt %)	GC Area %
0.249	1.6009
0.244	1.6240
0.245	1.6107
0.249	1.6194

To characterize the repeatability of the experimental results, a solution of dihydroindole (0.25 wt% nitrogen) in 1-methylnaphthalene was subjected to repeated identical reactions with sodium exchanged chabazite at 325°C. In each experiment, the same reactor was used. The initial mass of solution was 3 grams with 0.3 grams of catalyst. The reactor was pressurized to 2.76 MPa (400 psi) with nitrogen. The reactors were maintained at temperature for 60 minutes.

Mass balances of the materials were done during the experiment. Table 4.5, 4.6 and 4.7 shows the repeatability results of mass of solution, mass of catalyst and mass of gas, respectively, before and after the reaction.

Table 4.5 Mass of Solution (g)

Status	Reaction 1	Reaction 2	Reaction 3	Standard Deviation
Before Reaction	3.00	3.023	3.00	0.0132
After Reaction	2.7125	2.7536	2.6867	0.0337

Table 4.6 Mass of Catalyst (g)

Status	Reaction 1	Reaction 2	Reaction 3	Standard Deviation
Before Reaction	0.3016	0.3006	0.3010	0.0005
After Reaction	0.2215	0.2554	0.2072	0.0247

Table 4.7 Mass of Gas (g)

Status	Reaction 1	Reaction 2	Reaction 3	Standard Deviation
Before Reaction	0.47	0.48	0.46	0.01
After Reaction	0.52	0.54	0.51	0.015

The reacted samples were also analyzed by gas chromatography to analyze the area percentage of dihydroindole in the solution. Reproducibility of the dihydroindole conversion was 0.0275 area % or an average conversion of 0.4 with a standard deviation of 0.02

Table 4.8 Dihydroindole Area % (Reacted Solution)

Area % of Dihydroindole	Conversion
0.9846	0.3899
0.9369	0.4194
0.9783	0.3938

4.3 Thermal and Catalytic Cracking of Hexadecane

One of the natural zeolites used in this study (clinoptilolite) was characterized for the ability to catalytically crack hexadecane. As a comparison, both the thermal conversion of hexadecane and the catalytic cracking using commercial zeolite-Y were also studied in the micro-batch reactor. Table 4.9 and Figure 4.4 shows the results of the n-hexadecane cracking experiments.

Table 4.9 Hexadecane Conversion %

Temperature °C	Thermal (wt %)	Clinoptilolite (wt %)	Zeolite-Y (wt %)
410	16.78	14.57	7.75
425	34.53	26.49	23.92
435	51.20	35.36	34.90

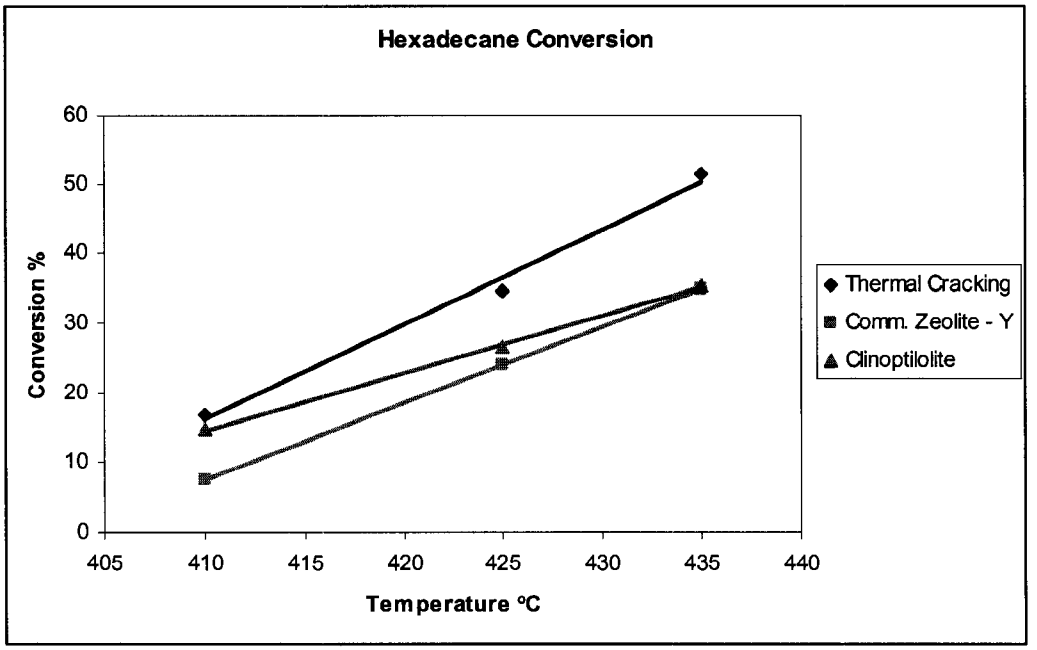

Figure 4.4 Plot of Temperature versus n-Hexadecane Percent Conversion

Gas chromatograms of the products from the hexadecane cracking reactions for the thermal reaction and the catalytic reactions using clinoptilolite and zeolite are presented in Figures 4.5 to 4.7, respectively. It is clear that the products from the catalytic cracking reactions are similar while the thermal reaction appears different.

.

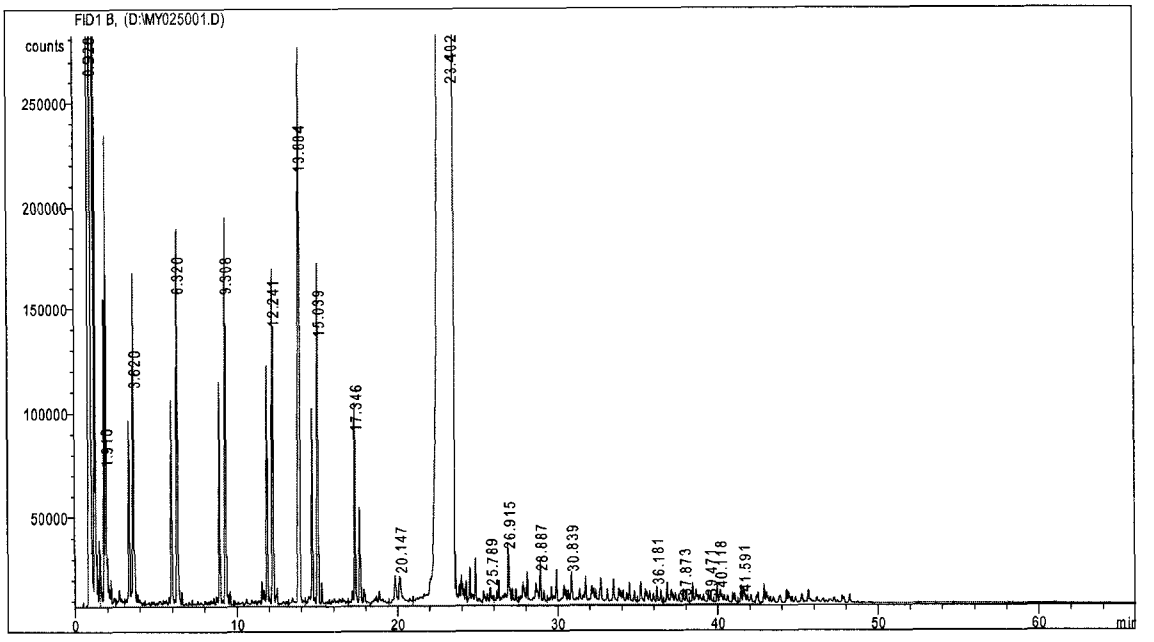

Figure 4.5 Gas Chromatogram of Thermal Cracked n-Hexadecane

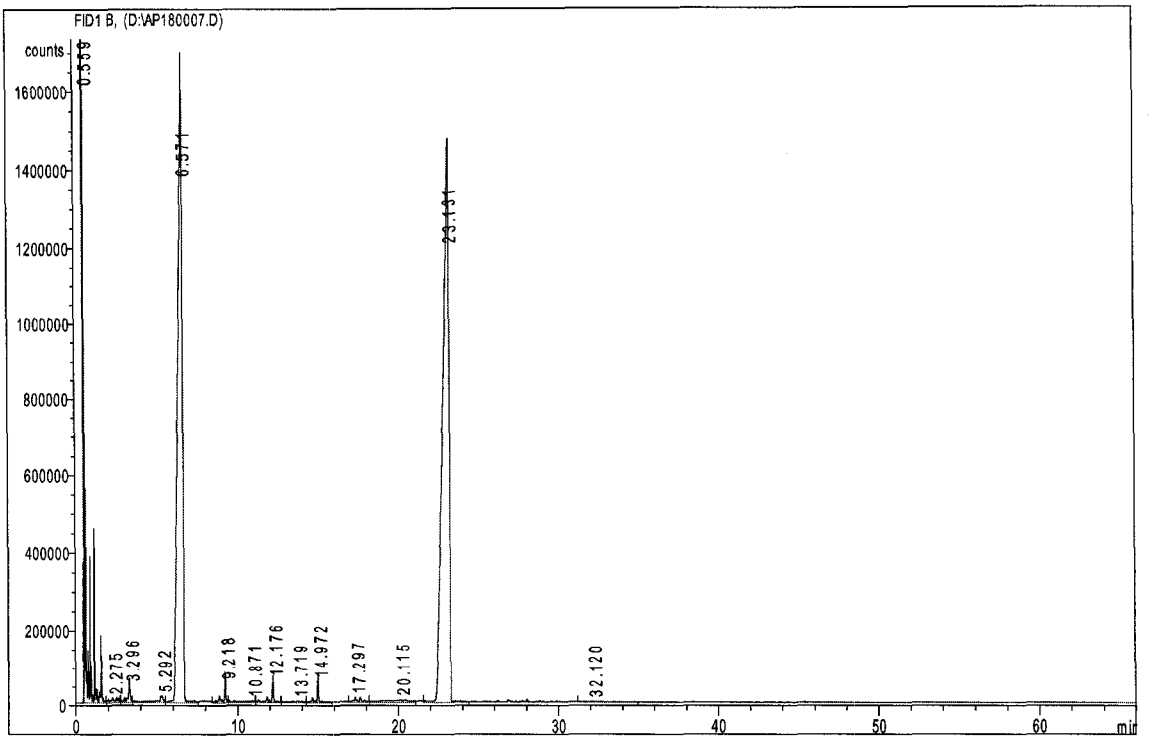

Figure 4.6 Gas Chromatogram of n-Hexadecane Cracking with Clinptilolite at 425°C

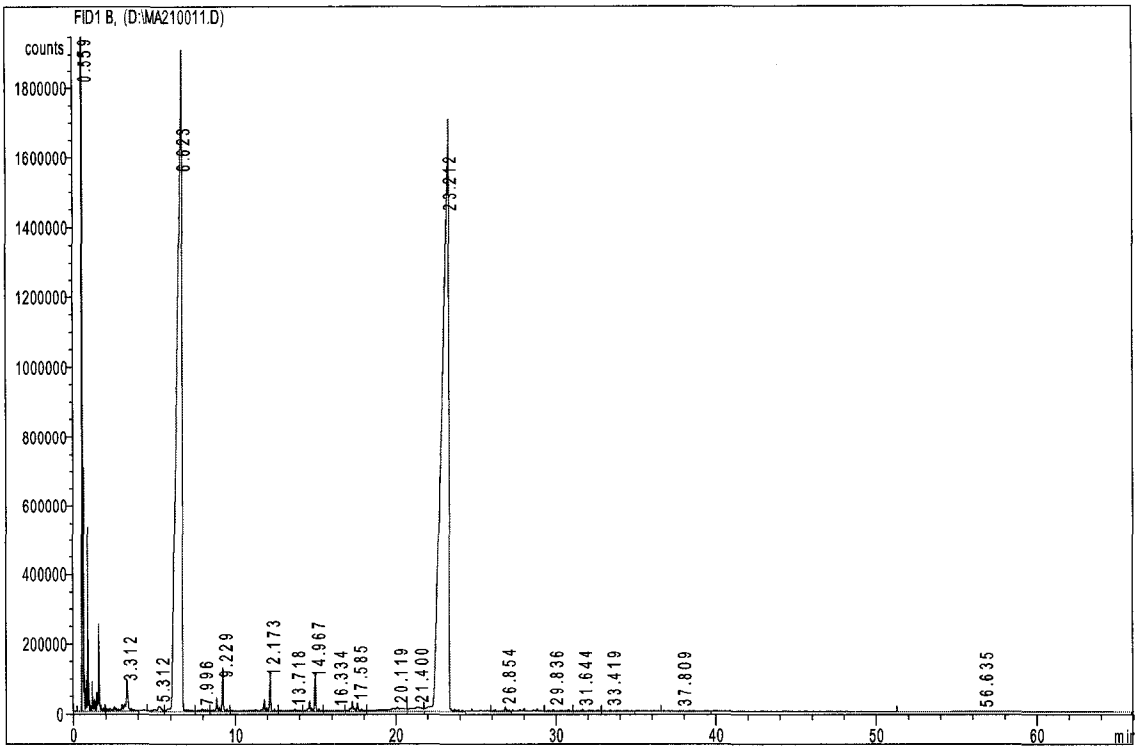

Figure 4.7 Gas Chromatogram of n-Hexadecane Cracking with Zeolite-Y at 425 °C

4.4 Dibenzothiophene Reaction

The ability of the natural zeolites to remove aromatic sulphur compounds was evaluated by studying the conversion of dibenzothiophene. A 10 mass % solution of di-benzothiophene in 1-methylnaphthalene was prepared and was reacted thermally and with 10 mass % of ammonium exchanged modified chabazite. Each type of reaction was done in triplicate. The reactions were carried out at 425 °C under nitrogen. GC analysis of the pure di-benzothiphene in 1-methylnaphthalene gave an area percent of 16.5732. The gas chromatograms of the reactants and products are presented in Appendix B. No new peaks were observed in the products from dibenzothiophene reactions.

Table 4.11 Dibenzothiophene Area Percent after Reaction

Thermal (Area %)	Conversion %	Modified Chabazite (Area %)	Conversion %
16.3178	1.54	15.4006	7.08
14.6333	11.7	15.1350	8.68
15.757	4.92	15.1913	8.34

4.5 Aromatic Nitrogen Conversion

Aromatic nitrogen compounds can be present in fuels in both pyridinic (six-membered rings) and pyrrolic type rings (five-membered rings). In this study on compound from each class was studied, quinoline (six-membered ring) and dihydroindole (five-membered ring).

4.5.1 Quinoline Cracking

A solution of quinoline (0.25 mass % nitrogen concentration) in 1-methylnaphthalene was reacted in presence of clinoptilolite catalyst at different temperatures ranging from 410°C to 425°C for 1 hour. The resultant products were analyzed by gas chromatography. Table 4.12 shows the results at different temperatures. GC analysis of the fresh solution of quinoline in 1-methylnaphthalene yielded an area percent of 1.9592.

Table 4.12 Quinoline Conversion

Temperature (° C)	Area %	Conversion %
400	1.81369	7.4270
410	1.76021	10.1560
425	1.44872	12.1750

GC analysis of the products from the catalytic quinoline reaction is presented in Figure 4.8. A small unidentified peak with a retention time of approximately 40 minutes can be observed in the chromatogram. This peak was not present in the pure quinoline solution.

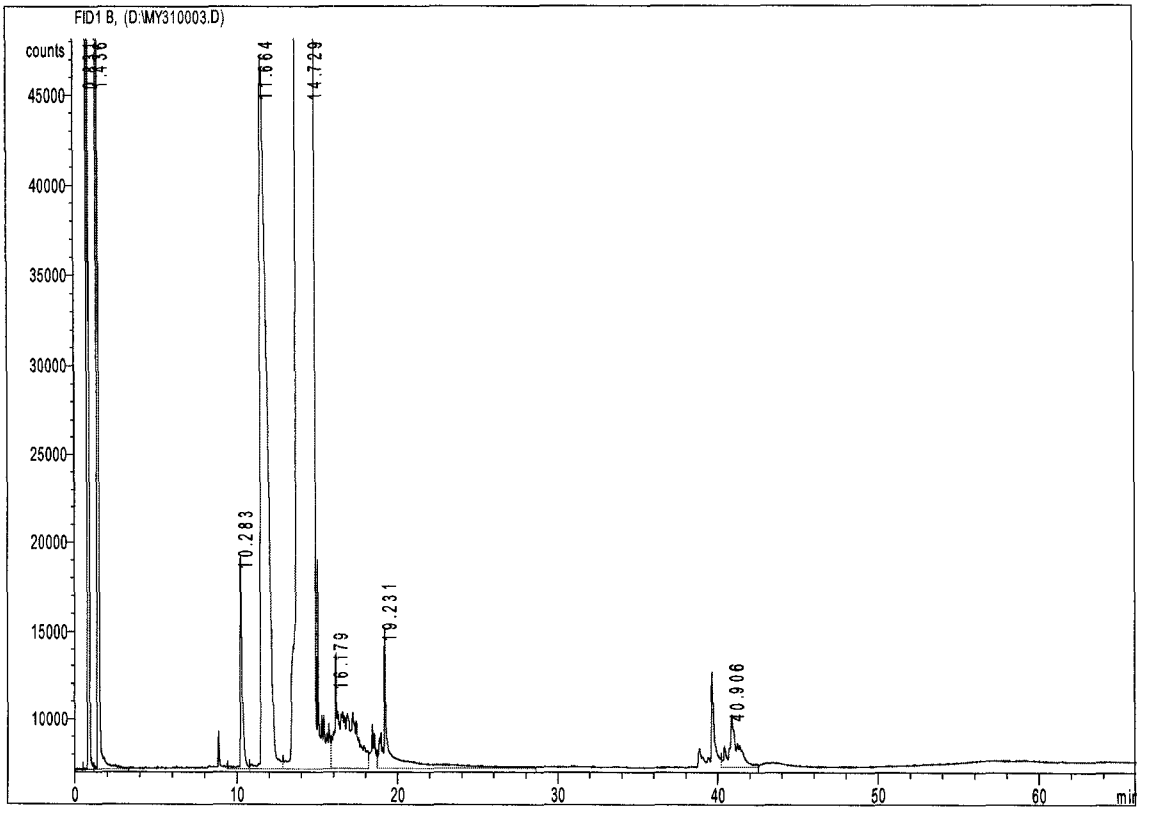

Figure 4.8 Gas Chromatogram of Quinoline in 1-Methylnaphthalene Solution reacted with Clinoptilolite at 425 °C

4.5.2 Dihydroindole Reactions

Reactions of dihydroindole were performed with two natural zeolite type catalysts (ammonium exchanged clinoptilolite and sodium exchanged modified upgraded chabazite) and a commercial zeolite-Y for comparison. Catalytic experiments were conducted under nitrogen using micro-batch reactors. The nitrogen pressure was adjusted to ensure that the reactions were in the liquid phase. For every experiment, catalyst used was 10 % by weight of the solution. The solution prepared was 0.25 mass % nitrogen concentration in 1-methylnaphthalene. Experiments were performed at temperatures ranging from 300 to 425 °C and the results are presented in Table 4.13 and Figure 4.9. GC analysis of the fresh 0.25 % nitrogen of dihydroindole in 1-methylnaphthalene gave an area percent of 1.6137 or dihydroindole mass % of 2.1165.

Table 4.13 Dihydroindole Mass Percent after Reaction

Temperature °C	**Clinoptilolite (mass %)**	**Chabazite (mass %)**	**Zeolite-Y (mass %)**
300	1.7358	1.4537	0.6409
325	1.6299	1.2681	0.3351
350	1.1412	0.8968	0.1778
375	0.5730	0.4118	0.2347
425	0	0	0

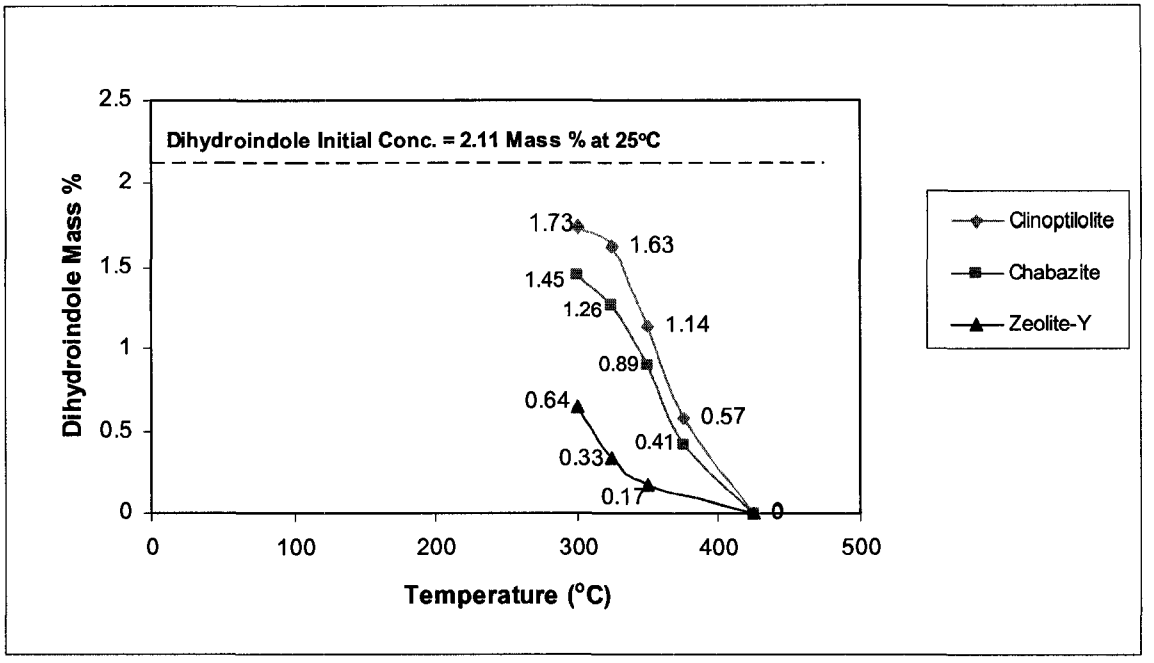

Figure 4.9 Reduction in Dihydroindole Mass Percent after Reaction

An example of a chromatogram from the products from a dihydroindole in 1-methylnaphthalene solution reacted with clinoptilolite at 425 °C is presented in Figure 4.10. Chromatograms for other conditions are presented in Appendix B.

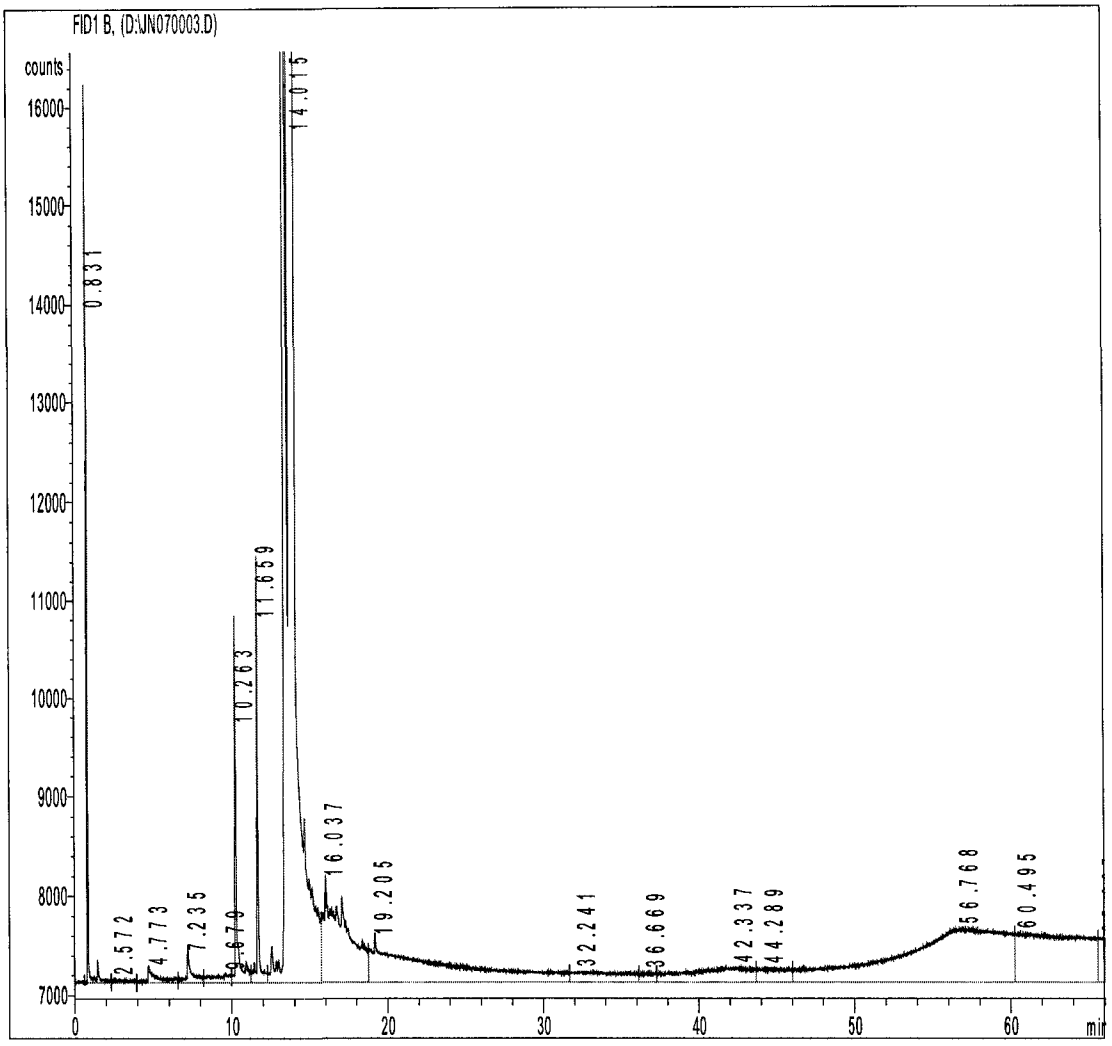

Figure 4.10 Gas Chromatogram of Dihydroindole in 1-Methylnaphthalene Solution reacted with Clinoptilolite at 425 °C

Surface analysis by X-ray photoelectron spectroscopy (XPS) was done on the uncalcined ammonium exchanged clinoptilolite and the recovered clinoptilolite catalyst after the reaction. The XPS results are presented in Figure 4.11. Two peaks are seen in Figure labeled as A and B. Peak 'A' occurs at the position 400.3 electron volt and peak 'B'

occurs at 402.4 electron volt. Both peaks are shifted to 284.8 electron volts (carbon 1-s line was set to 284.8 electron volt as an internal reference). Figure 4.12 presents the XPS analysis of the same catalyst but calcined and reacted with dihydroindole. Surface analysis shows two peaks 'A' and 'B' at 400.126 and 402.403 electron volts respectively. Both the peaks are shifted to 284.8 electron volt.

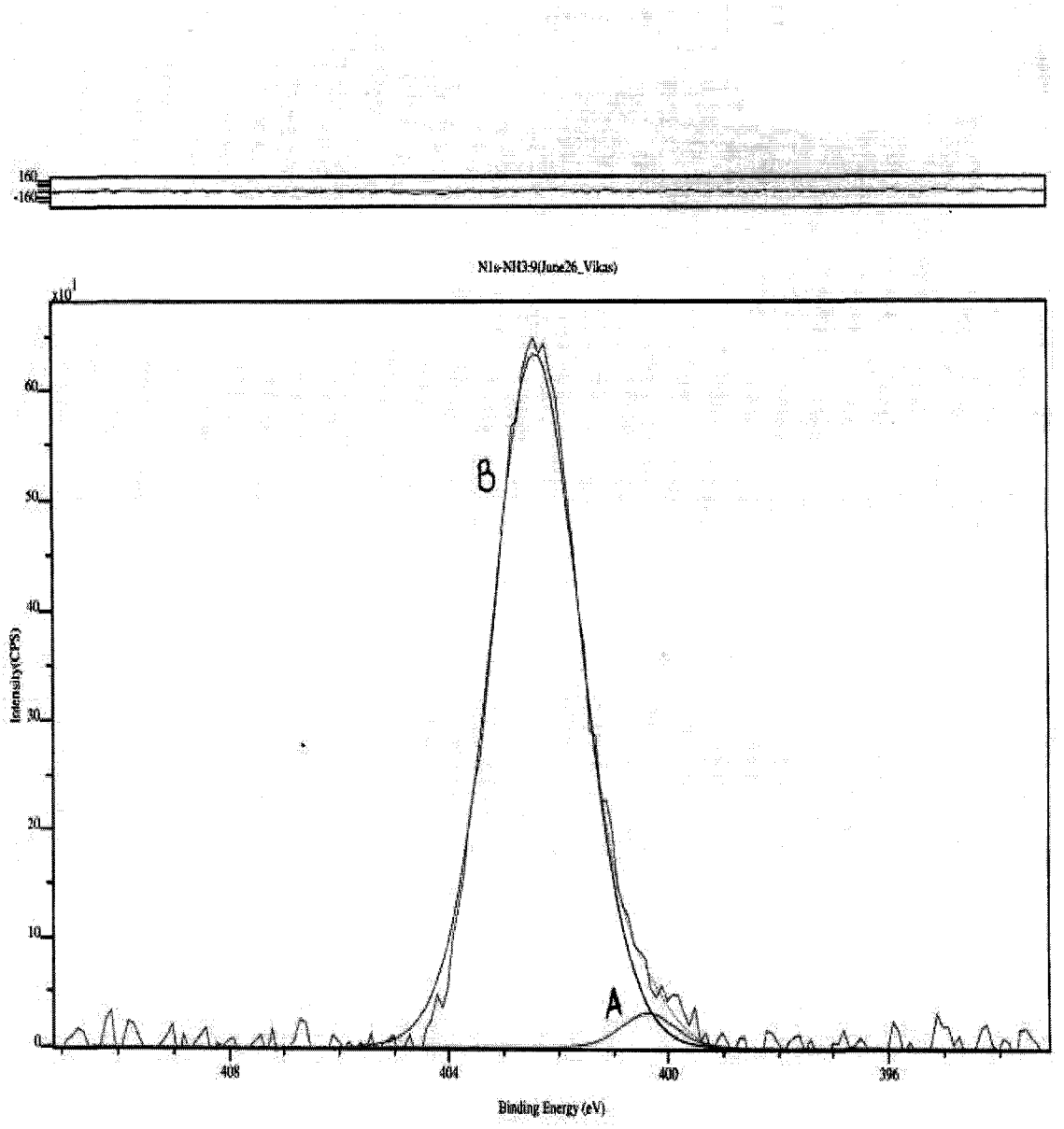

Figure 4.11 XPS of Uncalcined Ammonium Exchanged Clinoptilolite Catalyst

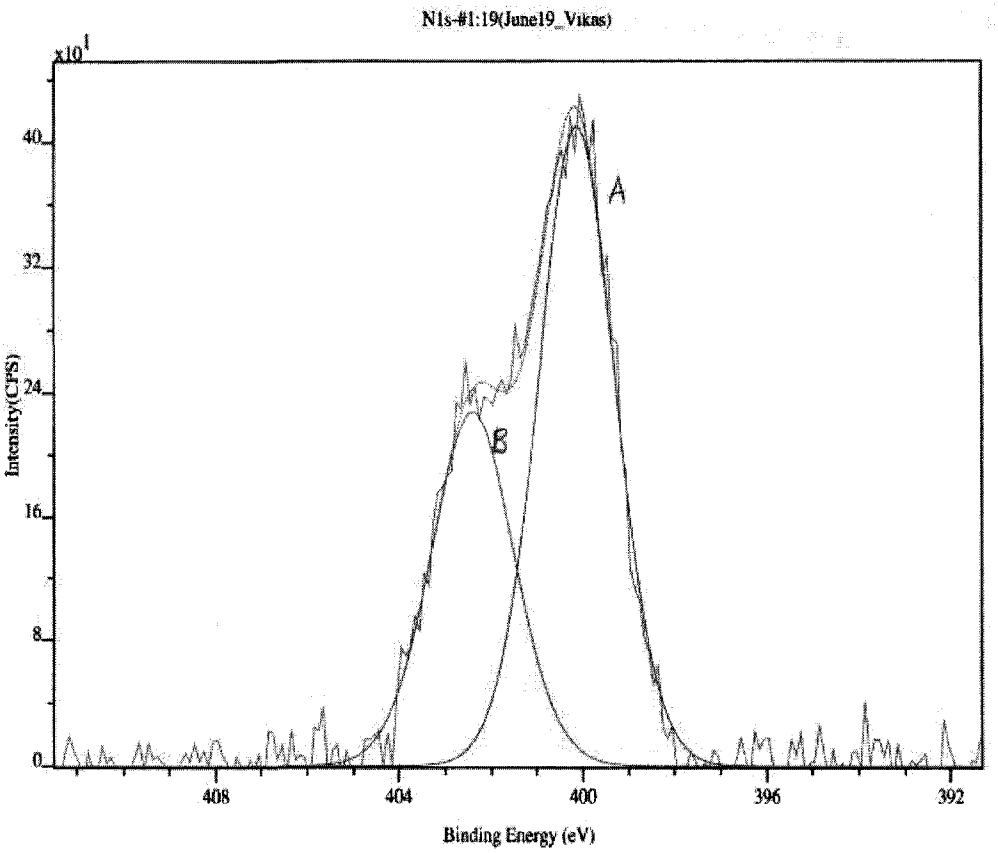

Figure 4.12 XPS of Dihydroindole Reacted Clinoptilolite

As a comparison, catalyst that was reacted with Cold Lake de-watered bitumen was also analyzed. The results from this experiment are presented in Figure 4.13. The Figure shows two peaks. Peak 'A' occurring at approximately the same position of 399.947 electron volt as dihydroindole reacted with clinoptilolite and a new peak 'C'. Both the peaks are shifted to 284.8 electron volt.

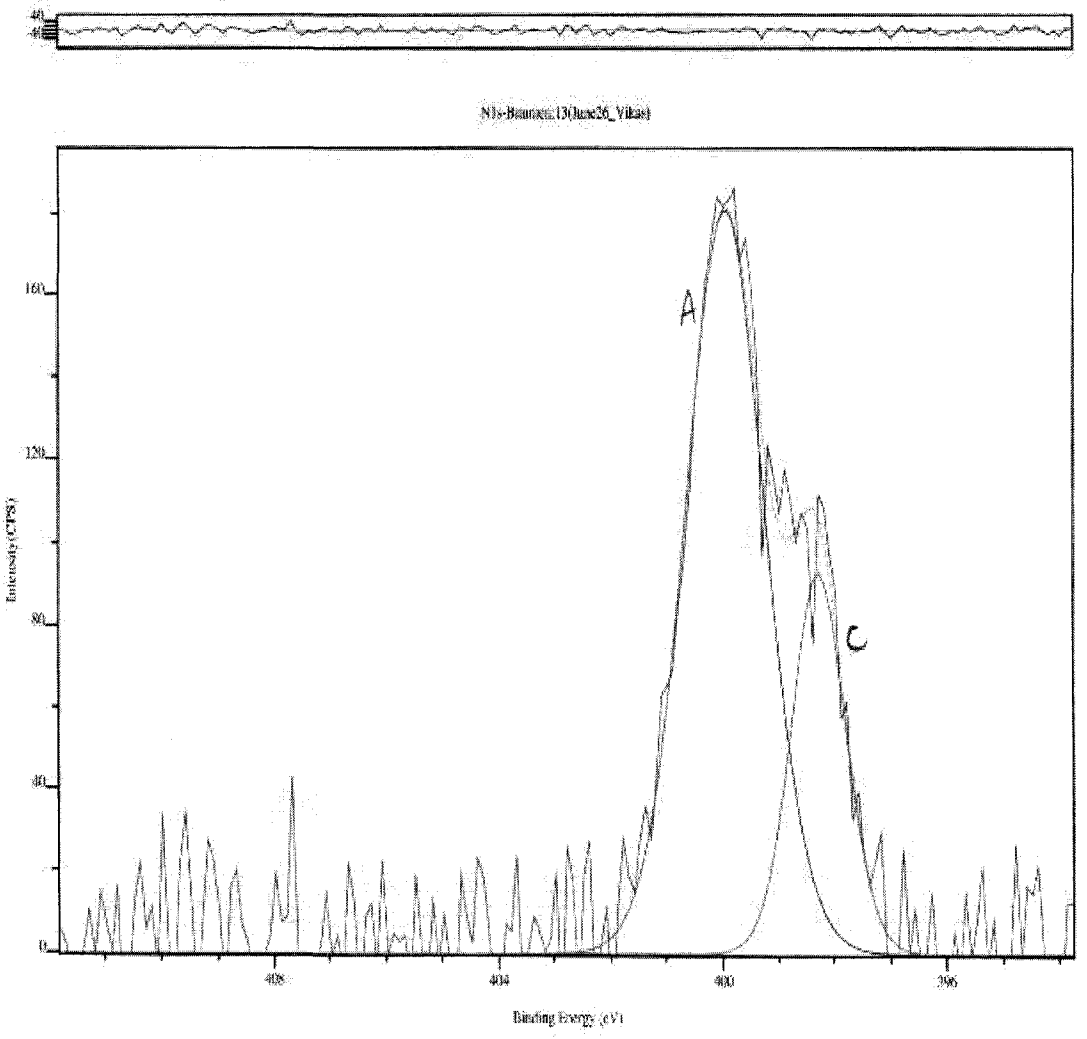

Figure 4.13 XPS of Clinoptilolite Reacted with Bitumen

To aid in the comparison of the XPS results, Figure 4.14 (a) and 4.14 (b) show the similarity between the two peaks resulting from reactions with dihydroindole and bitumen.

.

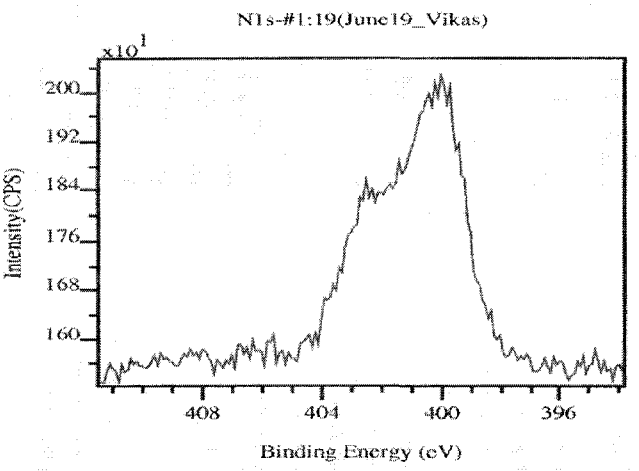

Figure 4.14 (a) XPS of Dihydroindole reacted Clinoptilolite

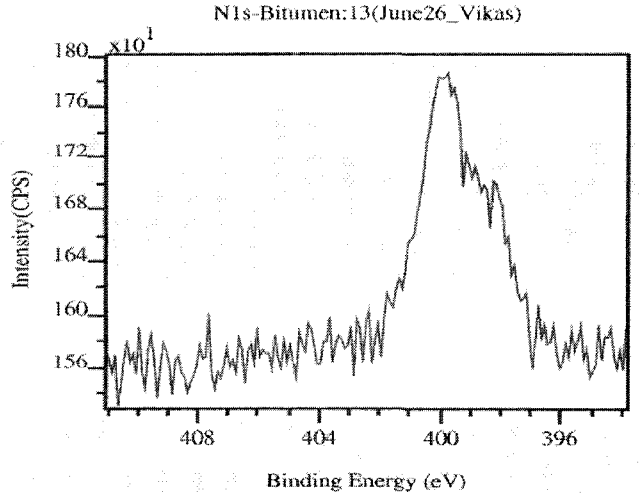

Figure 4.14 (b) XPS of Bitumen Reacted Clinoptilolite

To determine the amount of nitrogen adsorbed onto the clinoptilolite, a sample of the recovered dihydroindole reacted clinoptilolite was analyzed for nitrogen, carbon, hydrogen and sulphur by the Micro-analytical Services, Department of Chemistry at the University of Alberta. Analytical results in mass percent of 45.3754 units sample are given in Table 4.14

Table 4.14 Elemental Analysis of Dihydroindole Reacted Clinoptilolite

Element	Mass %
Nitrogen	0.8016
Carbon	1.4911
Hydrogen	1.0215
Sulphur	0.0422
Totals	3.3563

To test the recycling capacity of the catalyst, a saturation test of the catalyst was carried out. For this experiment 10% nitrogen solution of dihydroindole in 1-methylnaphthalene was prepared and the reaction was carried out under the same conditions at 425 ^{o}C with clinoptilolite catalyst. The catalyst was recovered, washed with pentane, dried and reused for the next experiment. The purpose was to determine the number of times the catalyst can be reused before it looses activity. In each of four successive experiments, the dihydroindole was completely removed in each pass. Figure 4.15 presents a gas chromatogram of the products from the third experiment. When compared with Figure 4.10, it can be seen that new peaks are appearing at a retention time of approximately 20 minutes.

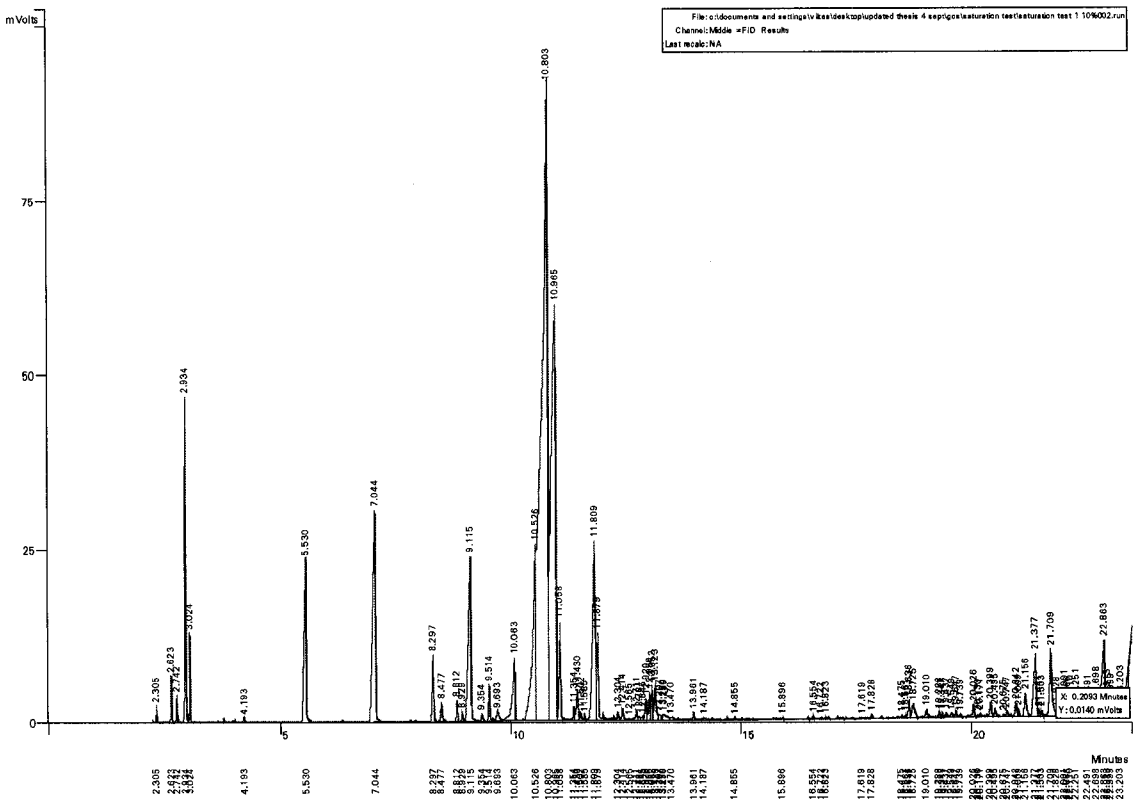

Figure 4.15 Gas Chromatogram of Dihydroindole in 1-Methylnaphthalene Solution reacted with clinoptilolite at 425 °C at 3rd recycle (Catalyst Saturation Test)

To determine the rate constants and the activation energies of all the used catalyst, it was essential to determine the order of reaction. Experiments were carried out by reacting 0.25 % nitrogen solution of dihydroindole in 1-methylnaphthalene in presence of 10 mass % ammonium exchanged sodium chabazite at a temperature of 425 °C. Conversion was measured at 30, 40, 50, and 60 minutes. GC analysis of the fresh solution yields a mass

percent of 1.6137 for the dihydroindole. The results of the area percent of dihydroindole after reactions are tabulated in 4.15

Table 4.15 Mass % of Dihydroindole at 425 °C

Time (mins.)	Mass %
0	2.1165
30	1.2061
40	1.1126
50	1.0281
60	0.8968

From the above data calculations were done and the results were plotted for 0.5 order, 1 order, 1.5 order and 2 order as presented in Figures 4.16 to 4.19. For the 0.5 order the linear regression R^2 value is 0.9492. By plotting the 1 order graph it is found that the linear trend line doesn't pass through the origin and has R^2 value of 0.9683. So half order and the first order reactions were ruled out. There was close proximity between 1.5 order and 2 order which have R^2 values of 0.9826 and 0.9902 respectively. Since second order plot fits the best and has highest regression value, order of reaction was considered to be second.

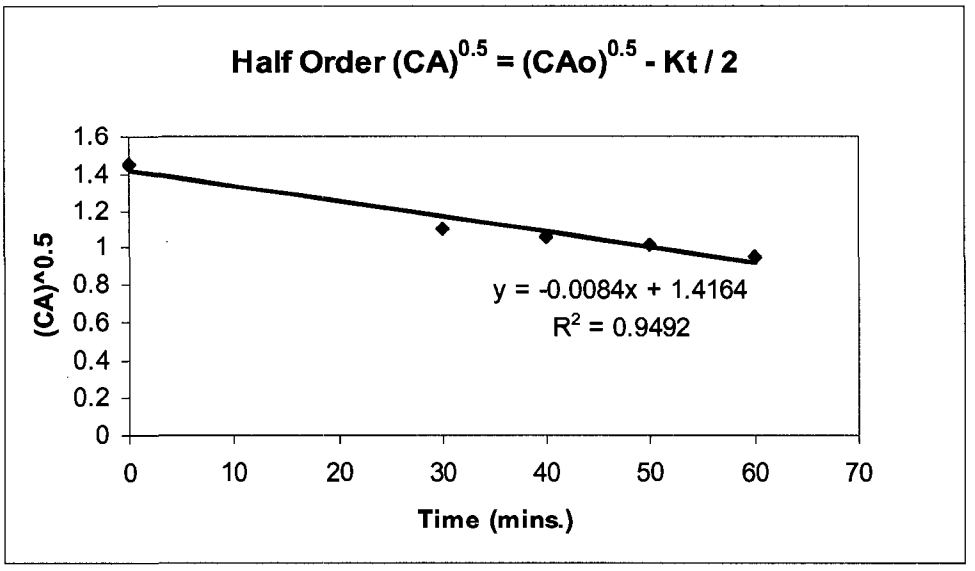

Figure 4.16 Plot for Half Order Reaction

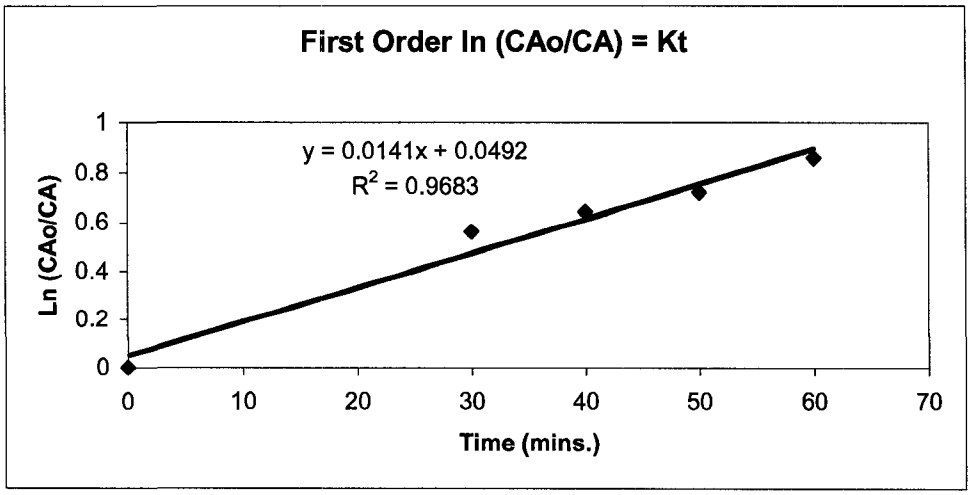

Figure 4.17 Plot for First Order Reaction

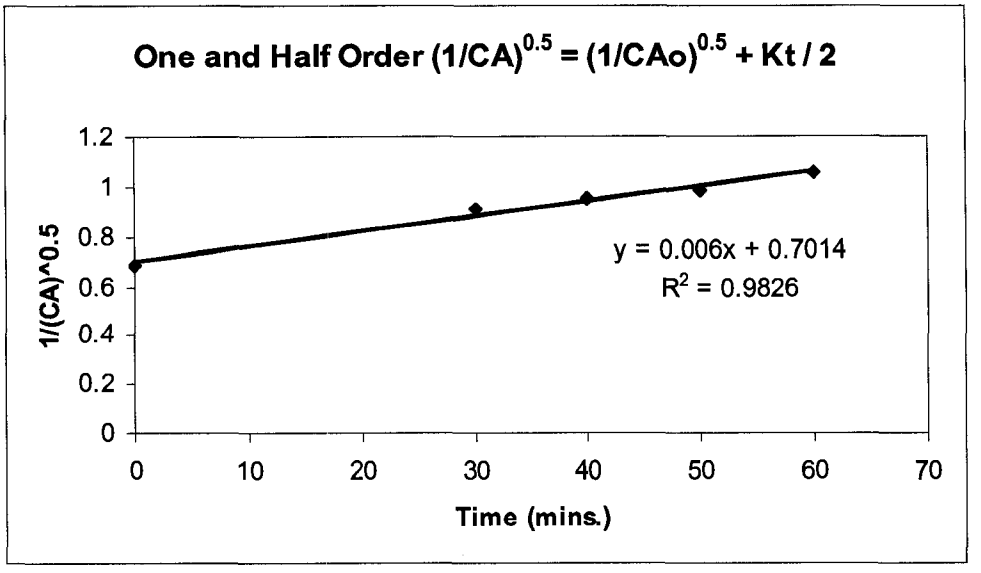

Figure 4.18 One and Half Order Plot

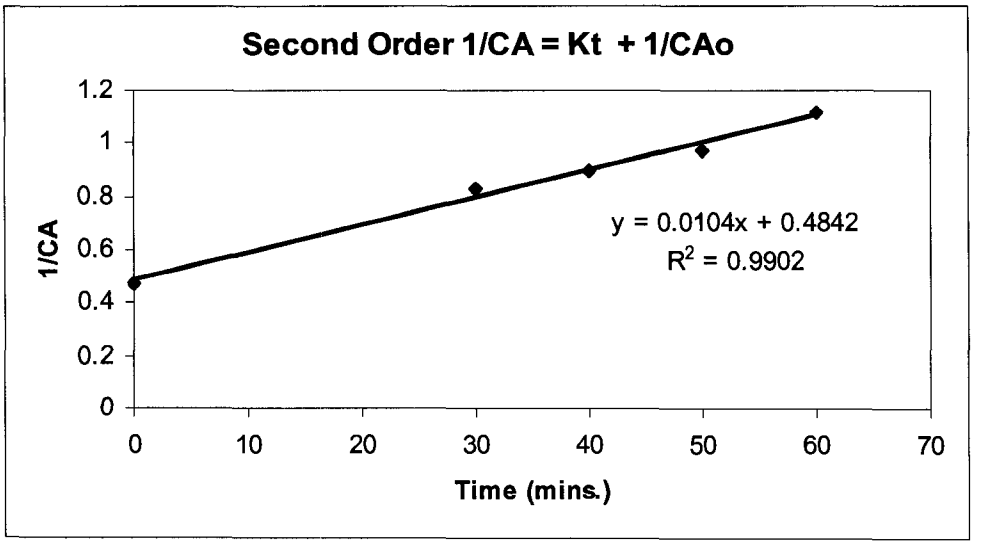

Figure 4.19 Second Order Plot

To quantify the effect of temperature on dihydroindole removal, an Arrhenius plot is presented in Figure 4.20 and the resulting activation energies are summarized in Table 4.16. Surface areas of all the catalysts used were taken into consideration for the calculation of the rate constant. Commercial Zeolite-Y has 400 m^2/gram of surface area, ammonium exchanged sodium chabazite has 70 m^2/gram and ammonium exchanged clinoptilolite gas 60 m^2/gram of surface area.

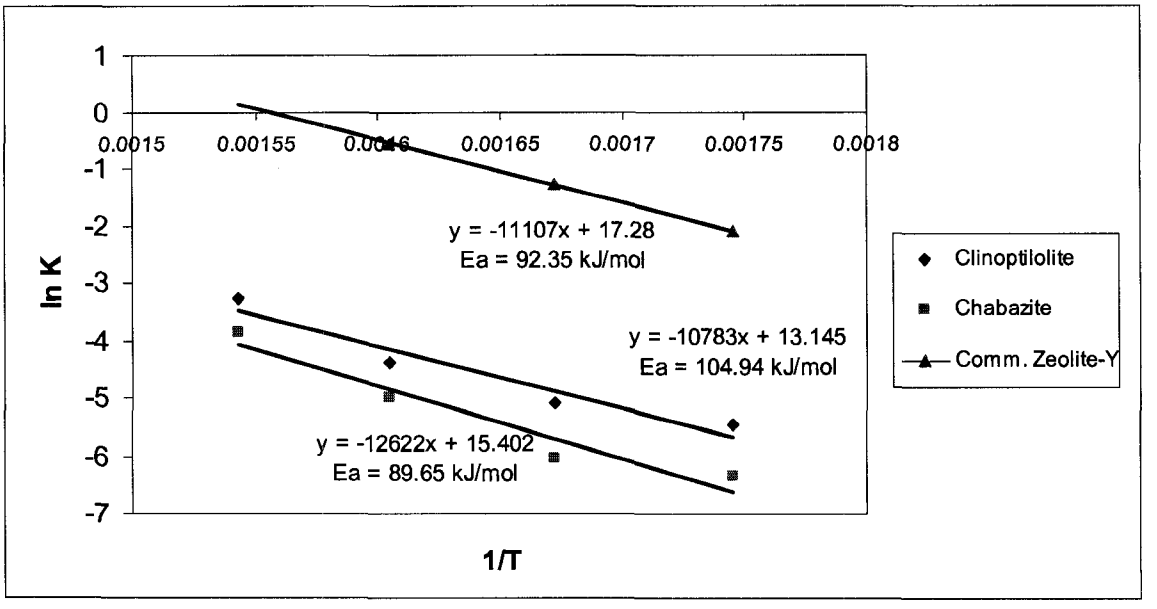

Figure 4.20 Arrhenius Plot for Determining Catalysts Activation Energy

Table 4.16 Activation Energy of Different Catalysts

Catalyst	Activation Energy (kJ / mol)
Commercial Zeolite-Y	92.3515
Chabazite	89.6576
Clinoptilolite	104.9483

Figure 4.12 shows the ammonia TPD of the some of the natural zeolite catalyst

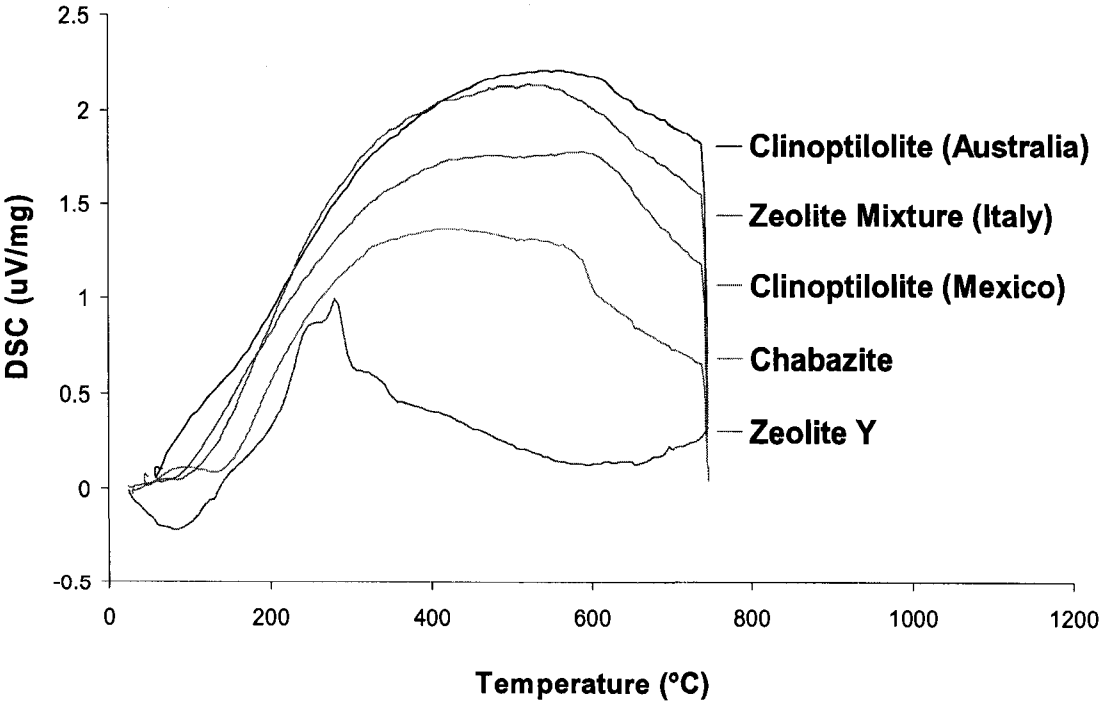

Figure 4.21 Ammonia TPD of Some Natural Zeolite Catalysts
(Courtesy: Dr S M Kuznicki's group)

5.0 Discussion

In the past, extensive work has been done on the removal of heteroatoms from fuels. Common processes for removing the heteroatoms include hydrodesulphurization (HDS) and hydrodenitrogenation (HDN). Both the processes use extensive amounts of hydrogen when upgrading high heteroatom containing streams such as those encountered in the upgrading of heavy oil. With reference to the work and paper published by Dr. S M Kuznicki and his group, some low cost natural zeolites such as clinoptilolite and chabazites have proved to be very effective in removing nitrogen and possibly sulphur and metals during the upgrading of oil sands without the addition of hydrogen. If such a process was possible it would provide a route for low cost upgrading of heavy oils as hydrogen would not be required in the reaction. Because of the low cost of the natural zeolite catalysts it would be possible to use them as once-through catalysts and consider them disposable

In the previous work, natural zeolite catalysts were mixed with unextracted oil bearing sand and reacted under nitrogen. A significant fraction of the heteroatoms were removed from the oil and the extractability of the oil from the sand was improved. It was not clear if the desulphurization and denitrogenation of the oil were due to adsorption or catalysis. Ultra-deep desulphurization and denitrogenation of diesel fuels have been reported using selective adsorption over a variety of adsorbents [21]. To validate the original observation that the natural zeolites were aiding the removal of heteroatoms, it was suggested that the natural zeolite catalysts prepared by Dr Kuznicki's group could be very effective if used with some of the model compounds. To test for cracking and

heteroatoms removal, two natural zeolite catalysts, ammonium exchanged upgraded sodium chabazite and ammonium exchanged clinoptilolite were used. Commercial Zeolite-Y was also used for comparison.

Very generally, heavy oil could be considered to be comprised of aromatic islands connected together by alkyl bridges. The aromatic islands contain both sulphur and nitrogen species. A general schematic of this structure is presented in Figure 5.1 Model compounds chosen for this experimental program included hexadecane, dibenzothiophene, quinoline and dihydroindole. Hexadecane was used to represents the long alkyl chains present in bitumen. Dibenzothiophene was used to represent the aromatic sulphur which accounts for approximately 60% of the total sulphur in heavy oil. Two types of aromatic nitrogen compounds, quinoline and dihydroindole, were selected for this study. Both are considered a basic (versus non-basic) type of nitrogen compound. This is relevant because the adsorption of nitrogen species has been reported to be in part due to acid-base interactions. Basic nitrogen compounds are also present in heavy oil and contribute highly towards catalyst poisoning. 1-methylnaphthalene was chosen as a solvent for dissolving the above compounds due to its non-reactive properties. Figure 5.1 shows the hypothetical model compound.

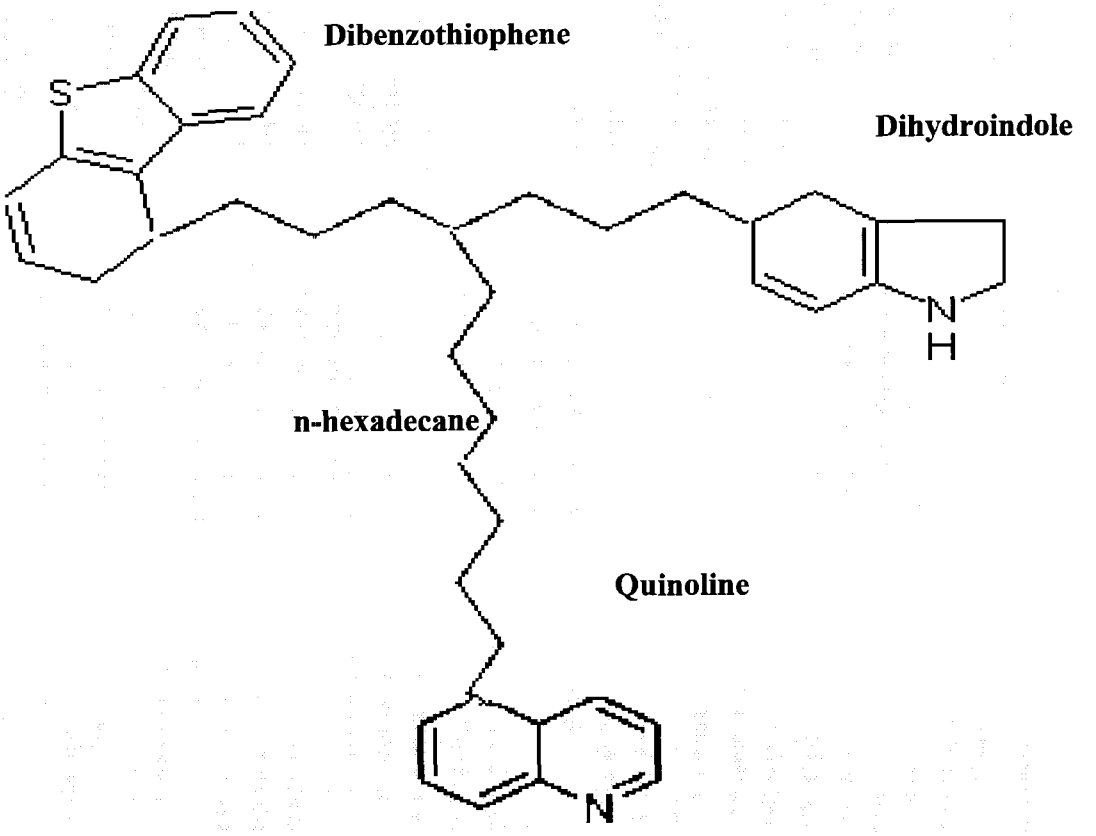

Figure 5.1 Hypothetical Model Compound

5.1 Cracking

One of the observations of the effect of natural zeolites on oilsands was improved extractability using aliphatic solvents such as hexane. This effect was attributed to possible cracking of the oil by the natural zeolites. To test this hypothesis, n-hexadecane was subjected to cracking thermally and with different catalysts at 425°C.

From the conversion data presented in Table 4.9 and the plot of conversion versus temperature presented in Figure 4.4, it is observed that thermal cracking yielded the highest conversion followed by clinoptilolite and zeolite-Y. Conversion of n-hexadecane by thermal cracking was more than 50% as compared to 35 % with zeolite-Y and 35 % with clinoptilolite at 425 °C. All the experiments were performed under the same operating conditions. The products from the clinoptilolite based natural zeolite, Figure 4.6, were similar to those produced by the commercial zeolite-Y, Figure 4.7. Both of these results were clearly different from the products achieved from thermal cracking, Figure 4.5. These results clearly show that the clinoptilolite based material is capable of catalyzing the cracking of hexadecane. These results are consistent with the literature reports of the ability of natural zeolites to catalyze cracking reactions [7] and shows that the transformation of the mineral into a natural zeolite was sucessful.

5.2 Desulphurization

One of the observation by Kuznicki et al. was that natural zeolite treated samples of oilsands had lower sulphur concentrations in the reacted products when compared with thermal treatment. To test this observation, dibenzothiophene was subjected to reaction thermally and in the presence of modified chabazite to determine the removal of sulphur from the solution. From Table 4.11, it can be seen that there was considerable scatter in the thermal conversion data with conversion ranging from 1.5 to 11.7%. There was less variability in the catalytic experiments with an average conversion of 8.03% with a standard deviation of 0.84% at 425 °C. Conversion levels of this magnitude are consistent with literature values for the catalytic cracking of

benzothiophene [39]. Compared with the experiments with oil sands, this level of conversion was low. Higher conversion levels of compounds such as dibenzothiophene usually require hydrogen and a supported metal catalyst such as CoMo sulfide on alumina. Otherwise, the aromatic ring of dibenzothiophenes is very stable.

5.3 Denitrogenation

Basic nitrogen model compounds were subjected to reactions with ammonium exchanged sodium chabazite, ammonium exchanged clinoptilolite and commercial Zeolite-Y as a control.

A 0.25 % basic nitrogen solution of quinoline in 1-methylnaphthalene was subjected to reaction at 400°C, 410°C and 425°C with the above mentioned catalysts. The resultant products were analyzed and showed a conversion ranging from 7.4 % to 12.2% over a temperature range from 400°C to 425°C., Table 4.12. This level of conversion is consistent with HDN data reported with FCC catalysts [38]. The chromatograms of the product, as shown in Figure 4.8, show that higher molecular weight products than the starting reactants were formed during the reaction. The conversion data, however, were lower than expected from the reported nitrogen concentration decreases observed with natural zeolites and oil sands.

The experiment was repeated but this time with a 0.25 mass % basic nitrogen solution of dihydroindole in 1-methylnaphthalene and ammonium exchanged clinoptilolite. Surprisingly, the gas chromatogram of the reacted sample showed complete removal of

dihydroindole compound. Initial GC of the solution of dihydroindole in 1-methylnaphthalene shows retention time at 10.76 minutes. In the reacted sample the peak of dihydroindole at the same retention time is eliminated. That was indicative that the conversion of dihydroindole was 100 %. Experiments were also carried out with ammonium exchanged upgraded chabazite and commercial zeolite-Y under the same conditions. These experiments also showed complete removal of dihydroindole compound as can be seen in Figure 4.9 and Table 4.13.

From the Figure 4.20 it is observed that from the experiments carried out, the activation energy of chabazite was 89.65 kJ/mol, clinoptilolite is 104.94 kJ/mol and commercial zeolite-Y is 92.35 kJ/mol and are almost comparable. Comparing the conversions and reduction in the dihydroindole concentration during the experiments, commercial Zeolite-Y by far has been more effective by virtue of its large surface area of approx 400 m^2/gram of catalyst. This large surface area, however, tends to plug very rapidly during the reaction and is not a very effective catalyst for cracking large molecules. On the other hand low cost catalysts such as clinoptilolite and chabazite natural zeolites are highly acidic and have a low surface area of 60 and 70 m^2/gram respectively and can be used as a disposable catalyst.

With the complete removal of dihydroindole from solution, two modes of actions were speculated: decomposition and/or adsorption on the surface of the catalyst. From the mass balance data presented for the dihydroindole reaction with exchanged chabazite at 325°C, presented in Tables 4.5 to 4.7, it can be seen that very little gas was formed. Additionally, there was not a significant generation of decomposition products in the solution, as observed by gas chromatography in Figure 4.10. It was hypothesized that the

dihydroindole was possibly adsorbed onto the surface of the catalyst. Interestingly, if the material was adsorbed onto the surface of the catalyst, it could not be due primarily to acid-base interactions since a significant amount of quinoline was not removed from solution during comparable experiments.

5.4 Analysis of Catalysts

To verify the adsorption of nitrogen on the surface of the catalyst, the recovered clinoptilolite catalyst and an uncalcined ammonium exchanged clinoptilolite control sample were analyzed by X-ray photoelectron spectroscopy by the University of Alberta ACSES surface chemistry laboratory.

For the uncalcined catalyst, two types of nitrogen were observed using XPS. The adsorbed ammonium nitrogen in the ammonium exchanged sample is apparent at "peak B" in Figure 4.11. The small peak "A" was consistent with nitrogen bound in an organic matrix. Peak "B" also had a binding energy that was consistent with ammonium salt. This could be found from the table of nitrogen compound type related to different binding energies, Appendix D. From the table of nitrogen compounds related to the binding energies, Peak "B" was completely removed when the sample was calcined.

Surface analysis of clinoptilolite catalyst reacted with dihydroindole was also performed using XPS, Figure 4.12. In this case, a significant peak was observed which corresponded to adsorbed dihydroindole (Peak 'A'). Peak 'A' occurred at 400.126 electron volt and generally corresponds with the category of nitrogen in an organic matrix. Also peak 'B'

occurring at 402.403 electron volts indicating an ammonium salt containing nitrogen was on the surface of the catalyst. Since this peak was completely removed during calcining, it must have been generated during the reaction. This is consistent with the results showing that indole was easily cracked on FCC catalysts to generate ammonia [40].

Since the purpose of the experimental study was to verify observations of the effect of natural zeolites on the upgrading of oil sands, the results of the XPS analysis of catalysts reacted with the model compounds were compared with the surface analysis of recovered catalyst from a reaction with extracted bitumen. Figures 4.14 (a) and 4.14 (b) show the similarity between the two XPS results from the model compound dihydroindole and bitumen. It can be seen from the two Figures that the organic matrix containing nitrogen peaks occurred at the same positions of approximately 400 electron volts.

A new peak, however, was observed with the bitumen derived samples and was labeled Peak 'C'. Peaks in this region are also assigned to the general group of nitrogen in an organic matrix. No further work was performed to identify this new peak. Interestingly, no adsorbed ammonia was observed on the more complicated bitumen derived sample.

To test if all of the nitrogen removed from the dihydroindole solution could be accounted for by adsorption onto the catalyst, the reacted catalyst sample was analyzed by elemental analysis. These results were presented in Table 4.14. The mass percent of nitrogen present in the dihydroindole and 1-methylnapthalene solution is 0.1926%. Therefore the mass of nitrogen in 3 grams of dihydroindole in 1-methylnaphtahlene solution is 0.0057 grams. Considering negligible nitrogen present in the calcined ammonium exchanged

clinoptilolite catalyst and 0.80 mass percent present in the recovered dihydroindole reacted clinoptilolite catalyst, mass of nitrogen present in 0.3 grams of catalyst used is 0.0024 grams. Some nitrogen in free state is present on the calcined fresh catalyst surface due to the fact that during calcinations process of the catalyst, flow of nitrogen is maintained in the tube furnace to protect the catalyst from burning and to aid desorption of ammonia from the catalyst surface. This nitrogen would easily be removed during the reaction. Elemental analysis of calcined ammonium exchanged clinoptilolite would reflect this nitrogen and hence is neglected in the analysis. These results suggest that not all of the nitrogen removed from the liquid is adsorbed onto the surface of the catalyst.

To further test the catalyst, a single batch of catalyst was reused four times in successive experiments with 10% dihydroindole. In each case, the dihydroindole was completely removed from solution. These results suggest that the mode of action of the catalyst was more likely reaction versus adsorption. On close inspection of the gas chromatogram of the products from the third recycle experiment, larger compounds were formed than the parent compound. One hypothesis for the observation is that the catalyst was polymerizing the dihydroindole. This hypothesis is supported by the fact that there is at least one paper in the literature that reports polyhydroindole [32]. Unfortunately, this hypothesis was not explored further in this study.

6.0 Conclusions

Hexadecane cracking experiments show that these natural forms of ammonium exchanged zeolites are definitely capable of performing cracking. However the results showed lower conversion than achieved with thermal cracking.

In the absence of hydrogen, the dibenzothiophene aromatic ring was relatively stable and was not significantly reduced with the natural forms of ammonium exchanged natural zeolites.

Quinoline was slightly reactive in the presence of natural forms of ammonium exchanged natural zeolites. The same ammonium exchanged natural zeolites were extremely effective in removing dihydroindole from a 1-methynaphthalene solution. Initially it was hypothesized that the whole amount of nitrogen eliminated would be adsorbed on the catalyst surface and the XPS analysis demonstrated the presence of dihydroindole adsorbed on the surface of the catalyst. From the elemental analysis it was determined that 0.0024 grams of nitrogen from the available 0.0057 grams was adsorbed on the surface of the catalyst i.e. approximately 42 %. Also, the saturation test performed on the chabazite catalyst showed that even 10 % concentration of nitrogen is completely removed four times repeateadly using the same catalyst. This gives rise to an open ended question about the rest of the nitrogen i.e. 58 %. It is known that these nitrogen species can undergo polymerization and due to the virtue of their heavy molecular weight, are not reflected in the gas chromatogram. These polymerized compounds also do not get attached to the catalyst surface and are removed once the catalyst is washed with a solvent.

7.0 Recommendations

The study definitely showed the positive effect of these ammonium exchanged natural form of zeolites in cracking and denitrogenation of the model compounds. As hypothesized earlier about the complete adsorption of nitrogen on the catalyst surface, the elemental analysis shows presence of 42 % nitrogen only adsorbed on the catalyst surface. It still requires study to verify the polymerization of these nitrogen species.

Past work and published paper from Dr. Kuznicki states the positive effect of these catalysts on the removal of heavy metals such as nickel and vanadium. It would be definitely beneficial to study the effect of these catalysts on the model compounds such as vanadium porphyrins.

During the course of the experiments 10 mass % of the catalyst was used. Further studies of optimizing the catalyst quantity and determining the optimum reaction temperature could be advantageous for economics.

Further studies are definitely required for more difficult nitrogen compound like non-basic nitrogen compounds such as carbazole. Also all these experiments were carried out in a micro batch reactor. It is highly recommended to evaluate the performance in fixed bed reactor.

8.0 References

[1] Bej, S. K., Dalai, A. K. and Adjaye, J., (2001), "Comparison of Hydrodenitrogenation of Basic and Non-basic Nitrogen Compounds Present in Oil Sands Derived Heavy Gas Oil", *Energy and Fuels*, **15**, 377-383

[2] Botchwey C., Dalai A.K. and Adjaye, J. (2004), "Kinetics of Bitumen-Derived Gas Oil Upgrading Using a Commercial NiMo/Al2O3 Catalyst", *The Canadian Journal of Chemical Engineering*, Volume 82

[3] Caeiro, G., Costa, A. F., Cerqueira, H. S., Magnoux, P., Lopes, J. M., Matias, P., Ribeiro, R.F. (2006), " Nitrogen poisoning Effect on the Catalytic Cracking of Gasoil", *Applied Catalysis A: General*, **320**, 8-15

[4] Calafat, A., Laine, J., and Lopez-Agudo, A., (1996), "Hydrodenitrogenation of Pyridine over Activated Carbon-Supported Sulfided Mo and NiMo Catalysts. Effects of Hydrogen Sulfide and Oxidation of the Support", *Catalysis Letters*, **40**, 229-234.

[5] Carrado, K.A., Kim, J. H., Song, C. S., Castagnola, N., Marshall, C. L. and Schwartz, M. M., (2006), "HDS and Deep HDS Activity of CoMoS-Mesostructured Clay Catalysts", *Catalysis Today*, **116**, 478-484

[6] Cejka, J. (2004), "Zeolites: Structures and Inclusion properties", Encyclopedia of Supramolecular Chemistry, *Marcel Dekker INC.*, 1623-1630

[7] Chang, C. D., Miale, J. N., Lago, R. M., Shihabi, D. S., Dessau, R. M., Chu, P., Garwood, W. E., Kuehl, G. H., Rosinski, E. J. (1985) "Treatment of Zeolites" European Patent EP0134333

[8] Ding, L., Zheng Y., Zhang Z., Ring and Chen J., (2006), "HDS, HDN, HDA, and Hydrocracking of Model Compounds over Mo-Ni Catalysts with Various Acidities", *Applied Catalysis A*: *General,* **319**, 25-37

[9] Dufresne. P, (2007), "Hydroprocessing Catalysts Regeneration and Recycling", *Applied Catalysis A: General*, **322**, 67-75

[10] Farag, H., Sakanishi, K., Kouzu, M., Matsumura, A., Sugimoto, Y and Saito, I., (2003), "Dual Character of H_2S as Promoter and Inhibitor for Hydrodesulfurization of Dibenzothiophene", *Catalysis Communications*, **4**, 321-326

[11] Ferdous, D, Dalai, A. K., Adjaye, J., (2002), "Comparison of Hydrodenitrogenation of Model Basic and Nonbasic Nitrogen Species in a trickle bed reactor Using Commercial $NiMo/Al_2O_3$ Catalyst", *Energy and Fuels*, **17**, 164-171

[12] Girgis, M. J. and Gates, B.C., (1991), "Reactivities, Reaction Networks, and Kinetics in High pressure Catalytic Hydroprocessing", *Ind. Eng. Chem. Res.*, **30**, 2021-2058.

[13] Gray, M.R., Khorasheh, F., Wanke, S.E., Achia, U., Krzywicki, A., Sanford, E.C., Sy, O.C.K., Ternan, M. (1992), "Role of Catalyst in Hydrocracking of Residues from Alberta Bitumens", *Energy and Fuels,* **6**, 476-485

[14] Jeong S.Y., Bunger, J.W., Suh J.K., and Lee J.M. (1995), "Dependence of Reaction Kinetics on Molecular Weight in Hydrodenitrogenation of Shale Oil", *J. of Chem. Eng. Of Japan*, **28 (1),** 122-124.

[15] Jokuty, P. L., Gray, M. R., (1991), "Resistant Nitrogen Compounds in Hydrotreated Gas Oil from Athabasca Bitumen", *Energy and Fuels*, **5**, 791-795

[16] Kanda, W. S., (2003), "Quinoline Conversion in the Presence of Athabasca Derived Heavy Gas Oil Fractions", Department of Chemical and Materials Engineering, University of Alberta.

[17] Khorasheh, F. and Gray, M. R., (1993), "High Pressure Thermal Cracking of Hexadecane", *Ind. Eng. Chem. Res.*, 32, 1853-1863

[18] Kim, S.C. and Massoth, F.E., (2000), "Kinetics of Hydronitrogenation of Indole", *Ind. Eng. Chem. Res.,* **39**, 1705-1712

[19] Kim, S.C. and Massoth, F.E., (2000), "Hydronitrogenation Activities of Methyl-Substituted Indoles", *Journal of Catalysis*, **189**, 70-78

[20] Kim, D., Yen, T. F., (2005), "Denitrogenation", Encyclopedia of Chemical Processing, *Marcel Dekker.*, 627-632

[21] Kim, J.H., Ma, X., Shou, A, Song, C. (2005), "Ultra-deep desulfurization and denitrogenation of diesel fuel by selective adsorption over three different adsorbents: A study on adsorptive selectivity and mechanism.", *Catalysis Today*, 111(1-2), 74-83

[22] Kowalczyk, P., Sprynskyy, M., Terzyk, A. P., Lebedynets, M., Namiesnik, J., Buszeuski, B., (2006), "Porous Structure of Natural and Modified Clinoptilolite", *Journal of Colloid and Interface Science*, **297**, 77-85

[23] Kuznicki, S. M., McCaffrey, W. C., Bian, J., Wangen, E., Koenig, A. and Lin, C.H. (2007), "Natural Zeolite Bitumen Cracking and Upgrading", *Microporous and Mesoporous Materials*, **105**, 268-272

[24] Liaw, S. J., Keogh, R. K., Thomas, G. A., and Davis, B.H., (1994), "Catalytic Hydrotreatment of coal-Derived Naphtha Using Commercial Catalysts", *Energy and Fuels*, **8**, 581-587

[25] Lavopa,V. and Satterfield C.N., (1988), "Response of Dibezothiophene Hydrodesulfurization to presence of Nitrogen compounds", *Chem. Eng. Comm.*, **70**, 171-176

[26] Ma, X., Sakanishi, K., Isoda, T., and Mochida, I, (1995), "Hydrodesulfurization Reactivities of narrow-Cut Fractions in a Gas Oil", *Chem. Eng. Comm.*, 34, 748-754

[27] Machida, M., Sakao, Y., and Ono, S. (2000), "Kinetics of Individual and Simultaneous Hydronitrogenations of Aniline and Pyridine", *Applied Catalysis A: General*, **201**, 115-120

[28] Maity, S.K., Perez, V. H., Ancheyta, J. and Rana M. S., (2007), "Catalyst Deactivation during Hydrotreating of Maya Crude in Batch Reactor", *Energy and Fuels*, **21**, 636-639

[29] Marcilly, C., (2004), "Zeolites in Petroleum Industry", Encyclopedia of Supramolecular Chemistry, *Marcel Dekker, INC*, 1599-1609

[30] Massoth, F.E. and Kim, S.C. (1998), "Polymer Formation during the HDN of Indole", *Catalysis Letters*, **57**, 129-134

[31] Miki, Y., Yamadaya, S., Oba M., and Sugimoto Y., (1983) "Role of Catalyst in Hydrocracking of Heavy Oil", *Journal of Catalysis*, **83**, 371-383

[32]Ozden M, Ekinci E, Karagozler AE (1998) "Synthesis and optimization of permselective polymer (polyindoline) film", *Journal of Solid State Electrochemistry,* **2**(6), 427-431

[33] Prins, R., Jian, M., and Flechsenhar, M., (1997), "Mechanism and Kinetics of Hydrodenitrogenation", *Polyhedron*, **16**(18), 3235-3246.

[34] Rana, S., Samano, V., Ancheyta, J. Diaz, J.A.I., (2007), "A Review of Recent Advances on Process Technologies for Upgrading of Heavy Oils and Residua", *Fuel*, **86**, 1216-1231

[35] Sanford, E. C., (1994), "Influence of Hydrogen and Catalyst on Distillate Yields and the Removal of Heteroatoms, Aromatics, and CCR during Cracking of Athabasca Bitumen Residuum Over a Wide Range of Conversion", *Energy and Fuels*, **8**, 1276-1288

[36] S.H. Yang and C. N. Satterfield, (1984), "Catalytic Hydrodenitrogenation of Quinoline in a Trickle-Bed Reactor - Effect of Hydrogen Sulphide", *Industrial & engineering chemistry process design and development*, 23, 20-25

[37] Tatsumi, T., (2004), "Zeolites: Catalysis", Encyclopedia of Supramolecular Chemistry, *Marcel Dekker, INC.*, New York, 1610-1616

[38] Trytten, L.C., Gray, M.R., and Sanford E.C., (1990), "Hydroprocessing of Narrow-Boiling gas Oil Fractions: Dependence of Reaction Kinetics on Molecular weight", *Ind. Eng. Chem. Res.*, **29**, 725-730

[39] Valla, J.A. Lappas A.A. and Vasalos I.A. (2006), "Catalytic cracking of thiophene and benzothiophene: Mechanism and kinetics", *Applied Catalysis A*: General **297**(1) 90-101

[40]Yu DY, Que GH, Xu H, Wang ZX (2003), "Co-cracking of indole and quinoline in catalytic cracking", *Abstracts Of Papers Of The American Chemical Society* **226**, U262-U262

Appendix A

Sample Preparation, Experimental Procedure and Mass Balance Data

This appendix presents the procedure of preparing the samples used during the course of the experiments. 0.25 mass percent of basic nitrogen quinoline and dihydroindole solution were prepared separately in 1- methylnaphthalene solvent. Ammonium exchanging procedure for zeolite as provided by Dr S.M. Kuznicki's group is also attached in this appendix.

This appendix also highlights the steps of experimental procedure implemented during the experiments. These steps were strictly followed for all the experiments.

.

Mass balance data sheet for one experimental procedure is also attached for the reference. This data is from one of the experiments performed during results repeatability (error tests).

A.1 Sample Preparation

The following procedure was implemented to prepare 0.53 % basic nitrogen concentration stock solution and 0.25 % basic nitrogen concentration experimental solution of quinoline in 1-methylnaphthalene.

Molecular formula of quinoline is C_9H_7N and Molecular weight is 129

Nitrogen present in quinoline is

14/129 = 10.85 % i.e. 10.85 g nitrogen in 100 g of Quinoline

For each trial of the experiment, 3 grams of solution was taken.

3 grams of 1-methylnaphthalene would contain

3*0.53/100 = 0.00159 grams of nitrogen

For 0.00159 grams of nitrogen, quinoline available is (0.0159 * 100) /10.85

= 0.1465 grams

For 0.53 % basic nitrogen solution of Quinoline and Dihydroindole the mix would be 0.1465 grams of quinoline and 2.8535 grams of 1-methylnaphthalene.

Solution was prepared for 10 trials therefore actually 1.4685 grams of quinoline was mixed with 28.5386 grams of 1-methylnaphthalene.

This stock solution was diluted to 0.25 % basic nitrogen solution of quinoline in 1-methylnaphthalene.

Total solution made was 30.0071 grams

In 1 gram of solution mass fraction of quinoline present is 1.4685/30.0071 = 0.04893

Mass fraction of nitrogen present is 10% of 0.04893 = 0.0053089

And mass fraction of 1-methylnaphthalene present is 28.5386/30.0071 = 0.95106

For nitrogen mass fraction of 0.0025, the quinoline mass fraction is

(0.0025 *0.04893)/ 0.0053089 = 0.023037

Volume of 1-methylnaphthalene required to make 0.25 % basic nitrogen solution is

0.04893 / X = 0.023037 = 2.123947 grams

Volume of 1- methylnaphthalene to be added is 2.123947 – 0.95106 = 1.172887 grams.

Mass of methylnaphthalene added was 1.17286 grams; therefore the concentration of nitrogen was 0.2443 %

The following procedure was implemented to prepare 0.53 % basic nitrogen concentration stock solution and 0.25 % basic nitrogen concentration experimental solution of dihydroindole in 1-methylnaphthalene

Molecular formula of dihydroindole is C_8H_9N and Molecular weight is 119

Nitrogen present in dihydroindole is

14/119 = 11.7647 % i.e. 11.7647 g nitrogen in 100 g of dihydroindole

For each trial of the experiment, 3 grams of solution was taken.

3 grams of 1-methylnaphthalene would contain

3*0.53/100 = 0.00159 grams of nitrogen

For 0.00159 grams of nitrogen dihydroindole available is (0.0159 * 100) /11.7647

= 0.13515 grams

For 0.53 % basic nitrogen solution of dihydroindole in 1-methylnaphthalene, the mix would be 0.13515 grams of dihydroindole and 2.86485 grams of 1-methylnaphthalene.

Solution was prepared for 10 trials therefore actually 1.3517 grams of dihydroindole was mixed with 28.6588 grams of 1-methylnaphthalene.

This stock solution was diluted to 0.25 % basic nitrogen solution of dihydroindole in 1-methylnaphthalene.

Total solution made was 30.0105 grams

In 1 gram of solution, mass fraction of dihydroindole present is 1.3517/30.0105 = 0.045040

Mass fraction of nitrogen present is 11.7647 % of 0.045040 = 0.0052988

And mass fraction of 1-methylnaphthalene present is 28.6588/30.0071 = 0.95495

For nitrogen mass fraction of 0.0025, the dihydroindole mass fraction is

(0.0025 *0.045040)/ 0.0052988 = 0.021250

Volume of 1-methylnaphthalene required to make 0.25 % basic nitrogen solution is

0.045040 / X = 0.021250 = 2.11952 grams

Volume of 1- methylnaphthalene added was 2.11952 – 0.95495 = 1.16457 grams.

Mass of methylnaphthalene added was 1.17286 grams; therefore the concentration of nitrogen was 0.245 %.

A 2 Ammonium Ion Exchange Procedure

- Zeolite sample is ground to a size passable through 200 mesh screen.
- 15 g of NH_4NO_3 salt and 20g (in case of Clinoptilolite) or 5 g (in case of Chabazite) of zeolite sample are mixed in approximately 200cc of deionized H_2O. The use of 1000 cc beaker or anything close to this size is recommended.
- Out of two 150 cc beakers one is filled with plenty of deionized H_2O and the other beaker with approximately 10 mL of 1M HCl.

- Calibration of the pH-Meter is checked and recalibrate if necessary. HCl is added drop wise using a disposable pipette and plastic bulb until the pH of the solution is approximately 3.5 – 4.pH-electrode is rinsed again before putting it back into the storage solution. Rest of the acid is disposed off very slowly and carefully in the sink.
- Magnetic stirring bullet (large enough to stir the solution in the beaker) is put into the 1000 mL beaker and the beaker is placed on a stirring hotplate. The stirring is quite fast to ensure no layer formation occurs. The temperature is set to a point sufficient to make the solution temperature approximately 80°C (recommended set-point temperature is 205°C).
- For clinoptilolites or chabazites the mixture is left stirring for 8 and 6 hours on the hot plates respectively.
- Beaker is removed from the hot plate and let the solution settle.Fines in the water are decanted away and new de-ionized water is mixed in the solution. This step is repeated 3-4 times, and then filtered under a vacuum with a Whatman # 4 (90 mm) filter paper.
- Filtered sample is put on a weighing dish and placed in the oven at 80°C or 100°C (watch glass used instead of the dish in this case) and left overnight.
- After that sample has dried it is ground so that all large clumps are gone.Three crucibles are filled with the sample and placed closely in the centre of the glass tube in the tube furnace. The program is set to ramp at 10°C per minute and settle at 450°C for 60 minutes. The entire calcination is done under mild nitrogen flow and vacuum. It is ensured that the yellow clamps are used to hold the glass joints.

- After the temperature has cooled to 200°C, the nitrogen flow is turned off and the top of the tube furnace opened. The sign warning of the high temperatures is put out. When the temperature reaches approximately 70°C, the catalyst is removed from the furnace.
- Final sample is ground to a size that makes through a 200 mesh screen.
- Ample is stored in closed plastic container and labeled properly.

A.3 Experimental Procedure

3 grams of prepared solution was weighed in a reactor and 10 mass % i.e. 0.3 grams of catalyst is added. The reactor was placed on the vice after finger tightening the main body nut and tightened ¼ turn. After this the reactor was subjected to leak test and nitrogen pressurization.

The reactor was attached to the nitrogen line with the help of a female connector provided at the end of the long tubing and tightened. Manifold was checked for all the valves from the nitrogen cylinder to the reactor were open and rest closed to avoid the intermixing. Nitrogen cylinder main valve was opened and the downstream pressure is adjusted to 1500 psi. The vent valve was opened to the atmosphere and the line flushed by opening the nitrogen cylinder downstream valve slightly to ensure no contamination in the line. The cylinder downstream valve and the vent valves are closed and the reactor's needle valve was opened. Care was taken that the vent valve was completely closed when pressurizing the reactor.

Reactor was pressurized with nitrogen to 1000 psi by opening the cylinder down stream valve and observing the pressure in the pressure gauge. The reactor was checked for leakage with snoop solution. Snoop solution was put on all the joints and fittings and observed for leakage for 2 minutes. Also the pressure gauge was observed continuously to see if there was any drop in the pressure from 1000 psi. If any leak was observed due to bubbling, reactor was depressurized by opening the vent valve slowly and disconnecting and the leaking joints further tightened. The leak test step was repeated. Once no leakage was found the reactor was depressurized by opening the vent valve slowly again. However the pressure was not made zero to ensure that no air from the atmosphere enters the reactor again. The reactor was now pressurized with nitrogen well above the vapor pressure of the respective compounds at 425 C.

Following were pressures applied on different compounds for performing reactions in liquid phase

Hexadecane	250 psi
Quinoline in 1-Methylnaphtahlene	400 psi
Dihydroindole in 1-Methylnaphtahlene	400 psi

The reactor was again pressurized to the respective pressure and depressurized to purge out any traces of air in the reactor and provide complete inert atmosphere in the reactor during the course of the reaction. The purging step was repeated five times. Care was taken not to reduce the pressure to zero. Once the desired pressure was set, the needle

valve on the reactor iclosed. The reactor was now pressurized to the desired pressure and ready to be placed in the Sand Bath.

Reactor in Sand Bath

Micro batch reactor with the desired pressure was fixed on the vertical arm of the sand bath and tightened with Allen keys. The sand bath was already preheated to the desired temperature and airflow adjusted. The vertical arm containing the reactor was lifted with the help of lever connected to the horizontal arm and placed in the sand bath. Care was taken that the horizontal arm rests on the cam and the guide goes into the slot provided. Function of the guide is to keep the horizontal arm in place on the cam so that while agitating it does not fall down. Motor is switched on to start the agitation of the reactor. Reactor is agitated in a vertical up and down motion.

Once the reaction was completed after 60 minutes the reactor was removed from the sand bath by lifting the lever attached to the horizontal arm and placing it outside the sand bath.

During the process of cooling the reactor was held from the long tubing attached to the top cap and very slowly rotated and also moved axially. It usually takes 3 to 4 minutes for the reactor to reach room temperature.

After venting the gas, the reactor was fixed on the bench vice horizontally with the top cap held in place and the nut of the main body loosened with a wrench slightly. The reactor was placed vertically on the vice with the bottom cap held in place and using two wrenches with the top cap held, the main body nut is loosened. This was done because there was a possibility of the product spillage if joint is loosened more in the horizontal

position. The product was carefully decanted in the vial. Transfer of clear liquid from the vial to the reactor and vice versa was repeated until almost the whole of the catalyst was recovered. The product was centrifuged in a micro centrifuge to recover the catalyst. The liquid product was analyzed in the gas chromatograph and catalyst washed with toluene dried in a vacuum oven and again washed with heptane or pentane to remove any aromatic compounds on the surface. Catalyst was reused or sent for the surface and elemental analysis

A.4 Mass Balance Data of Dihydroindole reaction with Chabazite at 325 °C (Error Test)

	(Grams)
1) Weight of the reactor	533.77
2) Weight of the reactor without cap	174.24
3) **Weight of dihydroindole and 1-methylnaphthalene solution**	**3.023**
4) **Weight of the Catalyst**	**0.3006**
5) Weight of the reactor w/o cap + Solution + Catalyst	177.57
6) Weight of the loaded reactor	537.09
7) Weight of the loaded reactor + nitrogen	537.57
8) **Weight of nitrogen**	**0.48**
9) Weight of the loaded reactor after reaction	537.56
10) Weight of the reactor after gas release	537.03
11) **Mass of gas**	**0.54**
12) Weight of Vial	27.3071
13) Weight of Vial + liquid product	30.0607
14) **Weight of liquid product**	**2.7536**
15) Mass of Petri dish	88.81
16) Mass of Petri dish + Catalyst	89.0654
17) **Mass of Catalyst recovered**	**0.2554**

Appendix B

Gas Chromatogram Results

This appendix details the chromatogram results of pure solvents and model compounds to find the retention time for calibration and the concentration or area percent after reacting thermally and in the presence of catalyst. Area percent from the GC analysis was used to calculate the conversions after the reaction and the mass % at a particular temperature. Results have been re-integrated on a different computer so there would be minor difference in the retention times on the report and the graphs shown.

In some cases internal standard have were used to calculate the conversion. Internal standard are introduced in the fresh and the reacted sample just before doing the gas chromatography. For the conversion calculations area percent of the model compound (A_{MC}) is divided by the area percent of the internal standard (A_{IS}) to find the area ratio (AR)

Therefore AR (Before Reaction) = A_{MC} / A_{IS}

AR (After Reaction) = A_{MC} / A_{IS}

Conversion % = $((AR_{(Before\ Reaction)} - AR_{(After\ Reaction)}) / AR_{(Before\ Reaction)}) * 100$

Calculations of conversion % for sample without internal standards are

($(A_{MC}$ % (before reaction) – A_{MC} % (after reaction)) / A_{MC} % (before reaction)) *100

Determining dihydroindole mass % at a particular temperature =

($(A_{MC}$ % (After Reaction) / A_{MC} (Before reaction))* Initial mass % of dihydroindole in fresh solution

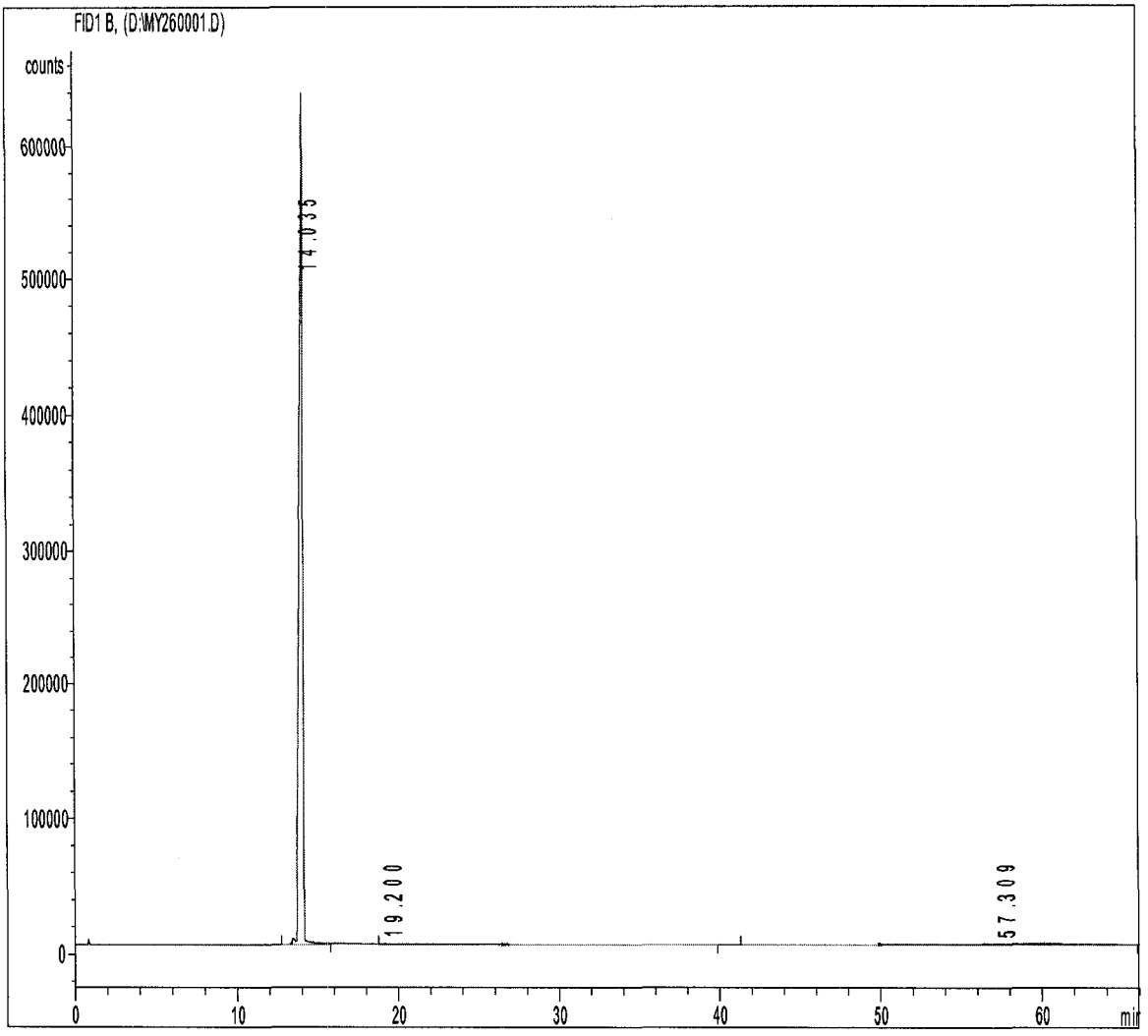

Figure B.01 Gas chromatogram of 1-Methylnaphyhalene

Analysis of pure 1-methylnphthalene shows retention time of 14.03 min

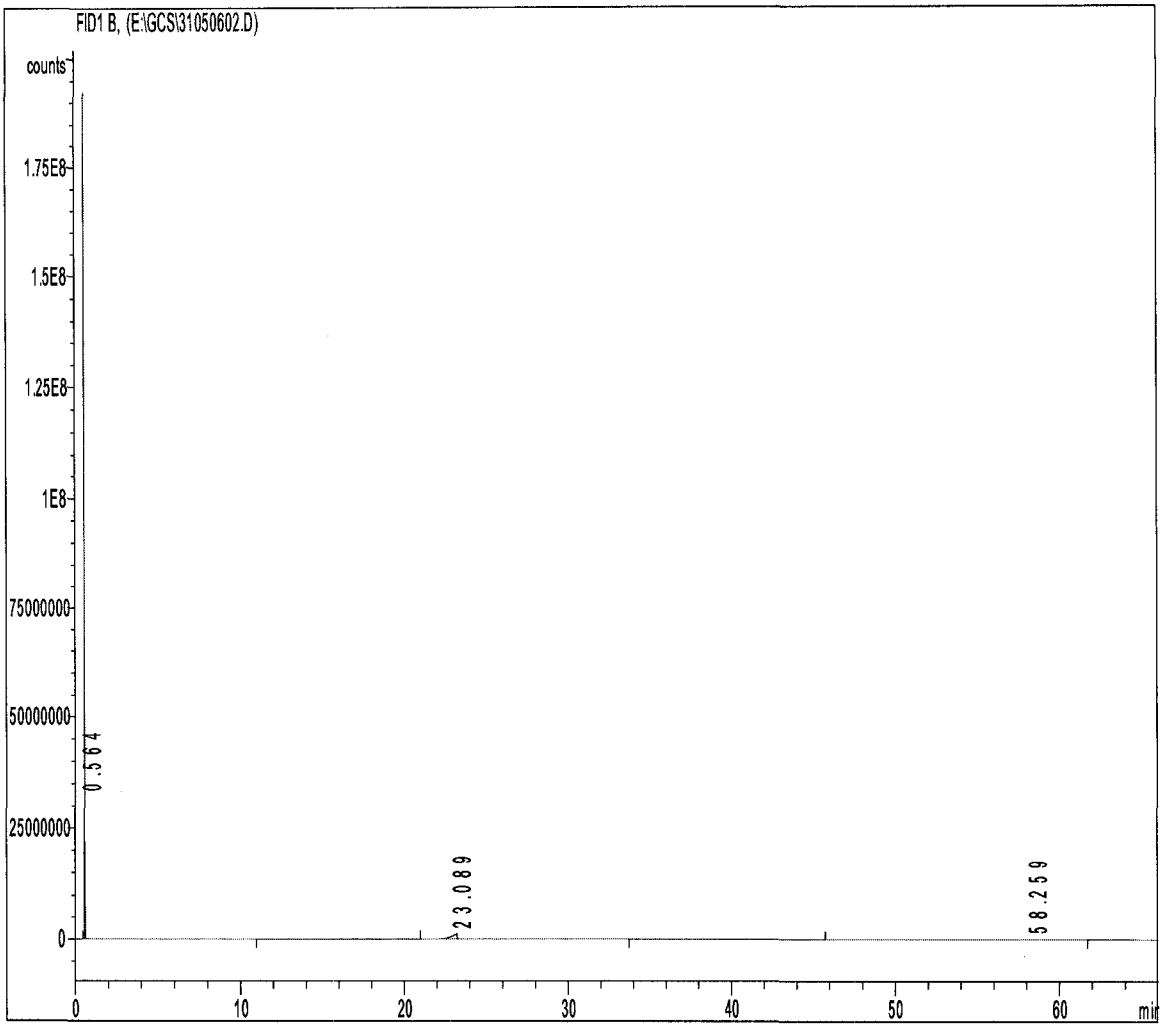

Figure B.02 Gas Chromatogram of n-Pentane

Analysis of pure pentane shows retention time of 0.56 minutes

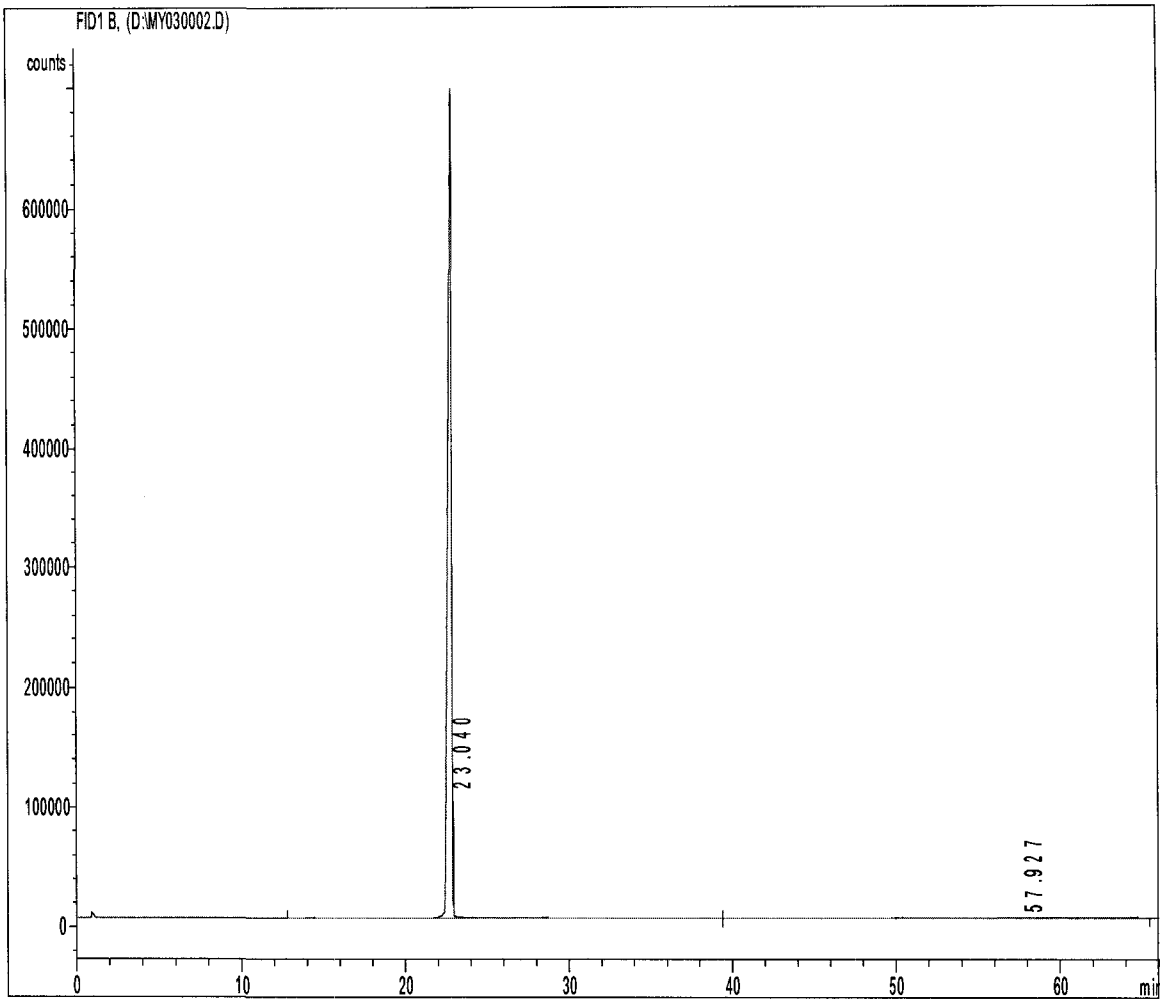

Figure B.03 Gas chromatogram of n-Hexadecane

Analysis of pure n-hexadecane shows retention time of 23.04 minutes

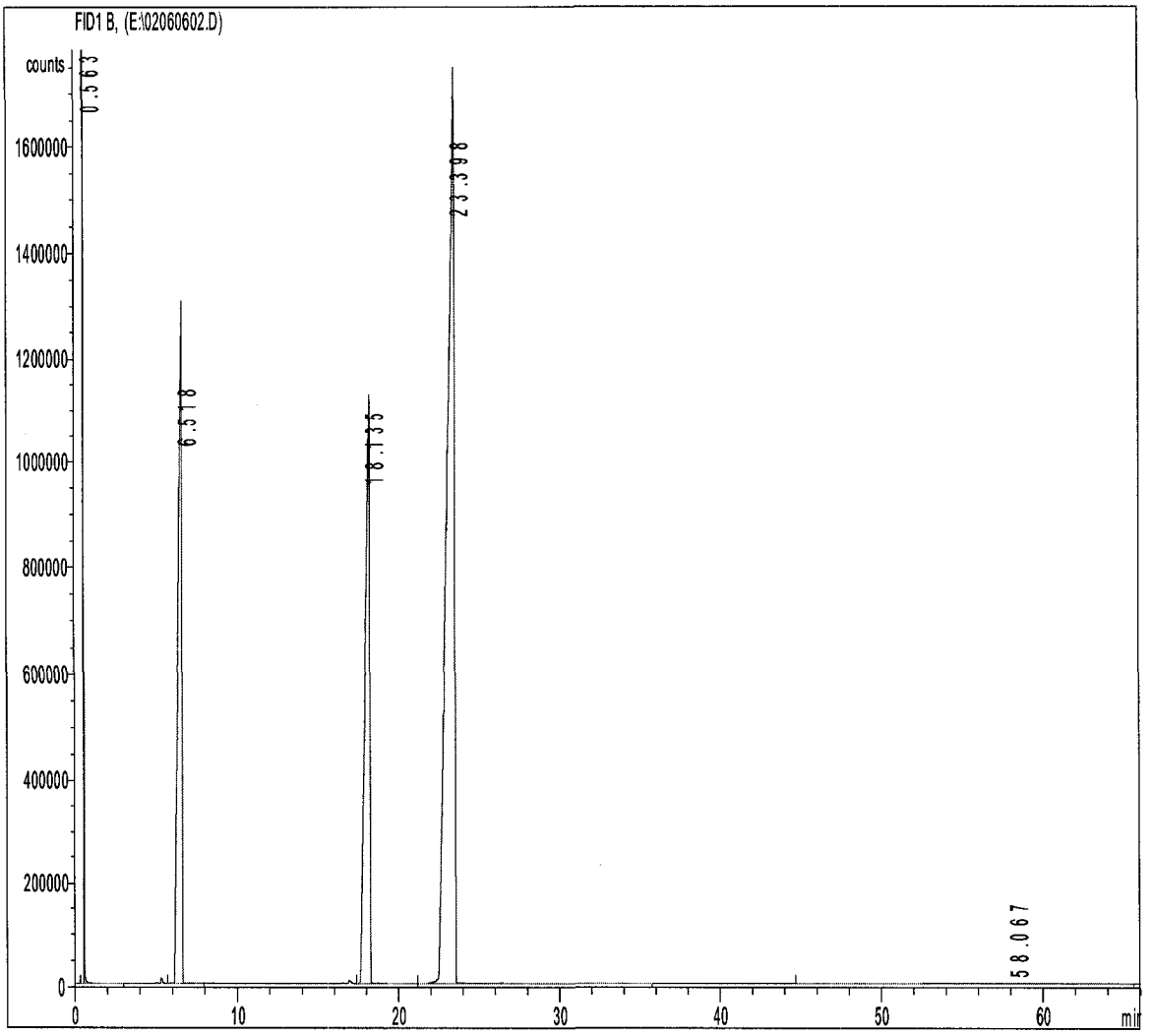

Figure B.04 Gas chromatogram of Decane

A mixture of alkanes was mixed and analyzed in the gas chromatograph. The mixture consisted of pentane, decane, tetradecane and hexadecane.

Retention time of decane from the analysis is 6.51 minutes

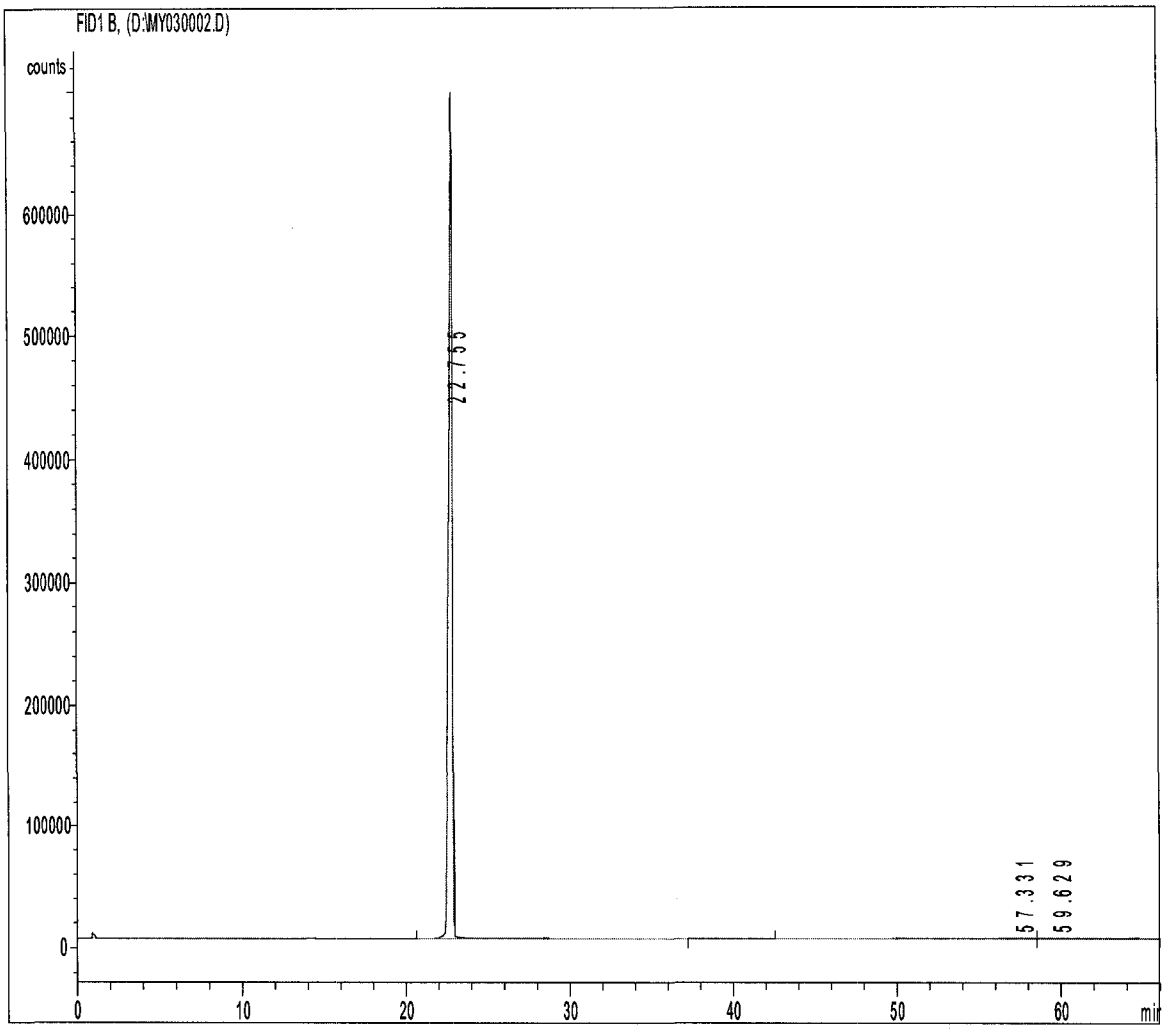

Figure B.05 GC of Pure n-Hexadecane without Internal Standard

Total area is 1.07152e7 area counts * s. Area of hexadecane is 1.06092e7. Therefore area percent of n-hexadecane is 99.01

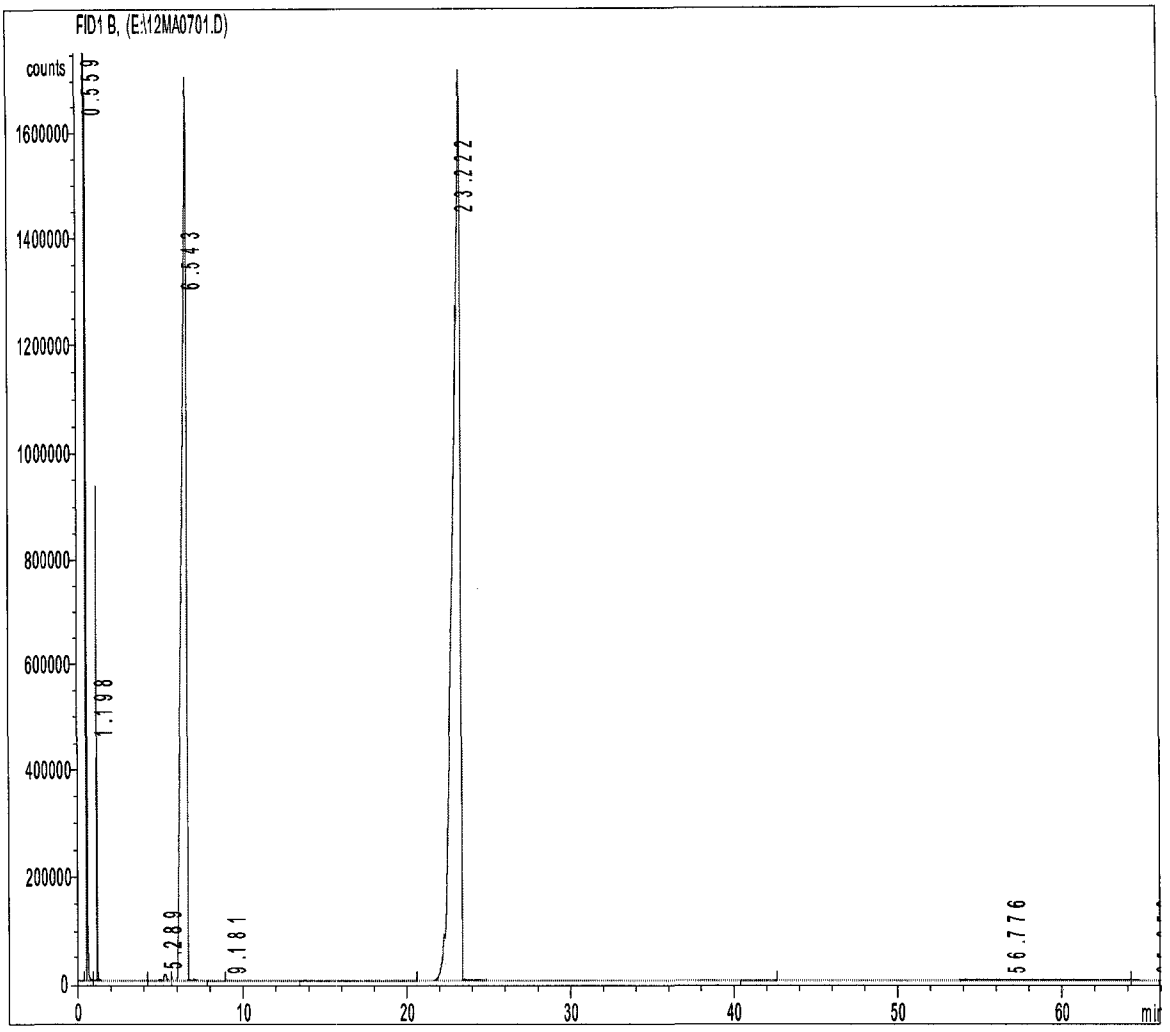

Figure B.06 Gas Chromatogram of n-Hexadecane with Internal Standard

Solution was prepared containing 2 mL of pentane, 0.2 mL of decane, 0.3 mL of n-hexadecane and analyzed in the gas chromatograph.

Total area was 4.83262e8. Area of n-hexadecane was 5.27109e7 and that of decane was 3.23169e7. Area percent of n-hexadecane and decane are 10.90731 and 6.68724 respectively. Area hexadecane/decane is 1.63

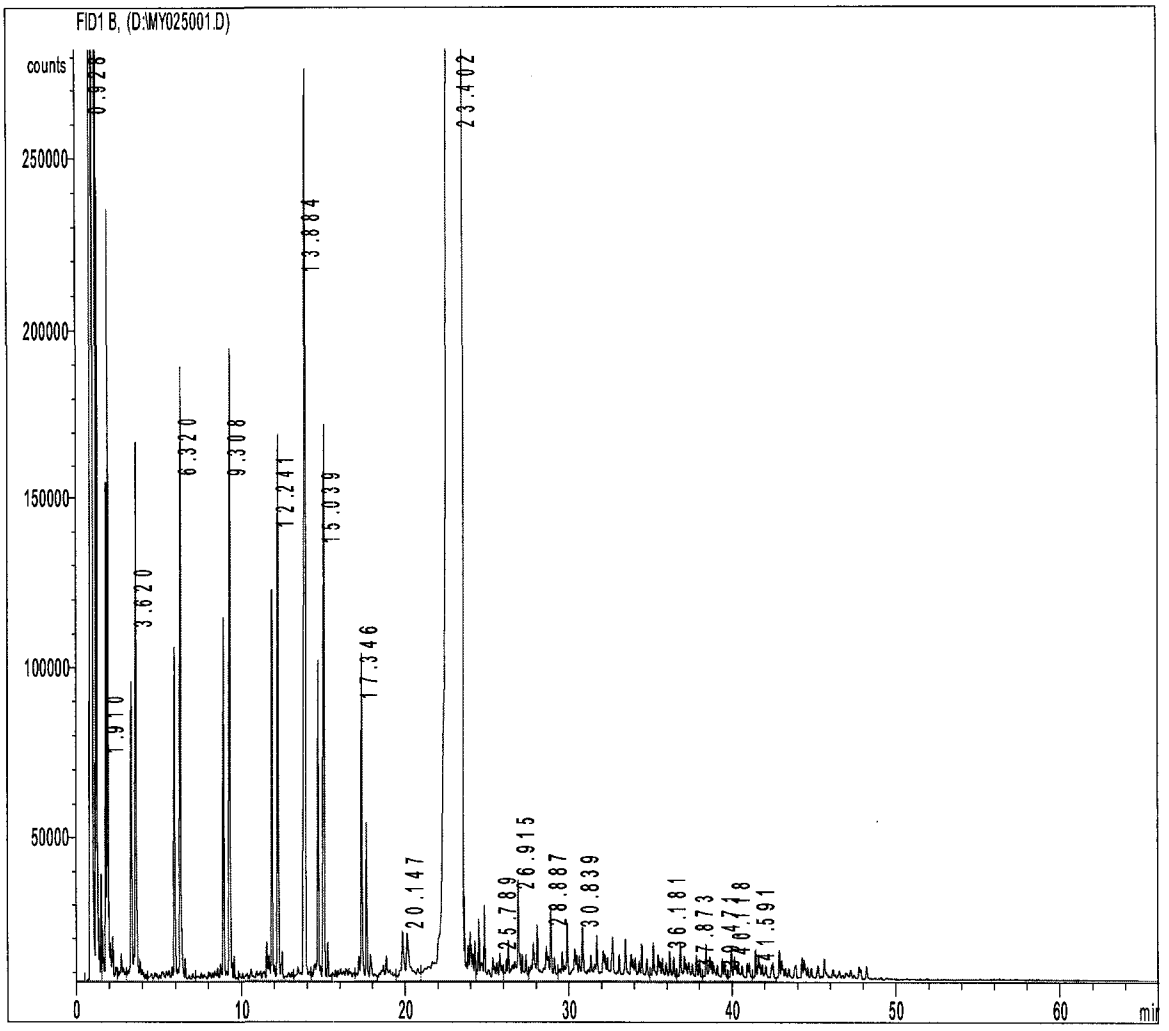

Figure B.07 Gas Chromatogram of Thermal Cracked n-Hexadecane

Total areas of the peaks were 1.01026e8 counts*s. Area of n-hexadecane peak was 6.54910e7 counts*s. Area percent of n-hexadecane was 64.82593. Therefore percent conversion is ((99.01095-64.82593)/ 99.01095) * 100 = 34.52

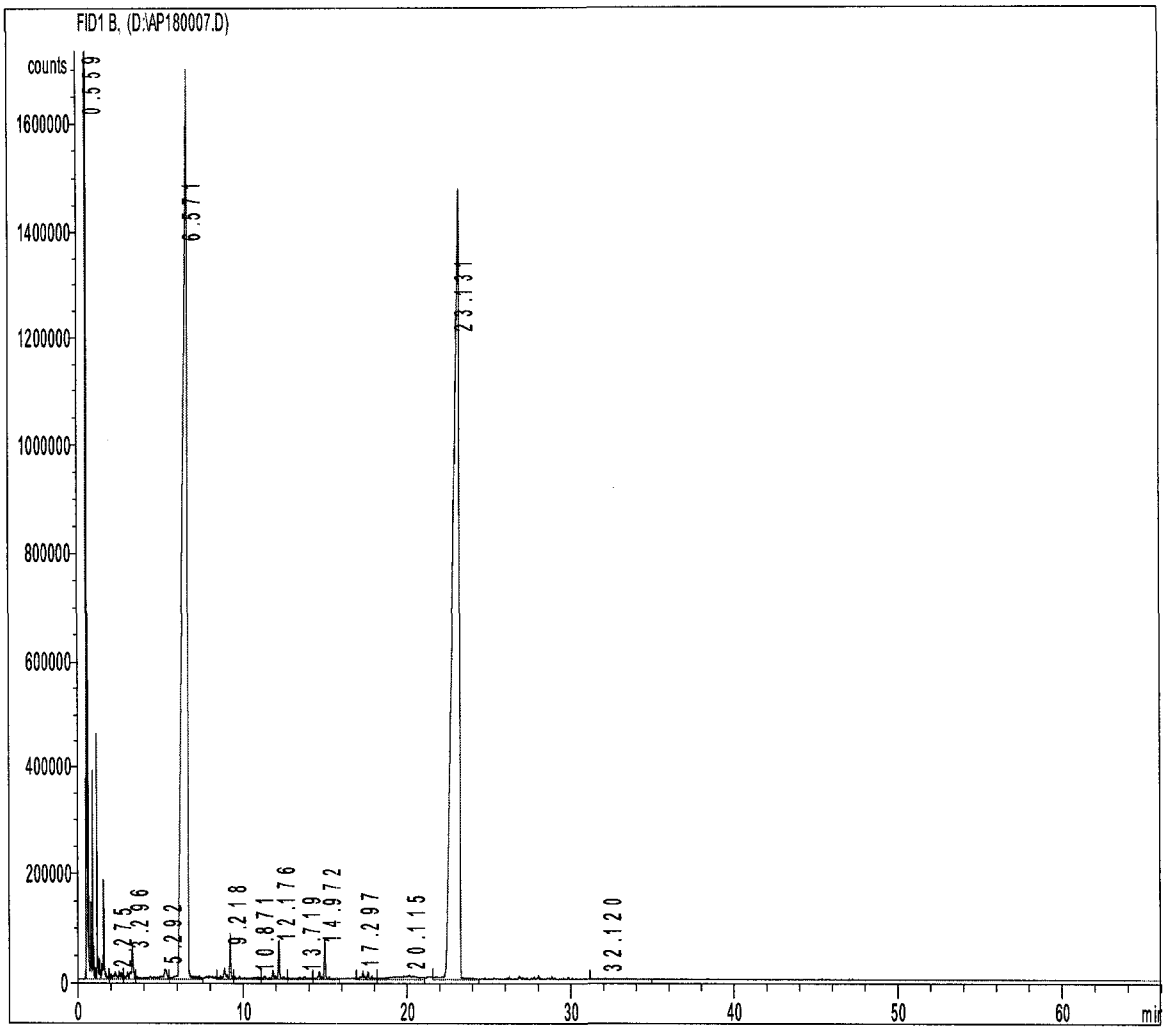

Figure B.08 Gas Chromatogram of n-Hexadecane Cracking with Clinptilolite at 425°C

Solution was prepared containing 2 mL of pentane, 0.2 mL of decane, 0.3 mL of cracked n-hexadecane and analyzed in the gas chromatograph.

Total areas of the peaks are 3.45807e8 counts*s. Area of n-hexadecane was 3.92371e7 counts*s and that of decane was 3.27259e7 counts*s. Area percent of n-hexadecane and decane are 11.34693 and 9.46395 respectively. Area hexadecane /decane is 1.19. Therefore percent conversion is ((1.63106-1.19896)/1.63106)*100 = 26.49

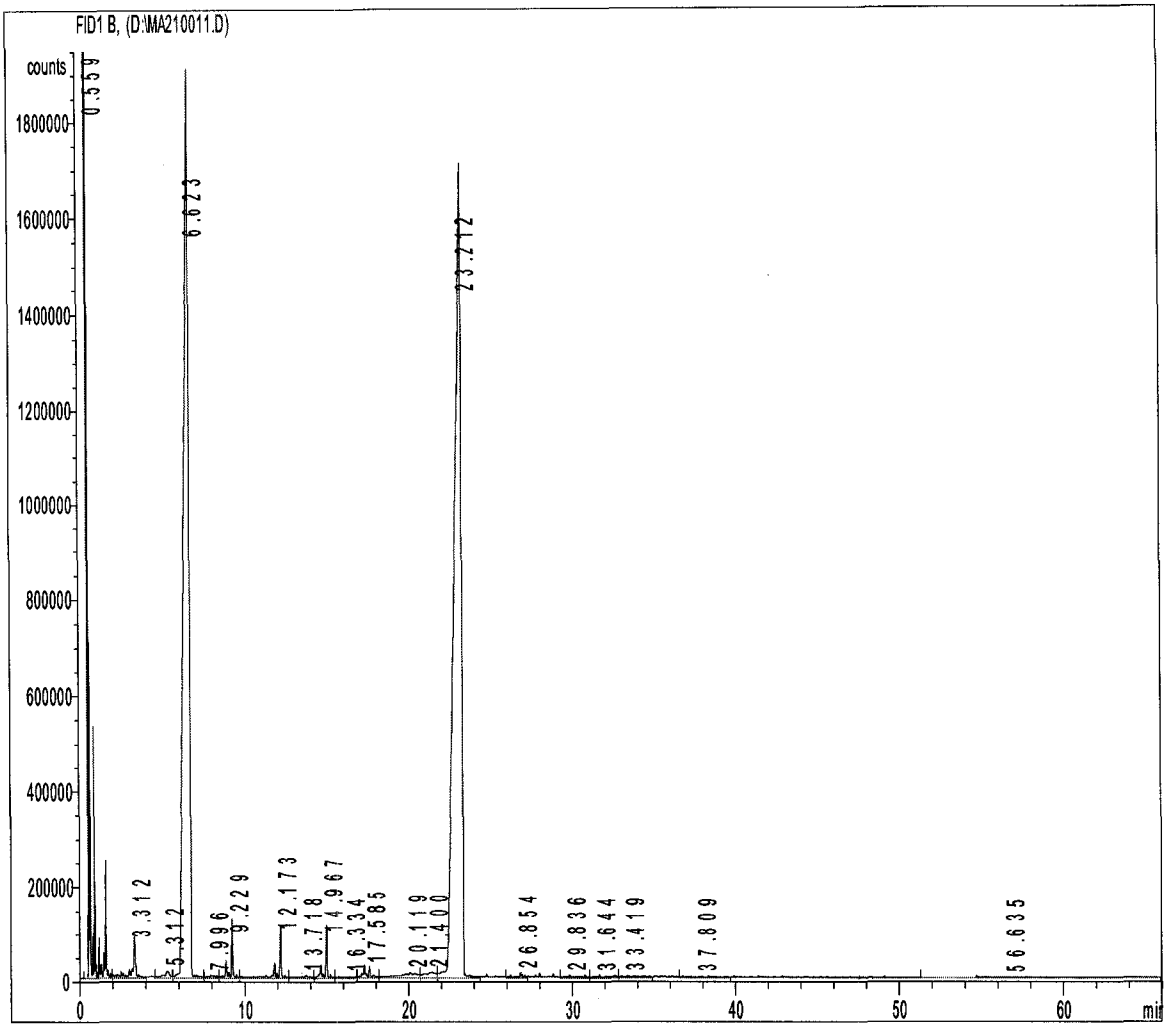

Figure B.09 Gas Chromatogram of n-Hexadecane Cracking with Zeolite-Y at 425°C

Solution was prepared containing 2 mL of pentane, 0.2 mL of decane, 0.3 mL of cracked n-hexadecane and analyzed in the gas chromatograph.

Total areas of the peaks are 3.45807e8 counts*s. Area of n-hexadecane is 4.97241e7 counts*s and that of decane was 4.00718e7 counts*s. Area percent of n-hexadecane and decane are 11.18 and 9.01 respectively. Area hexadecane /decane is 1.24. Therefore percent conversion is ((1.63-1.24) /1.63)*100 = 23.92

Pure DBT GC analysis

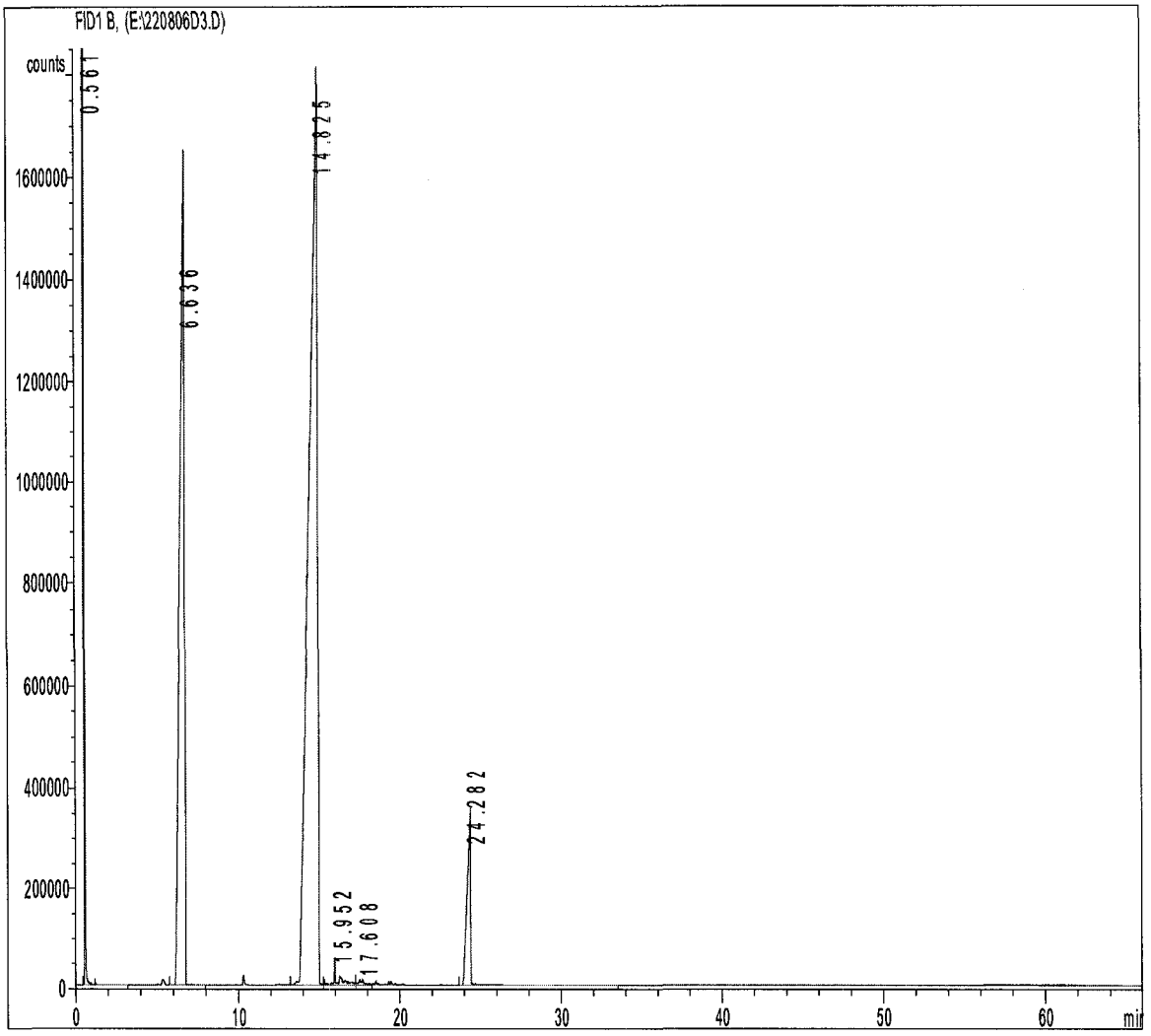

Figure B.10 Gas Chromatogram of Dibenzothiophene

Analysis shows the retention time of dibenzothiophene at 24.39 minutes.

Solution was prepared containing 2 mL of pentane, 0.2 mL of decane, 0.25 mL of 10 mass % solution of dibenzothiophene in 1- methylnaphthalene and analyzed in the gas chromatograph. Total areas of the peaks are 4.01883e8. Area of Dibenzothiophene is 5.19542e6 and that of decane is 3.13482e7. Area percent of dibenzothiophene and decane are 1.29277 and 7.80032. Area dibenzothiophene/decane is 0.16

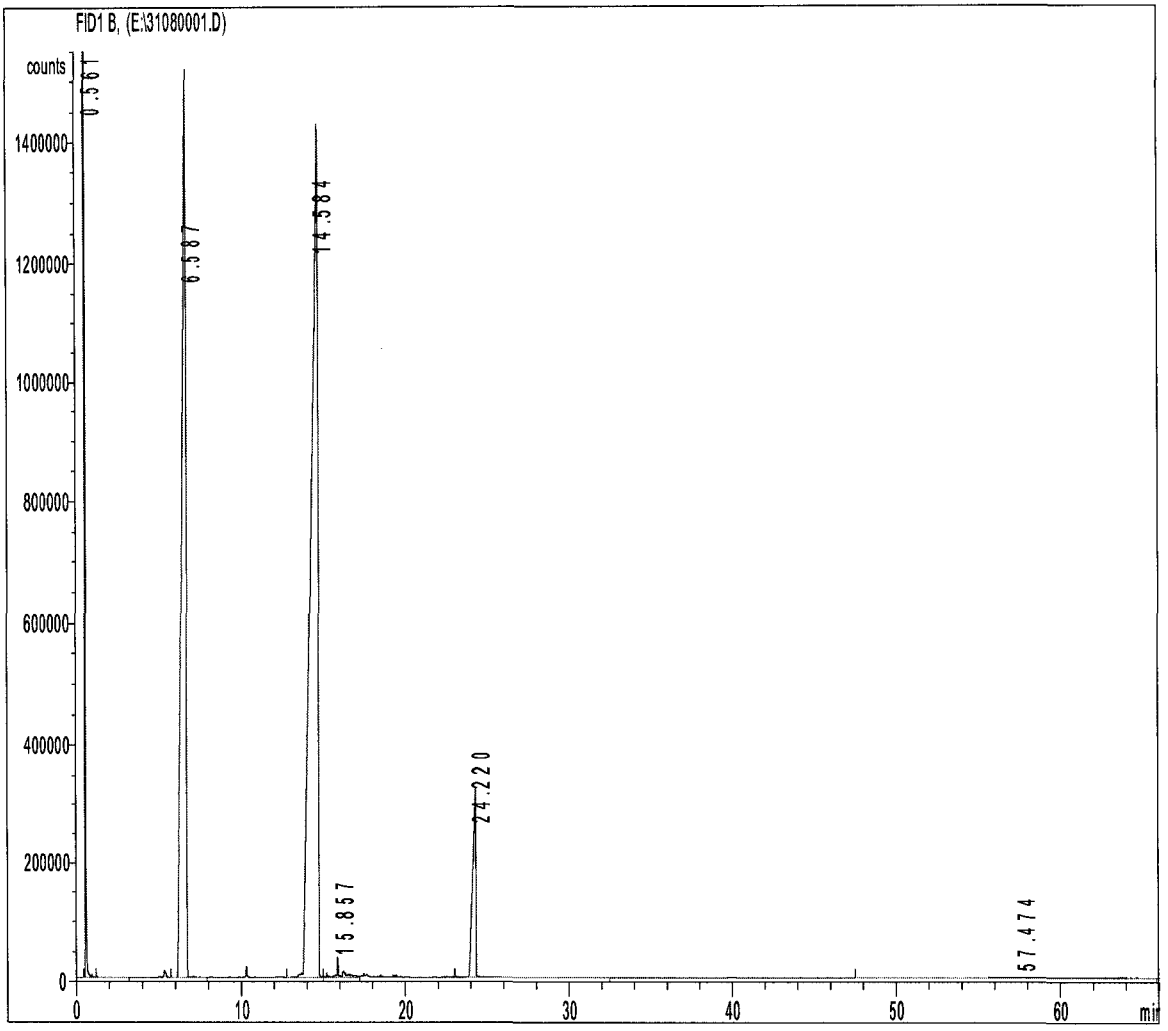

Figure B.11 Gas Chromatogram of Dibenzothiophene Thermally Reacted at 425°C

Solution was prepared containing 2 mL of pentane, 0.2 mL of decane, 0.25 mL of reacted dibenzothiophene and 1- methylnaphthalene solution.

Total areas of the peaks are 3.57455e8 counts*s. Area of dibenzothiophene is 4.27895e6 counts*s and that of decane is 2.62226e7 counts*s. Area percent of dibenzothiophene and decane are 1.19 and 7.33 respectively. Area dibenzothiophene /decane is 0.16.

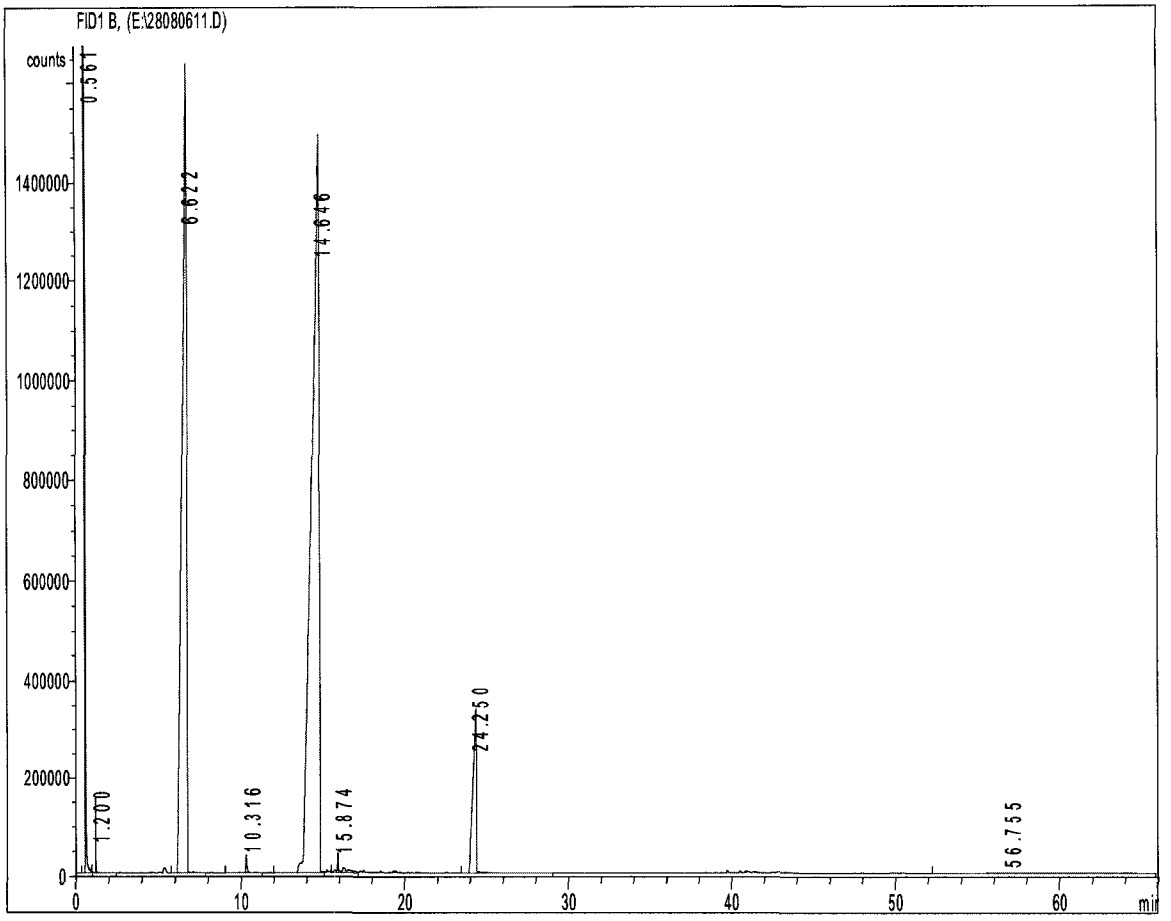

Figure B.12 Gas Chromatogram of Dibenzothiophene Reacted with Modified Chabazite at 425°C

Solution was prepared containing 2 mL of pentane, 0.2 mL of decane, 0.25 mL of reacted dibenzothiophene and 1- methylnaphthalene solution with modified chabazite..

Total areas of the peaks are 3.79974e8 counts*s. Area of dibenzothiophene is 4.68141e6 counts*s and that of decane is 3.03976e7 counts*s. Area percent of dibenzothiophene and decane are 1.23 and 7.99 respectively. Area dibenzothiophene /decane is 0.15.

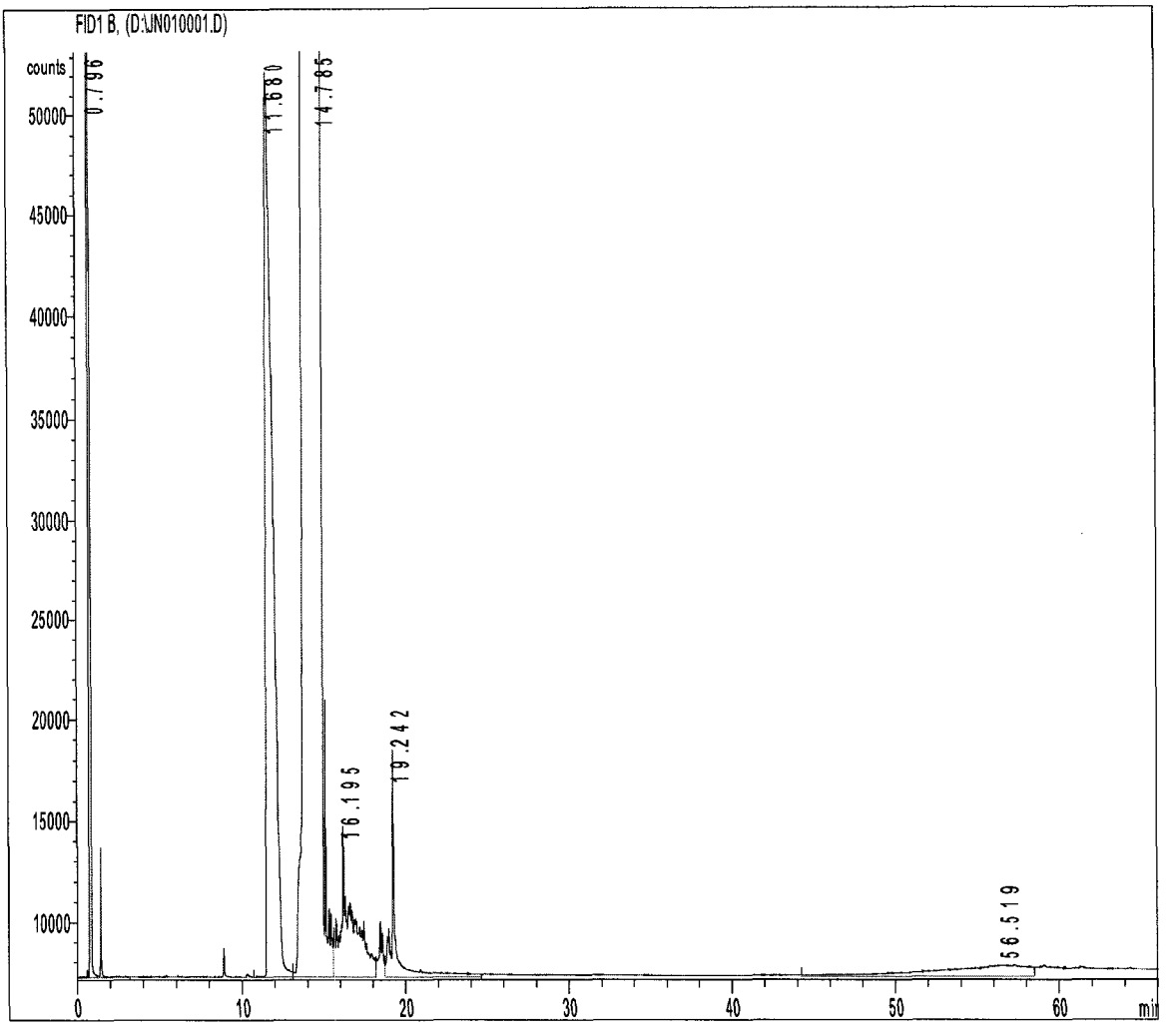

Figure B.13 Gas Chromatogram of Quinoline in 1-Methylnaphthalene Solution

0.25 mass percent concentration solution of quinoline in 1-methylnaphthalene is prepared and analyzed in a gas chromatograph. As per the analysis quinoline peaks appears at retention time of 11.680 minutes. Total areas of the peaks are 7.05392e7 counts*s and the area of quinoline is 1.38200e6 counts*s. Therefore the area percent of quinoline is (1.38200e6 /7.05392e7)*100 = 1.95.

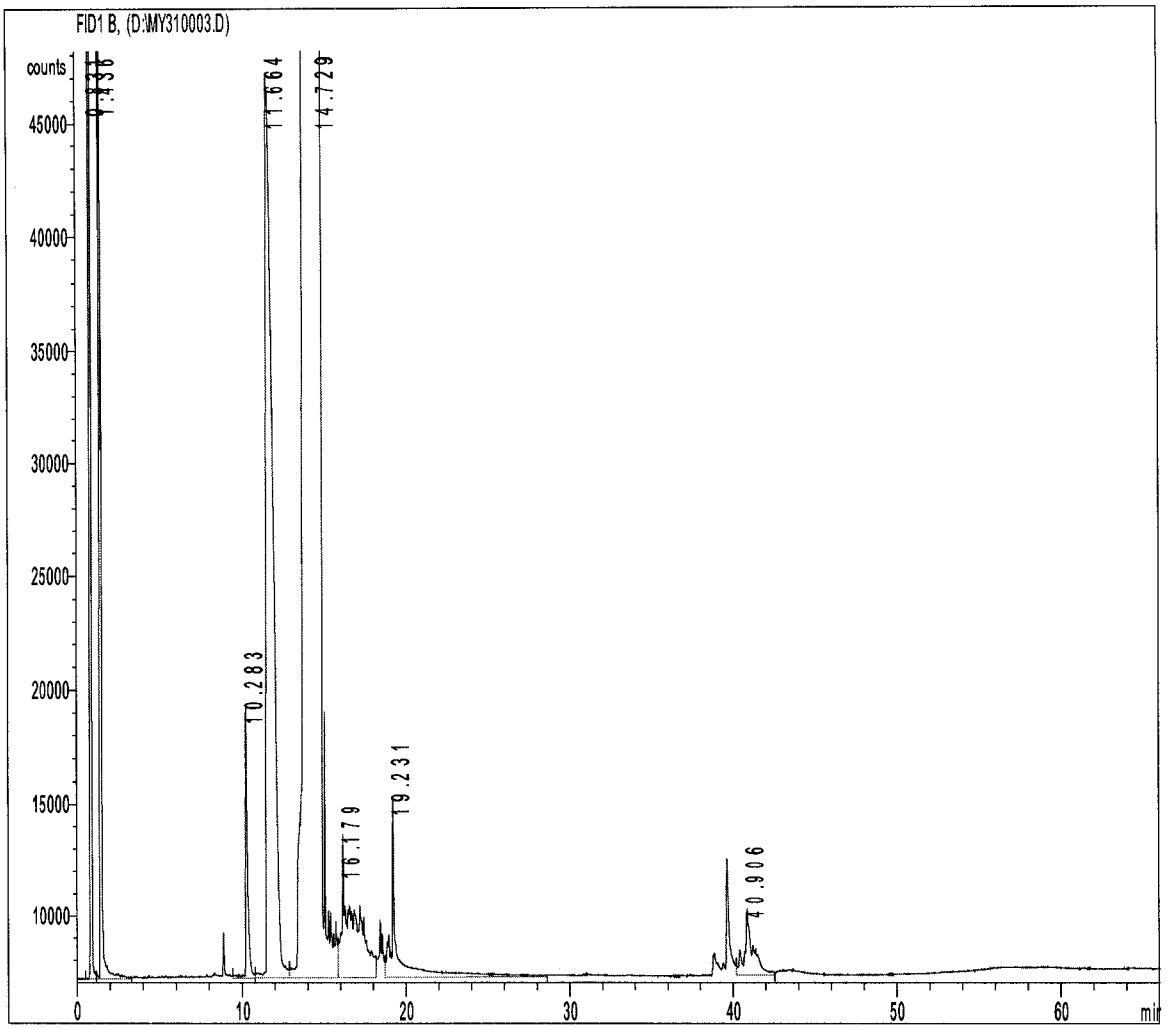

Figure B.14 Gas Chromatogram of Quinoline in 1-Methylnaphthalene Solution reacted with Clinoptilolite at 425°C

Total areas of the peaks are 6.74203e7 counts*s. Area of quinoline is 1.16006e6. Therefore area percent of quinoline is 1.16006e6 / 6.74203e7 = 1.72 and the conversion is ((1.95-1.72)/1.95)*100 = 12.17 %

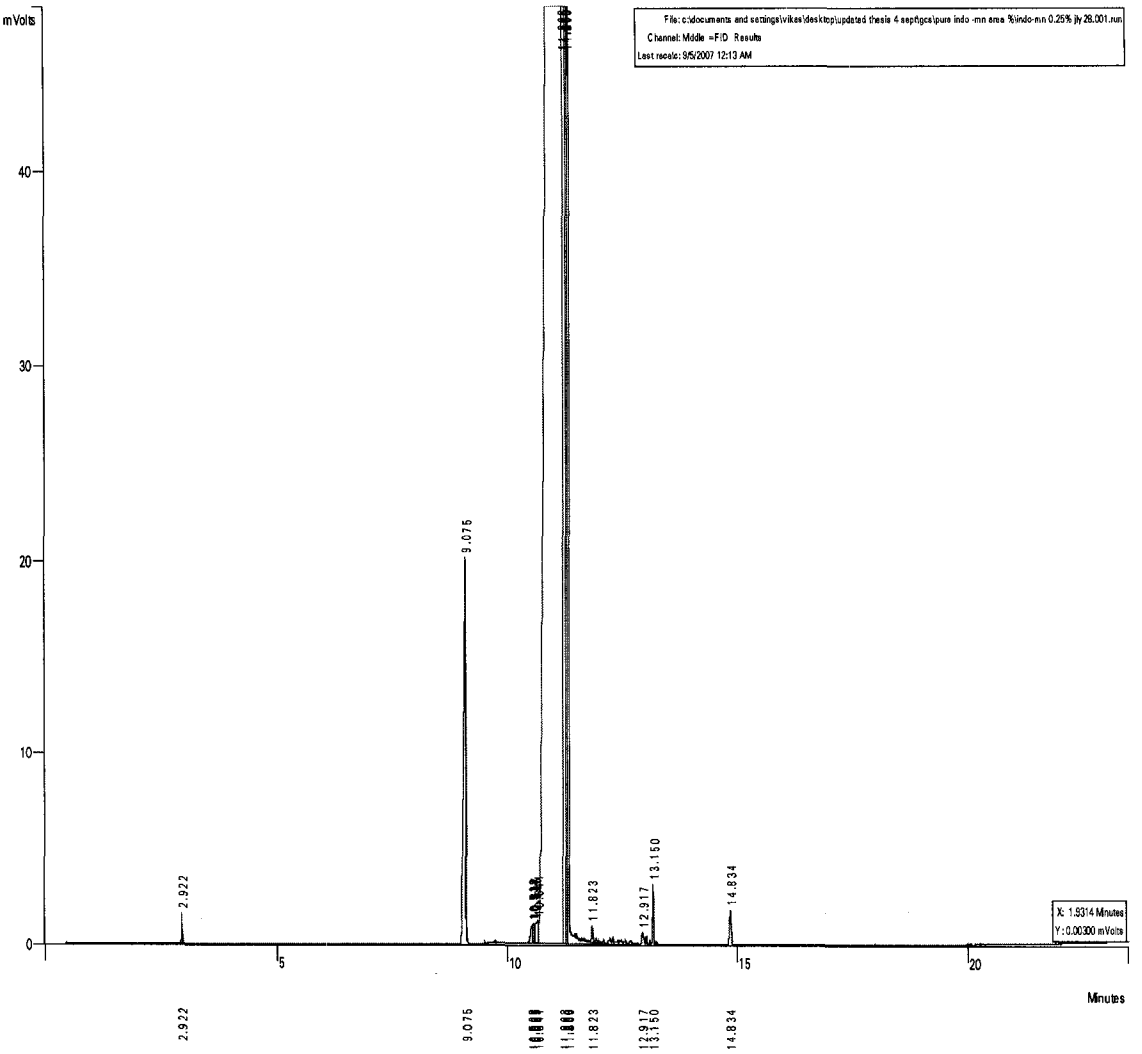

Figure B.15 Gas Chromatogram of Dihydroindole in 1-Methylnaphthalene Solution

0.25 mass percent concentration solution of dihydroindole in 1-methylnaphthalene is prepared and analyzed in a gas chromatograph. As per the analysis dihydroindole peaks appears at retention time of 9.07 minutes. Total areas of the peaks are 4374437 counts and the area of dihydroindole is 71041 counts. Therefore the area percent of dihydroindole is (71041/ /4374437)*100 = 1.61. Initial concentration of dihydroindole at 0.249 % nitrogen concentration is 2.11 mass %

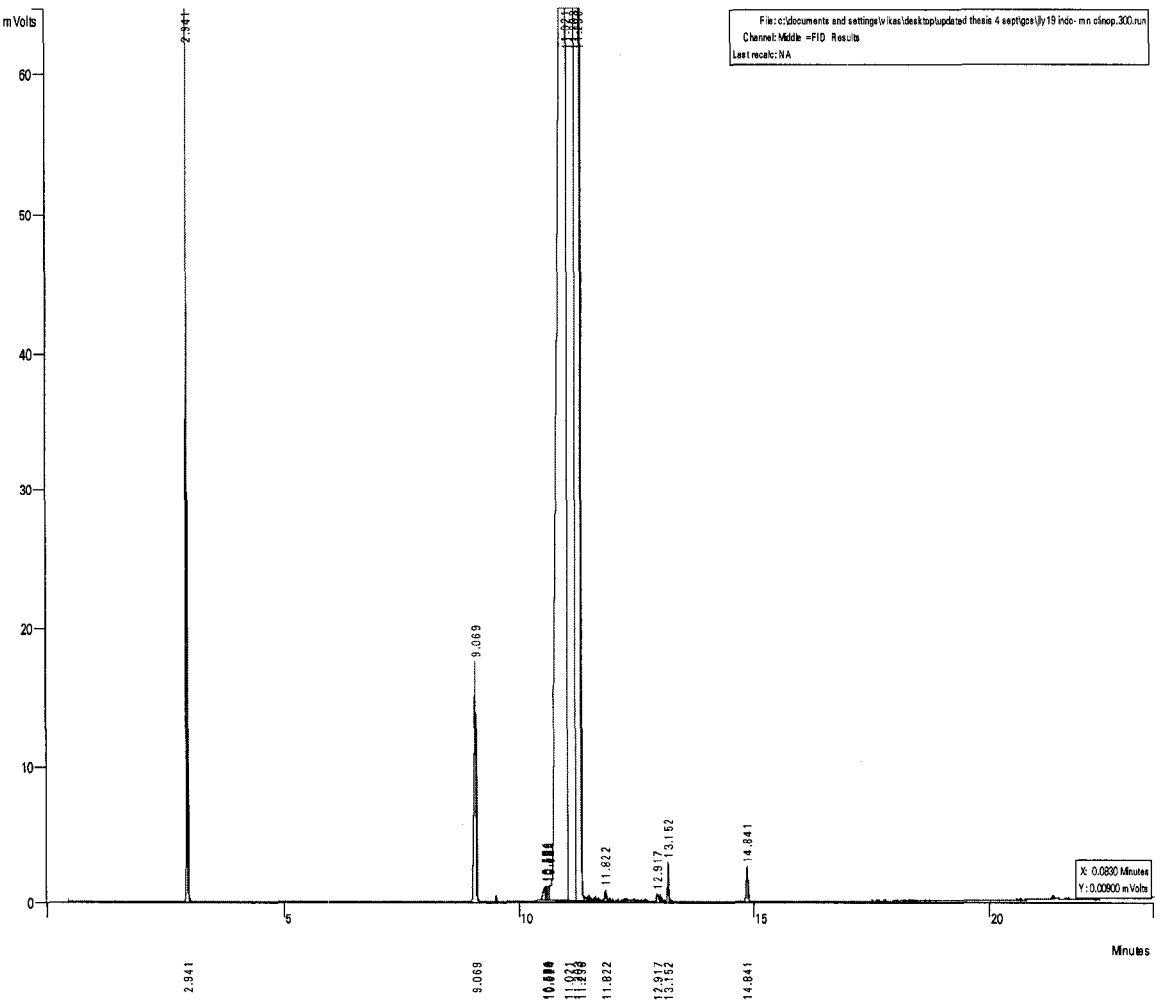

Figure B.16 Gas Chromatogram of Dihydroindole in 1-Methylnaphthalene Solution Reacted with Clinoptilolite at 300°C

Total areas of the peaks are 4203040 counts. Area of dihydroindole is 55629 counts. Therefore area percent of dihydroindole is 55629/ 4203040= 1.32 and the conversion is ((1.6137-1.3235)/1.6240)*100 = 17.98 %. And mass % of dihydroindole at 300°C is (1.32/1.61)* 2.11 = 1.73

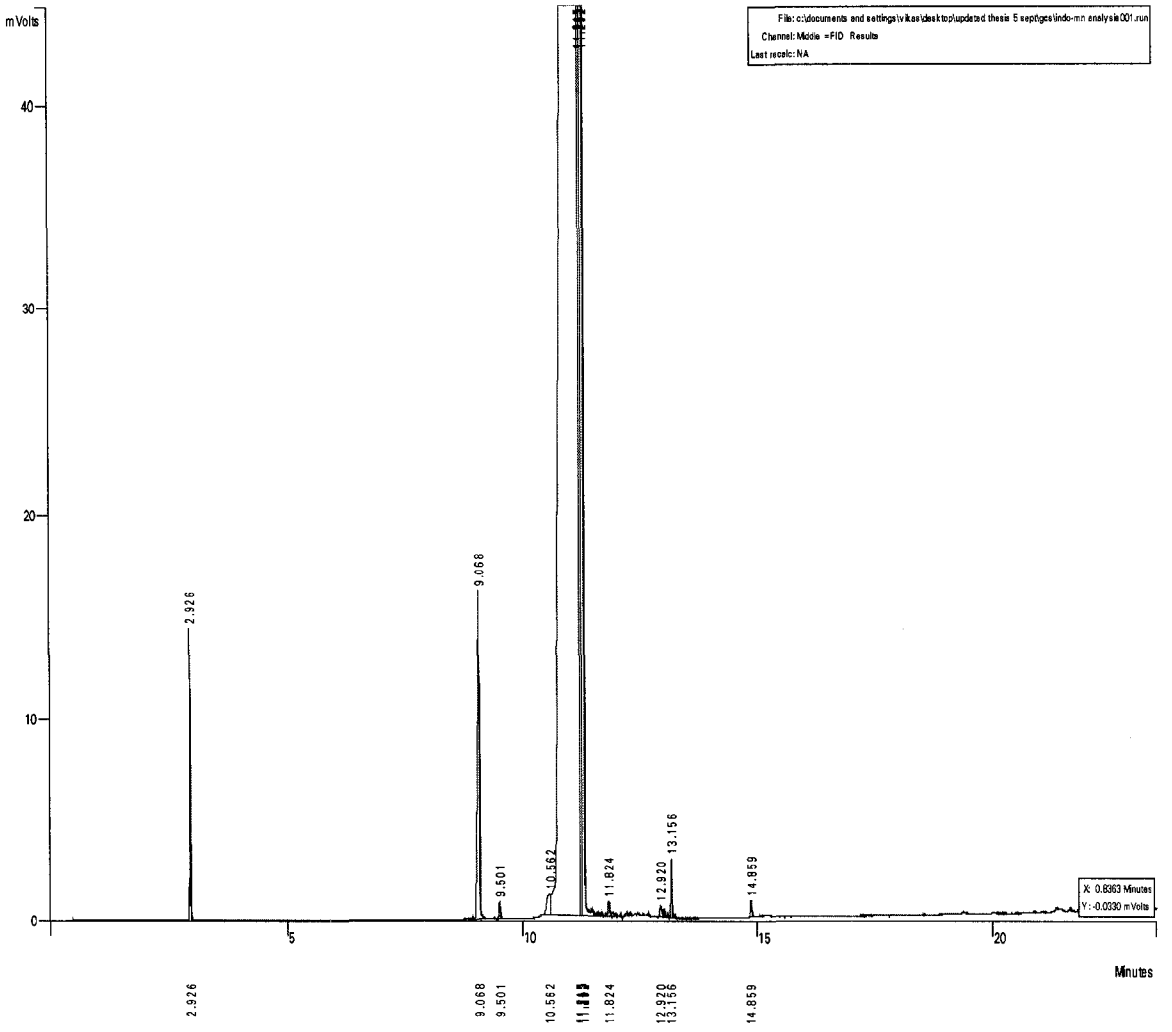

Figure B.17 Gas Chromatogram of Dihydroindole in 1-Methylnaphthalene Solution Reacted with Clinoptilolite at 325°C

Total areas of the peaks are 3954185 counts. Area of dihydroindole is 49139 counts. Therefore area percent of dihydroindole is 49139/ 3954185 = 1.24 and the conversion is ((1.61-1.24)/1.61)*100 = 22.99 % and the mass percent of dihydroindole at 325°C (1.24/1.61)*2.11 = 1.63

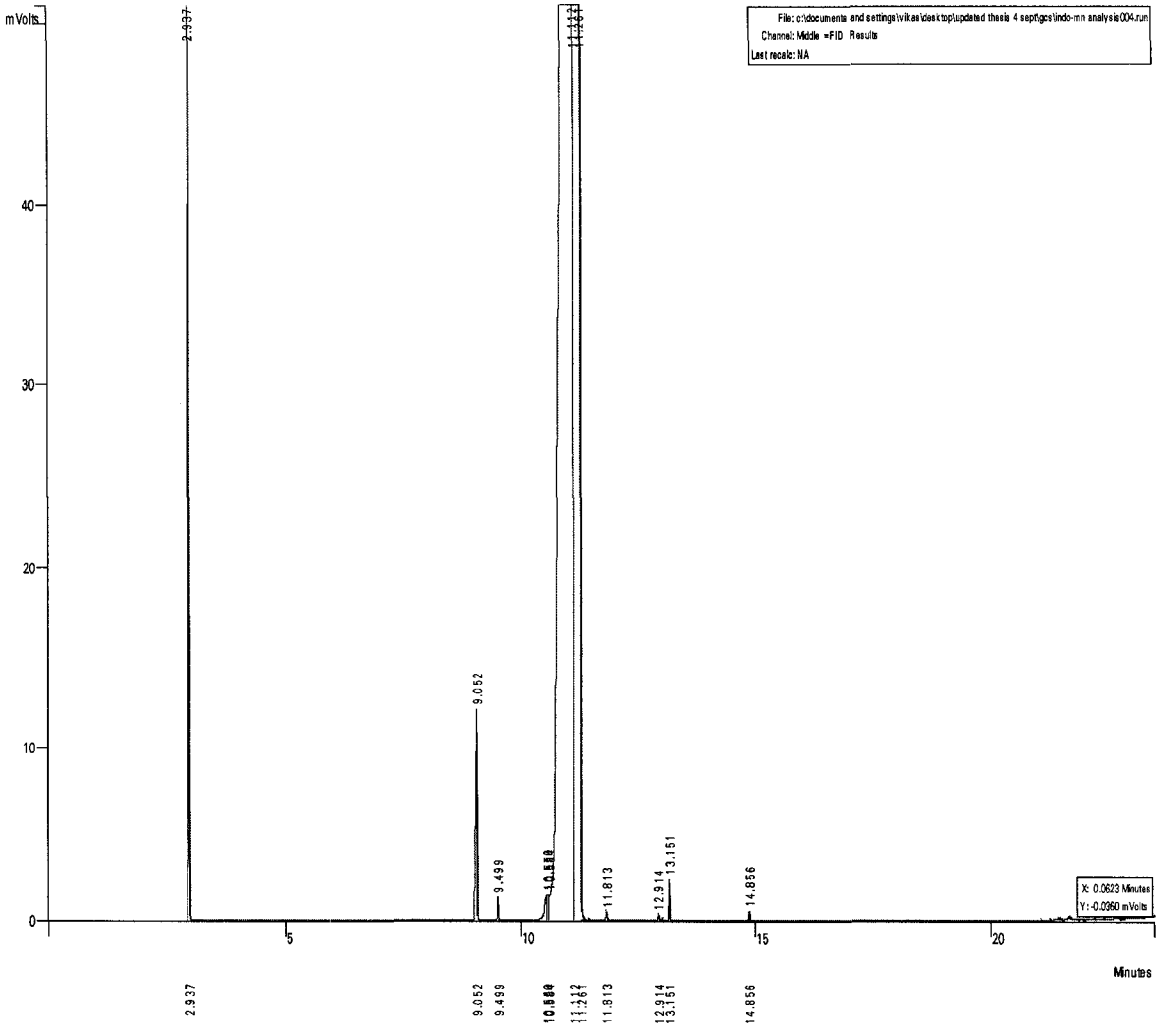

Figure B.18 Gas Chromatogram of Dihydroindole in 1-Methylnaphthalene Solution Reacted with Clinoptilolite at 350°C

Total areas of the peaks are 3638280 counts. Area of dihydroindole is 31658 counts. Therefore area percent of dihydroindole is 31658/ 3638280 = 0.8701 and the conversion is ((1.6137-0.8701)/1.6137)*100 = 46.08 %. Mass percent of dihydroindole at 350°C is (0.87/1.61)*2.11 = 1.14

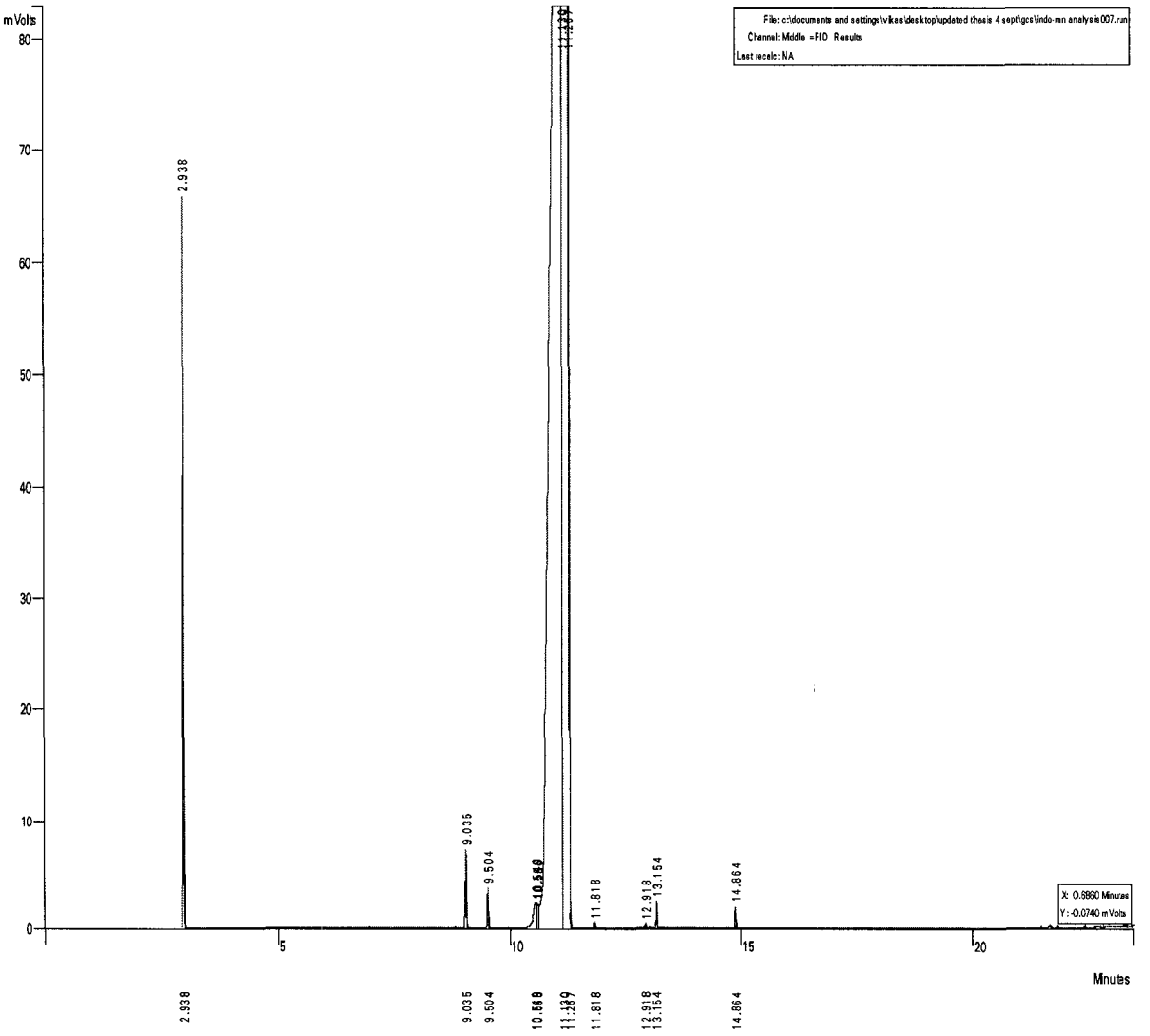

Figure B.19 Gas Chromatogram of Dihydroindole in 1-Methylnaphthalene Solution Reacted with Clinoptilolite at 375°C

Total areas of the peaks are 3688201 counts. Area of dihydroindole is 16114 counts. Therefore area percent of dihydroindole is 16114 / 3688201 = 0.43 and the conversion is ((1.61-0.43)/1.6137)*100 = 72.92 % and the mass % of dihydroindole at 375°C is (0.44/1.61)*2.1165 = 0.57

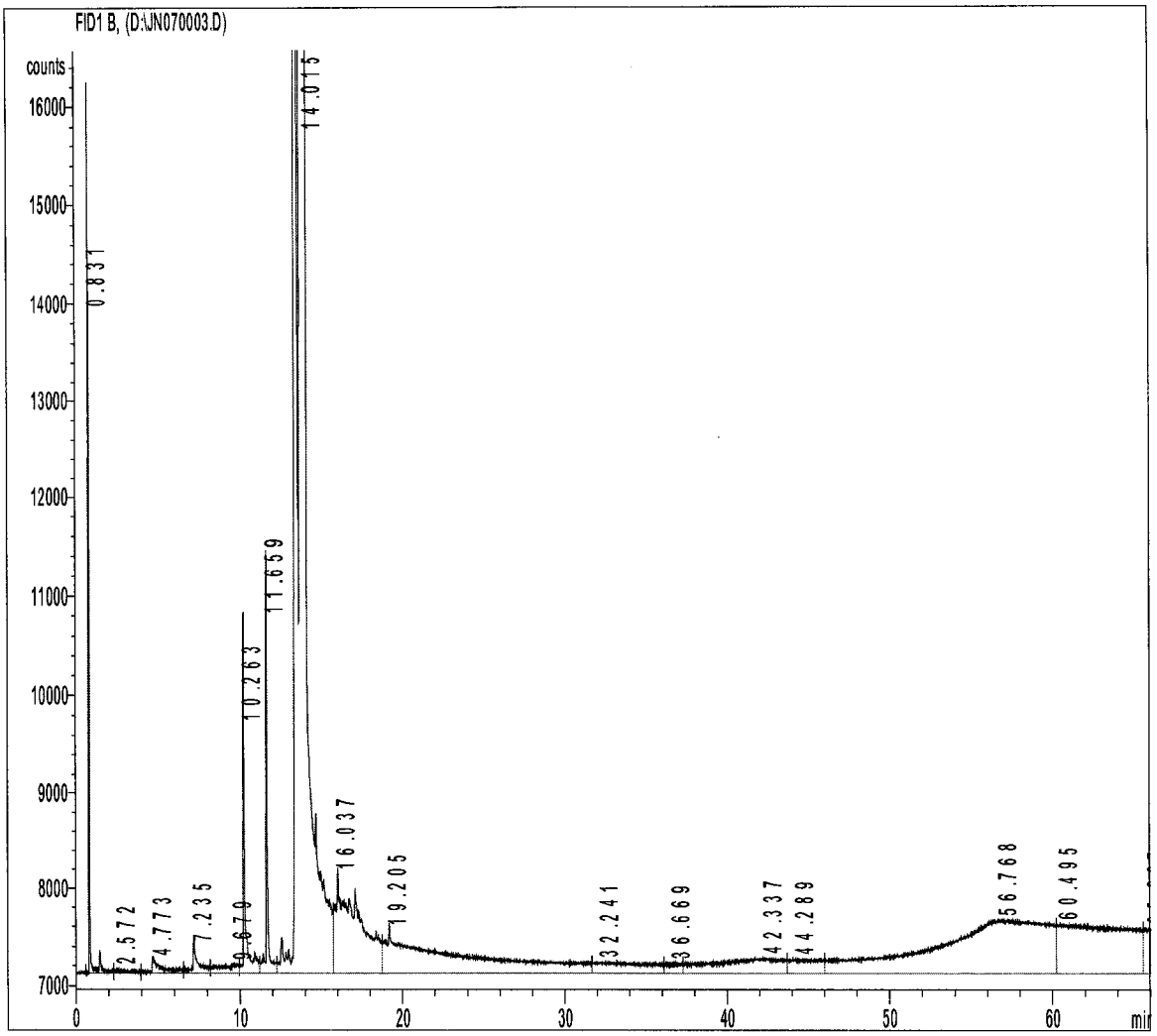

Figure B.20 Gas Chromatogram of Dihydroindole in 1-Methylnaphthalene Solution Reacted with Clinoptilolite at 425°C

GC analysis of 0.25 mass percent solution of dihydroindole in 1-methylnaphthalene showing complete elimination of dihydroindole peak at 425°C

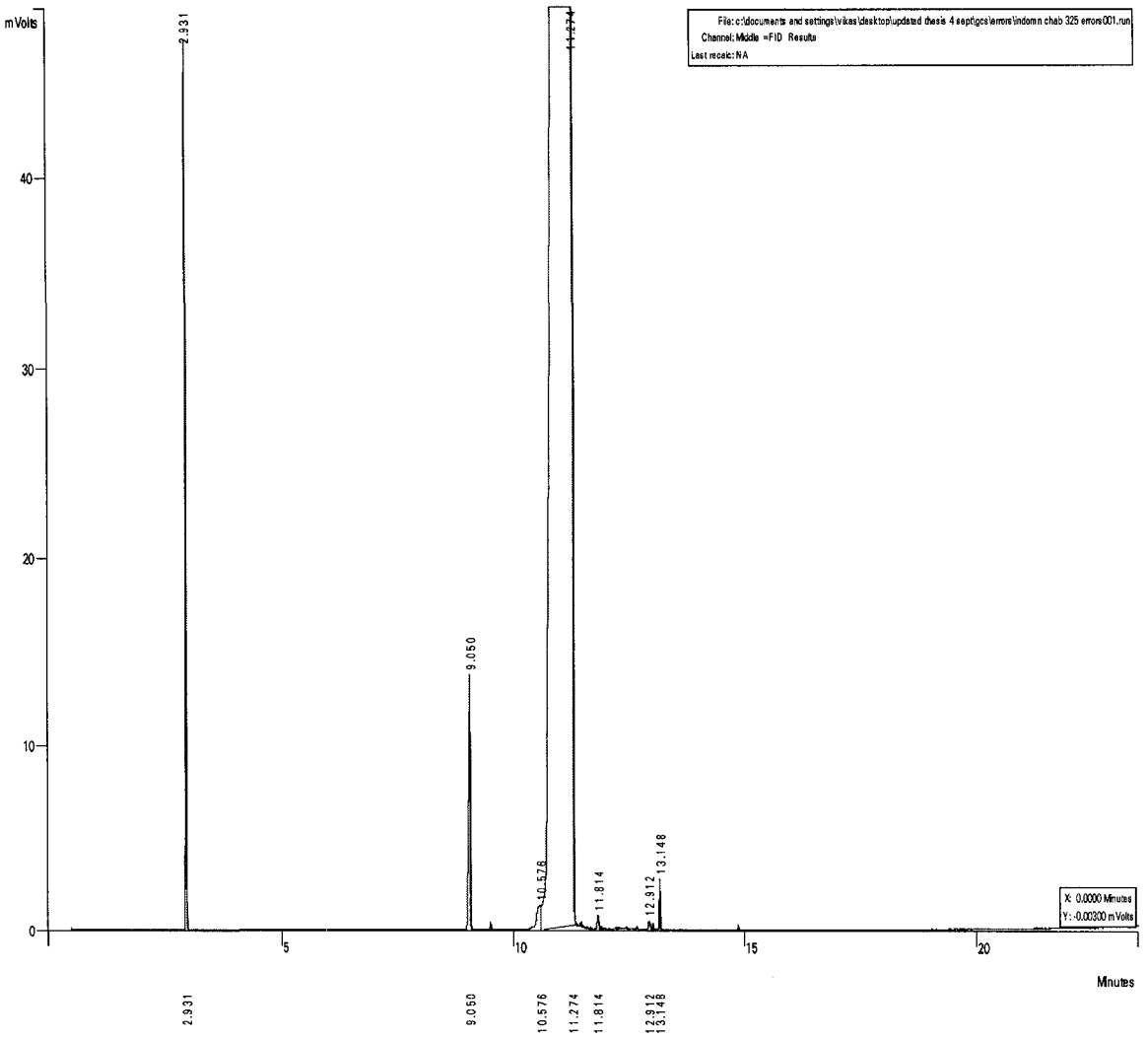

Figure B.21 Gas Chromatogram of Dihydroindole in 1-Methylnaphthalene Solution Reacted with Chabazite at 325°C (Error Test)

Total areas of the peaks are 3925812 counts. Area of dihydroindole is 36779 counts. Therefore area percent of dihydroindole is 36779 / 3925812 = 0.9369 and the conversion is ((1.62-0.94)/1.62)*100 = 42.30 %

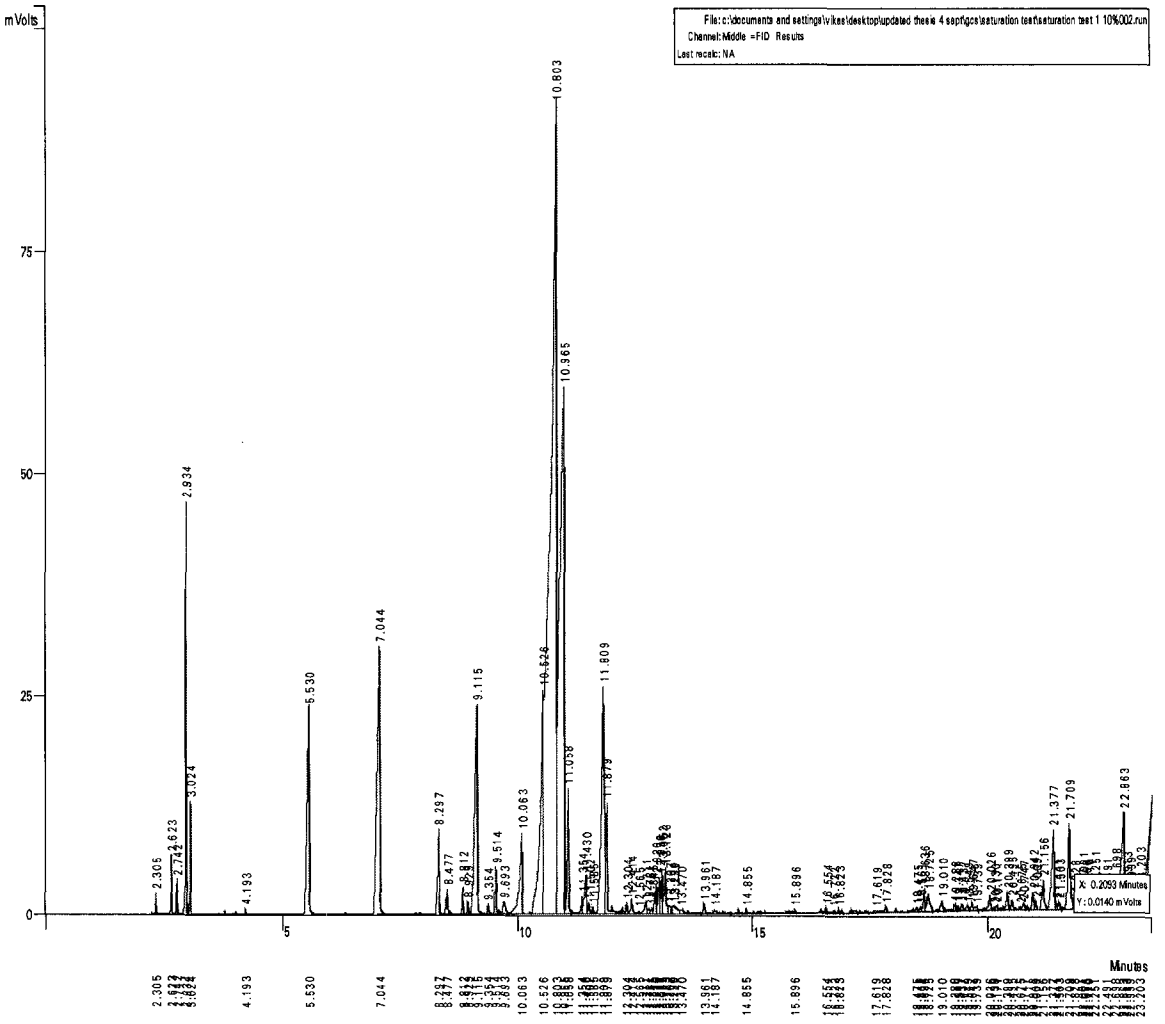

Figure B.22 Gas Chromatogram of Dihydroindole in 1-Methylnaphthalene Solution Reacted with clinoptilolite at 425°C at 3rd recycle (Catalyst Saturation Test)

GC analysis of the dihydroindole in 1-methylnaphthalene solution reacted with clinoptilolite at 425°C at 3rd recycle of the catalyst shows complete elimination of dihydroindole

Appendix C

Gas Chromatogram Integration Data and Elemental Analysis Reports

These each integration data report corresponds to the respective chromatogram graph in Appendix A. Area counts of the solvent or model compounds AC_{MC} is divided by the total area counts of all the peaks AC_{Total} to find the area percent. Area percent is then used to calculate the conversion.

$$\text{Area Percent} = (AC_{MC} / AC_{Total}) * 100$$

Also the elemental analysis report of the catalyst is included for reference.

Data File D:\MY030002.D Sample Name: HEXADECANE

Integration Results

Signal 1: FID1 B,

Peak #	Time [min]	Type	Area [counts*s]	Height [counts]	Width [min]	Start [min]	End [min]
1	0.992	BV	4.29443e4	3401.82300	0.2113	0.398	3.038
2	14.029	VV	1.24259e4	190.88068	0.8395	13.321	17.154
3	22.786	VV	1.06084e7	5.56180e5	0.3025	20.398	35.310
4	57.253	VV	1.06668e4	186.68001	0.7306	43.185	58.268
5	59.798	VV	3.99414e4	144.64027	3.4297	58.268	65.846

Figure C.01 Integration Results of Pure Hexadecane Analysis

Data File E:\12MA0701.D Sample Name: Purehexadcn

Integration Results

Signal 1: FID1 B,

Peak #	Time [min]	Type	Area [counts*s]	Height [counts]	Width [min]	Start [min]	End [min]
1	0.559	BV	3.96603e8	1.20751e8	0.0547	0.398	0.926
2	1.198	VV	1.52579e6	4.42290e5	0.1042	0.926	4.206
3	5.289	VV	1.35491e5	1.02686e4	0.2179	4.206	5.673
4	6.543	VV	3.23362e7	1.28420e6	0.3738	5.673	7.819
5	23.222	VV	5.28205e7	1.43030e6	0.5108	20.623	40.399
6	56.776	VV	6.12926e5	893.75330	8.3369	42.639	64.182

Figure C.02 Integration Results of Pure Hexadecane with Internal Standard

Data File D:\MY025001.D Sample Name: PHEXATHERMAL 425

Integration Results

Signal 1: FID1 B,

Peak #	Time [min]	Type	Area [counts*s]	Height [counts]	Width [min]	Start [min]	End [min]
1	0.928	BV	1.72368e7	2.94070e6	0.1484	0.528	1.566
2	1.910	VV	1.43860e6	6.55468e4	0.3201	1.566	2.493
3	2.747	VV	1.09222e5	6619.78760	0.2565	2.493	3.040
4	3.620	VV	1.36063e6	1.02598e5	0.2987	3.040	4.308
5	6.320	VV	1.56340e6	1.47986e5	0.1873	4.308	7.221
6	9.308	VV	1.60807e6	1.47574e5	0.1911	7.221	9.794
7	12.241	VV	1.71490e6	1.31995e5	0.2156	9.794	13.178
8	13.884	VV	1.92416e6	2.07445e5	0.1722	13.178	14.227
9	15.039	VV	1.40957e6	1.27057e5	0.1934	14.227	15.510
10	16.402	VV	1.90751e5	3465.86475	0.6741	15.510	16.895
11	17.346	VV	8.53123e5	8.14415e4	0.1702	16.895	18.283
12	18.856	VV	1.82326e5	6400.98486	0.4123	18.283	19.447
13	20.147	VV	4.14263e5	1.37719e4	0.5109	19.447	20.955
14	23.402	VV	6.54910e7	1.59218e6	0.5599	20.955	24.328
15	25.789	VV	4.68432e5	7510.92871	0.7916	24.328	25.998
16	26.915	VV	5.06545e5	2.53657e4	0.2970	25.998	27.550
17	28.887	VV	5.72593e5	1.45421e4	0.5234	27.550	29.339
18	30.839	VV	1.49102e6	1.40289e4	1.2880	29.339	34.952
19	36.181	VV	3.65459e5	7729.46191	0.5836	34.952	36.604
20	37.873	VV	3.25069e5	2397.11865	1.6621	36.604	38.201
21	39.471	VV	2.88511e5	2238.37720	1.5678	38.201	39.746
22	40.118	VV	2.62522e5	5990.30713	0.5433	39.746	41.237
23	41.591	VV	2.53495e5	4230.34424	0.7631	41.237	42.680
24	42.969	VV	1.62393e5	2783.97778	0.7445	42.680	43.652
25	44.382	VV	1.96792e5	5241.79443	0.5020	43.652	45.030
26	45.655	VV	1.12070e5	4147.88232	0.3952	45.030	45.892
27	46.183	VV	1.60201e5	3067.11572	0.8705	45.892	47.539
28	48.232	VV	1.46624e5	3668.61499	0.5303	47.539	50.371

Figure C.03 Integration Results of Hexadecane Thermal Cracking

Data File D:\AP180007.D

Sample Name: HexaClinop425

Integration Results

Signal 1: FID1 B,

Peak #	Time [min]	Type	Area [counts*s]	Height [counts]	Width [min]	Start [min]	End [min]
1	0.559	BV	2.67517e8	8.20719e7	0.1020	0.452	1.881
2	2.275	VV	3.34583e5	1.08020e4	0.4094	1.881	2.745
3	3.296	VV	5.59068e5	4.55065e4	0.2233	2.745	3.492
4	5.292	VV	5.63017e5	1.69261e4	0.4681	3.492	5.518
5	6.571	VV	3.27265e7	1.36609e6	0.3595	5.518	7.530
6	7.976	VV	1.97207e5	5760.57422	0.5114	7.530	8.404
7	9.218	VV	6.09201e5	5.13673e4	0.3144	8.404	9.412
8	10.871	VV	3.03068e5	3927.16016	1.0490	9.412	11.080
9	12.176	VV	6.52026e5	5.93681e4	0.1921	11.080	12.681
10	13.719	VV	2.55211e5	4504.61816	0.7250	12.681	14.244
11	14.972	VV	6.21655e5	5.61350e4	0.1932	14.244	15.858
12	16.341	VV	1.39310e5	2888.67725	0.6266	15.858	16.886
13	17.297	VV	3.46629e5	1.23086e4	0.3926	16.886	18.187
14	20.115	VV	7.86133e5	7535.49609	1.2651	18.187	21.071
15	21.367	VV	1.42344e5	5727.09619	0.3540	21.071	21.572
16	23.131	VV	3.92383e7	1.19248e6	0.4639	21.572	24.363
17	26.873	VV	1.92856e5	6860.65283	0.3920	25.928	27.483
18	28.021	VV	1.30144e5	6801.72607	0.3192	27.483	28.371
19	28.857	VV	1.05031e5	3597.23804	0.3726	28.371	29.277
20	29.868	VV	1.26682e5	3275.65088	0.4832	29.277	30.555
21	32.120	VV	2.61518e5	1868.36975	1.6970	31.184	34.935

Figure C.04 Integration Results of Hexadecane Cracking with Clinoptilolite at 425°C

Data File D:\MA210011.D Sample Name: ZeoHexa425REP1

Integration Results

Signal 1: FID1 B,

Peak #	Time [min]	Type	Area [counts*s]	Height [counts]	Width [min]	Start [min]	End [min]
1	0.559	BV	3.45096e8	1.03206e8	0.1030	0.239	1.965
2	3.312	VV	1.27445e6	7.45643e4	0.2794	1.965	4.018
3	5.312	VV	4.02522e5	1.58103e4	0.3610	4.558	5.624
4	6.623	VV	4.00770e7	1.54130e6	0.3674	5.624	7.509
5	7.996	VV	2.20853e5	6149.12354	0.4990	7.509	8.417
6	9.229	VV	9.70867e5	8.57063e4	0.1962	8.417	9.679
7	12.173	VV	1.27649e6	9.24041e4	0.2092	9.679	12.662
8	13.718	VV	3.09107e5	5822.16455	0.6834	12.662	14.196
9	14.967	VV	9.27342e5	8.74123e4	0.1878	14.196	15.467
10	16.334	VV	2.41415e5	4282.90381	0.7056	15.467	16.819
11	17.585	VV	5.50047e5	1.97852e4	0.5003	16.819	18.172
12	20.119	VV	8.90584e5	1.16174e4	0.9424	18.172	20.703
13	21.400	VV	6.13105e5	1.29727e4	0.6314	20.703	21.760
14	23.212	VV	4.97494e7	1.42632e6	0.4869	21.760	24.338
15	26.854	VV	2.50103e5	1.06534e4	0.3379	25.928	27.232
16	29.836	VV	2.74954e5	6326.39111	0.5551	29.270	31.059
17	31.644	VV	2.51063e5	4746.19922	0.6811	31.059	32.843
18	33.419	VV	2.46818e5	4397.42578	0.7028	32.843	34.898
19	37.809	VV	2.94006e5	2468.60181	1.9850	36.548	39.690
20	56.635	VV	4.95108e5	668.14655	8.7572	51.287	65.882

Figure C.05 Integration Results of Hexadecane Cracking with Zeolite-Y at 425°C

Data File E:\220806D3.D Sample Name: pent/puredbt30

Integration Results

Signal 1: FID1 B,

Peak #	Time [min]	Type	Area [counts*s]	Height [counts]	Width [min]	Start [min]	End [min]
1	0.561	BV	3.00608e8	8.43396e7	0.0594	0.452	3.191
2	5.370	VV	1.33225e5	1.03740e4	0.2138	4.049	5.759
3	6.636	VV	3.13874e7	1.28589e6	0.3488	5.759	7.955
4	10.325	VV	1.38328e5	1.75502e4	0.1560	9.518	11.317
5	12.542	VV	6.24729e4	1102.70081	0.7410	11.317	13.203
6	14.825	VP	6.42688e7	1.58598e6	0.5368	13.203	15.251
7	15.952	VV	8.07460e5	3.21446e4	0.3571	15.251	17.241
8	17.608	VV	2.81560e5	6960.04932	0.5840	17.241	18.258
9	18.526	VV	8.19250e4	6298.07861	0.2158	18.258	18.745
10	19.363	VV	1.87624e5	1715.68896	1.3558	18.745	22.241
11	24.282	VV	5.29990e6	2.70391e5	0.3087	23.655	33.515

Figure C.06 Integration Results of Pure Dibenzothiophene

Data File E:\31080001.D

Sample Name: T DBT25

Integration Results

Signal 1: FID1 B,

Peak #	Time [min]	Type	Area [counts*s]	Height [counts]	Width [min]	Start [min]	End [min]
1	0.561	BV	2.85260e8	8.20648e7	0.0579	0.452	3.193
2	5.364	VV	1.16205e5	1.03235e4	0.1953	4.053	5.736
3	6.587	VV	2.62593e7	1.15031e6	0.3303	5.736	7.892
4	10.304	VV	1.01348e5	1.20712e4	0.1780	9.600	11.205
5	14.584	VV	4.15922e7	1.19917e6	0.4846	12.755	14.985
6	15.857	VV	5.57315e5	2.73340e4	0.3179	14.985	17.183
7	17.532	VV	1.63837e5	3431.71533	0.6690	17.183	18.231
8	19.350	VV	1.07957e5	1717.47070	0.7973	18.825	20.562
9	24.220	VV	4.39006e6	2.49321e5	0.2854	23.010	32.473
10	57.474	VV	4.01603e5	521.21521	9.1173	47.499	65.827

Figure C.07 Integration Results of Dibenzothiophene Thermal Reaction at 425°C

Data File E:\28080611.D Sample Name: mchbckddbt

Integration Results

Signal 1: FID1 B,

Peak #	Time [min]	Type	Area [counts*s]	Height [counts]	Width [min]	Start [min]	End [min]
1	0.561	BV	2.97812e8	8.35394e7	0.0594	0.345	0.978
2	1.200	VV	2.04952e5	4.89166e4	0.0698	0.978	2.420
3	5.364	VV	1.32249e5	1.05650e4	0.2100	4.805	5.757
4	6.622	VV	3.04371e7	1.29827e6	0.3535	5.757	7.816
5	10.316	VV	2.16584e5	2.93217e4	0.1502	9.039	11.250
6	14.646	VV	4.63766e7	1.22793e6	0.5206	11.972	15.038
7	15.874	VV	5.42988e5	2.70472e4	0.2982	15.469	17.105
8	17.362	VV	1.70753e5	3486.47534	0.6514	17.105	18.253
9	19.352	VV	1.11119e5	3179.49805	0.4717	18.745	19.932
10	24.250	VV	4.75709e6	2.36750e5	0.2984	23.425	29.001
11	40.927	VV	1.84387e5	3874.95996	0.6511	40.178	42.186
12	56.755	VV	4.06886e5	577.20703	8.4321	52.236	65.800

Figure C.08 Integration Results of Dibenzothiophene with Modified Chabazite at 425°C

Data File D:\JN010001.D

Sample Name: MN-QN 0.25

Integration Results

Signal 1: FID1 B,

Peak #	Time [min]	Type	Area [counts*s]	Height [counts]	Width [min]	Start [min]	End [min]
1	0.796	BV	1.54530e6	2.47420e5	0.1369	0.612	3.172
2	11.680	VV	1.38200e6	4.14640e4	0.5329	10.698	13.092
3	14.785	VV	6.65330e7	1.58475e6	0.5858	13.092	15.559
4	16.195	VV	3.57038e5	6520.08447	0.7029	15.559	18.187
5	19.242	VV	1.83872e5	9320.37891	0.3288	18.731	24.611
6	56.519	VV	2.35285e5	575.16461	4.9645	44.253	58.491

Figure C.09 Integration Results of Quinoline Solution in 1- Methylnaphthalene

Data File D:\MY310003.D Sample Name: QN-MN CLINOP 42!

Integration Results

Signal 1: FID1 B,

Peak #	Time [min]	Type	Area [counts*s]	Height [counts]	Width [min]	Start [min]	End [min]
1	0.831	BP	1.79971e6	4.35591e5	0.1122	0.511	1.172
2	1.436	VV	1.79645e6	2.93909e5	0.1019	1.172	3.297
3	10.283	VV	1.01931e5	1.10288e4	0.1718	9.416	10.796
4	11.664	VV	1.16006e6	3.88074e4	0.5088	10.796	12.864
5	14.729	VV	6.16999e7	1.50729e6	0.5736	12.864	15.837
6	16.179	VV	3.05510e5	4190.47852	0.9146	15.837	18.190
7	19.231	VV	1.95195e5	6956.02734	0.3914	18.726	28.624
8	40.906	VV	1.08871e5	2302.61206	0.6156	40.205	42.547

Figure C.10 Integration Results of Quinoline Reaction with Clinoptilolite at 425°C

Run File : c:\documents and settings\vikas\desktop\updated thesis 4 sept\gcs\pure indo -mn area %\ir
Method File : c:\star\untitled.mth
Sample ID : INDOMN 0.25% JLY28R

Injection Date: 7/28/2007 12:32 PM Calculation Date: 9/5/2007 12:13 AM

Operator : Vikas
Workstation:
Instrument : Varian3800
Channel : Middle = FID

Detector Type: 3800 (1 Volt)
Bus Address : 44
Sample Rate : 10.00 Hz
Run Time : 23.477 min

** Star Chromatography Workstation Version 5.31 ** 00664-7068-5CF-20D0 **

Run Mode : Analysis
Peak Measurement: Peak Area
Calculation Type: Percent

Peak No.	Peak Name	Result ()	Ret. Time (min)	Time Offset (min)	Area (counts)	Sep. Code	Width 1/2 (sec)	Status Codes
1		0.0482	2.922	0.000	2108	BB	1.0	
2		1.6240	9.075	0.000	71041	VB	3.4	
3		0.0720	10.528	0.000	3152	BV	5.6	
4		0.0391	10.557	0.000	1712	VV	0.0	
5		0.0395	10.585	0.000	1726	VV	0.0	
6		0.0923	10.641	0.000	4037	VV	0.0	
7		64.8091	11.203	0.000	2835034	VV	0.0	
8		17.6690	11.259	0.000	772919	VV	0.0	
9		7.6245	11.290	0.000	333530	VV	0.0	
10		7.6492	11.306	0.000	334609	VP	1.8	
11		0.0467	11.823	0.000	2043	TF	0.0	
12		0.0486	12.917	0.000	2128	BV	3.7	
13		0.1240	13.150	0.000	5424	VB	1.6	
14		0.1137	14.834	0.000	4974	PB	2.7	
Totals:		99.9999		0.000	4374437			

Figure C.11 Integration Results of Dihydroindole in 1-Methylnaphthalene

Run File : c:\documents and settings\vikas\desktop\updated thesis 4 sept\gcs\jly19 indo- mn clinop.300.run
Method File : c:\star\indo-mn analysis\indo-mn clinop. 300.mth
Sample ID : INDO-MN CLINOP 300

Injection Date: 7/19/2007 4:37 PM Calculation Date: 7/19/2007 5:02 PM

Operator : Vikas
Workstation:
Instrument : Varian3800
Channel : Middle = FID

Detector Type: 3800 (1 Volt)
Bus Address : 44
Sample Rate : 10.00 Hz
Run Time : 23.477 min

** Star Chromatography Workstation Version 5.31 ** 00664-7068-5CF-20D0 **

Run Mode : Analysis
Peak Measurement: Peak Area
Calculation Type: Percent

Peak No.	Peak Name	Result ()	Ret. Time (min)	Time Offset (min)	Area (counts)	Sep. Code	Width 1/2 (sec)	Status Codes
1		2.0420	2.941	0.000	85827	BB	1.2	
2		1.3235	9.069	0.000	55629	PB	3.1	
3		0.0975	10.554	0.000	4096	BV	8.2	
4		0.0260	10.570	0.000	1093	VV	0.0	
5		0.0264	10.586	0.000	1108	VV	0.0	
6		0.0428	10.624	0.000	1797	VV	0.0	
7		26.6444	11.021	0.000	1119874	VV	0.0	
8		40.4759	11.203	0.000	1701217	VV	0.0	
9		28.9553	11.296	0.000	1217003	VB	6.7	
10		0.0454	11.822	0.000	1910	VP	2.4	
11		0.0474	12.917	0.000	1993	BV	3.6	
12		0.1147	13.152	0.000	4822	PB	1.6	
13		0.1587	14.841	0.000	6671	BB	2.7	
	Totals:	100.0000		0.000	4203040			

Figure C.12 Integration Results of Dihydroindole Reacted with Clinoptilolite at 300°C

Run File : c:\documents and settings\vikas\desktop\updated thesis 3 sept\gcs\indo-mn analysis001.run
Method File : c:\star\indo-mn analysis\indo-mn zeo 325.mth
Sample ID : INDO-MN CLINOP 325

Injection Date: 7/18/2007 6:06 PM Calculation Date: 7/19/2007 11:03 AM

Operator : Vikas
Workstation:
Instrument : Varian3800
Channel : Middle = FID

Detector Type: 3800 (1 Volt)
Bus Address : 44
Sample Rate : 10.00 Hz
Run Time : 23.477 min

** Star Chromatography Workstation Version 5.31 ** 00664-7068-5CF-20D0 **

Run Mode : Analysis
Peak Measurement: Peak Area
Calculation Type: Percent

Peak No.	Peak Name	Result ()	Ret. Time (min)	Time Offset (min)	Area (counts)	Sep. Code	Width 1/2 (sec)	Status Codes
1		0.4311	2.926	0.000	17046	BB	1.0	
2		1.2427	9.068	0.000	49139	PB	2.9	
3		0.0373	9.501	0.000	1474	BB	1.6	
4		0.1366	10.562	0.000	5403	BV	8.5	
5		72.0935	11.215	0.000	2850711	VV	0.0	
6		12.1914	11.253	0.000	482069	VV	0.0	
7		13.6055	11.292	0.000	537987	VB	3.2	
8		0.0479	11.824	0.000	1892	VP	2.4	
9		0.0493	12.920	0.000	1948	BV	2.0	
10		0.1216	13.156	0.000	4808	PB	1.6	
11		0.0432	14.859	0.000	1708	BB	1.7	
	Totals:	100.0001		0.000	3954185			

Figure C.13 Integration Results of Dihydroindole with Clinoptilolite at 325°C

Run File : c:\documents and settings\vikas\desktop\updated thesis 4 sept\gcs\indo-mn analysis004.run
Method File : c:\star\indo-mn analysis\indo-mn zeo 350.mth
Sample ID : INDO- MN CLINOP 350

Injection Date: 7/18/2007 7:41 PM Calculation Date: 7/19/2007 11:05 AM

Operator : Vikas
Workstation:
Instrument : Varian3800
Channel : Middle = FID

Detector Type: 3800 (1 Volt)
Bus Address : 44
Sample Rate : 10.00 Hz
Run Time : 23.477 min

** Star Chromatography Workstation Version 5.31 ** 00664-7068-5CF-20D0 **

Run Mode : Analysis
Peak Measurement: Peak Area
Calculation Type: Percent

Peak No.	Peak Name	Result ()	Ret. Time (min)	Time Offset (min)	Area (counts)	Sep. Code	Width 1/2 (sec)	Status Codes
1		2.1179	2.937	0.000	77054	BB	1.2	
2		0.8701	9.052	0.000	31658	PB	2.5	
3		0.0792	9.499	0.000	2881	BB	1.6	
4		0.2432	10.550	0.000	8850	BV	7.9	
5		0.0910	10.584	0.000	3312	VV	7.9	
6		50.0708	11.112	0.000	1821716	VV	0.0	
7		46.2816	11.261	0.000	1683854	VB	10.0	
8		0.0445	11.813	0.000	1620	VP	2.4	
9		0.0474	12.914	0.000	1726	BV	1.9	
10		0.1147	13.151	0.000	4173	PB	1.6	
11		0.0395	14.856	0.000	1436	BB	1.8	
	Totals:	99.9999		0.000	3638280			

Figure C.14 Integration Results of Dihydroindole with Clinoptilolite at 350°C

Run File : c:\documents and settings\vikas\desktop\updated thesis 4 sept\gcs\indo-mn analysis007.run
Method File : c:\star\indo-mn clinop 375.mth
Sample ID : INDO-MN CLINOP 375

Injection Date: 7/18/2007 9:15 PM Calculation Date: 7/19/2007 11:28 AM

Operator : Vikas
Workstation:
Instrument : Varian3800
Channel : Middle = FID

Detector Type: 3800 (1 Volt)
Bus Address : 44
Sample Rate : 10.00 Hz
Run Time : 23.477 min

** Star Chromatography Workstation Version 5.31 ** 00664-7068-5CF-20D0 **

Run Mode : Analysis
Peak Measurement: Peak Area
Calculation Type: Percent

Peak No.	Peak Name	Result ()	Ret. Time (min)	Time Offset (min)	Area (counts)	Sep. Code	Width 1/2 (sec)	Status Codes
1		2.3603	2.938	0.000	87053	BB	1.2	
2		0.4369	9.035	0.000	16114	PB	2.0	
3		0.1852	9.504	0.000	6829	BB	1.6	
4		0.4151	10.549	0.000	15308	BV	7.5	
5		0.1496	10.566	0.000	5516	VV	7.5	
6		52.7184	11.130	0.000	1944360	VV	0.0	
7		43.4196	11.267	0.000	1601403	VB	9.5	
8		0.0491	11.818	0.000	1811	VP	2.2	
9		0.0463	12.918	0.000	1709	BV	2.0	
10		0.1216	13.154	0.000	4486	VB	1.6	
11		0.0979	14.864	0.000	3612	BB	1.6	
	Totals:	100.0000		0.000	3688201			

Figure C.15 Integration Results of Dihydroindole with Clinoptilolite at 375°C

Data File D:\JN070003.D Sample Name: INDO-MN 0.25 425

Integration Results

Signal 1: FID1 B,

Peak #	Time [min]	Type	Area [counts*s]	Height [counts]	Width [min]	Start [min]	End [min]
1	0.831	BV	3.05848e4	6785.54395	0.1166	0.612	2.311
2	2.572	VV	1748.01135	28.78640	0.7724	2.311	3.943
3	4.773	VV	6679.48291	123.15848	0.6967	3.943	6.553
4	7.235	VV	7705.18701	265.06830	0.4031	6.553	8.188
5	9.679	VV	6907.12256	74.24319	1.1654	8.188	9.972
6	10.263	VV	2.57419e4	2559.07397	0.1814	9.972	11.217
7	11.659	VV	2.48697e4	3637.71558	0.1438	11.217	12.276
8	14.015	VV	8.07190e6	4.09431e5	0.2940	12.276	15.739
9	16.037	VV	1.00581e5	1007.08673	1.2292	15.739	18.763
10	19.205	VV	1.30827e5	423.85977	3.6650	18.763	31.672
11	32.241	VV	2.44890e4	99.15786	2.9133	31.672	36.116
12	36.669	VV	5989.59863	86.57601	0.8551	36.116	37.279
13	42.337	VV	4.36259e4	140.58553	3.7643	37.279	43.689
14	44.289	VV	1.79344e4	131.23828	1.6423	43.689	46.007
15	56.768	VV	2.68201e5	531.86902	5.9630	46.007	60.254
16	60.495	VV	1.47061e5	487.12851	3.5861	60.254	65.541
17	65.897	VBA	1.19063e4	445.55707	0.4454	65.541	65.987

Figure C.16 Integration Results of Dihydroindole with Clinoptilolite at 425°C

Run File : c:\documents and settings\vikas\desktop\updated thesis 5 sept\gcs\errors\indomn chab 325 errors001.run
Method File : c:\star\indo mn chab. 325 error1.mth
Sample ID : INDOMNCHAB325ERR2

Injection Date: 7/28/2007 4:06 PM Calculation Date: 7/28/2007 4:39 PM

Operator : Vikas Detector Type: 3800 (1 Volt)
Workstation: Bus Address : 44
Instrument : Varian3800 Sample Rate : 10.00 Hz
Channel : Middle = FID Run Time : 23.477 min

** Star Chromatography Workstation Version 5.31 ** 00664-7068-5CF-20D0 **

Run Mode : Analysis
Peak Measurement: Peak Area
Calculation Type: Percent

Peak No.	Peak Name	Result ()	Ret. Time (min)	Time Offset (min)	Area (counts)	Sep. Code	Width 1/2 (sec)	Status Codes
1		1.4764	2.931	0.000	57962	BB	1.1	
2		0.9369	9.050	0.000	36779	PB	2.6	
3		0.2483	10.576	0.000	9749	BV	11.7	
4		97.1184	11.274	0.000	3812687	VB	7.3	
5		0.0472	11.814	0.000	1852	VP	2.2	
6		0.0484	12.912	0.000	1900	BV	3.3	
7		0.1244	13.148	0.000	4883	VB	1.6	
	Totals:	100.0000		0.000	3925812			

Figure C.17 Integration Result of Error Test of Dihydroindole with Chabazite at 325°C

Run File : c:\documents and settings\vikas\desktop\updated thesis 4 sept\gcs\saturation test\saturation test 1 10%002.run
Method File : c:\star\indo mn clinop 10% saturation test3.mth
Sample ID : SATURATION TEST 3

Injection Date: 8/1/2007 5:38 PM Calculation Date: 8/1/2007 6:03 PM

Operator : Vikas Detector Type: 3800 (1 Volt)
Workstation: Bus Address : 44
Instrument : Varian3800 Sample Rate : 10.00 Hz
Channel : Middle = FID Run Time : 23.477 min

** Star Chromatography Workstation Version 5.31 ** 00664-7068-5CF-20D0 **

Run Mode : Analysis
Peak Measurement: Peak Area
Calculation Type: Percent

Peak No.	Peak Name	Result ()	Ret. Time (min)	Time Offset (min)	Area (counts)	Sep. Code	Width 1/2 (sec)	Status Codes
1		0.1151	2.305	0.000	2718	VV	0.9	
2		0.3224	2.623	0.000	7610	VV	1.0	
3		0.2539	2.742	0.000	5994	VV	1.2	
4		2.4846	2.934	0.000	58649	VV	1.1	
5		0.6575	3.024	0.000	15521	VP	1.0	
6		0.0477	4.193	0.000	1126	TF	0.0	
7		3.2962	5.530	0.000	77807	PB	3.1	
8		5.4652	7.044	0.000	129009	VB	4.2	
9		0.9101	8.297	0.000	21483	VV	2.0	
10		0.2763	8.477	0.000	6522	VB	1.9	
11		0.2304	8.812	0.000	5438	BV	1.6	
12		0.1096	8.929	0.000	2588	VV	1.6	
13		4.1398	9.115	0.000	97723	VP	4.0	
14		0.0927	9.354	0.000	2187	TS	0.0	
15		0.4273	9.514	0.000	10088	PV	1.7	
16		0.2309	9.693	0.000	5450	VV	3.5	
17		1.5965	10.063	0.000	37686	VB	3.1	
18		5.5727	10.526	0.000	131547	VV	6.6	
19		34.3714	10.803	0.000	811350	VV	6.7	
20		17.1317	10.965	0.000	404401	VV	7.0	
21		1.4239	11.058	0.000	33612	VV	2.1	
22		0.1860	11.354	0.000	4391	VV	2.0	
23		0.5566	11.430	0.000	13139	VV	2.9	
24		0.1095	11.502	0.000	2584	VV	2.0	
25		0.0707	11.585	0.000	1669	VV	2.0	
26		4.7542	11.809	0.000	112226	VV	4.0	
27		1.4079	11.879	0.000	33235	VV	2.7	

Figure C.18 Integration Results of Chabazite Saturation Test with Dihydroindole at 425°C

Appendix D

D.1 Reaction Order and Activation Energy Calculations

This appendix presents the plots and calculations for reaction order and activation energy of the reaction. For determining the order of reaction, experiments were performed with dihydroindole and 1-methylnaphthalene solution at time intervals of 30, 40, 50 and 60 minutes and temperature of 425°C. The experiments were done in presence of chabazite catalyst.

To determine the energy of activation, experiments were performed with dihydroindole and 1-methylnaphthalene solution at temperature of 300°C, 325°C, 350 °C, 375°C and 425°C. Time of the reaction was 60 minutes. Reaction was carried out in presence of chabazite catalyst.

Once order of reaction was determined activation energy was calculated by plotting a graph between ln (k) and 1/T to determine – Ea/R as slope and subsequently calculate the energy of activation.

D.1.1 Order of Reaction

To determine the activation energy of the catalysts, it was important to determine the order of the reaction. 3 grams of dihydroindole and 1-methylnaphthalene solution was taken with 10 mass % of ammonium exchanged sodium upgraded chabazite. The reactions were performed at 425°C. The reactions were carried out at different time intervals of 30, 40, 50 and 60 minutes. Equations used to calculate and plot the graphs are mentioned in the Table D.01

Table D.01 Equations for Different Reaction Orders

Serial No.	Reaction Order	Equation
1	Half	$C_A^{1/2} = C_{Ao}^{1/2} - (K\,t / 2)$
2	First	$\ln (C_{Ao} / C_A) = Kt$
3	One and half	$1 / C_A^{1/2} = 1/C_{AO}^{1/2} + K\,t / 2$
4	Second	$1/C_A - 1/C_{Ao} = K\,t$

Results of concentration of the products are given in the Table D.02 at different times

Table D.02 Dihydroindole Mass Percent

Sl No.	Time (mins.)	Final Concentration, C_A in mass %
1	0	2.1165
2	30	1.2061
3	40	1.1126
4	50	1.0281
5	60	0.8968

Table D.03 shows the calculated values of $C_A^{0.5}$, ln (C_{Ao}/C_A), 1/ (C_A) and 1/ CA. Initial concentration C_A is 2.1165 mass percent

Table D.03 Calculation for Concentration

Sl no.	Time	$C_A^{0.5}$	ln (C_{Ao}/C_A)	$1/(C_A)^{0.5}$	1/ CA
1	0	1.4548	0	0.6873	0.4724
2	30	1.0982	0.5623	0.9105	0.8290
3	40	1.0548	0.6430	0.9480	0.8987
4	50	1.0139	0.7220	0.9862	0.9726
5	60	0.9470	0.8586	1.0559	1.1150

D.1.2 Half Order Reactions Plot

Initial concentration C_{Ao} is 2.1165 mass percent. A graph is plotted between $C_A^{0.5}$ versus time t. The slope is –K/2 i.e. -0.0084 with intercept as $C_{Ao}^{1/2}$ i.e. 1.4164 R^2 value is 0.9492

Figure D.01 shows the plot for the half order reaction

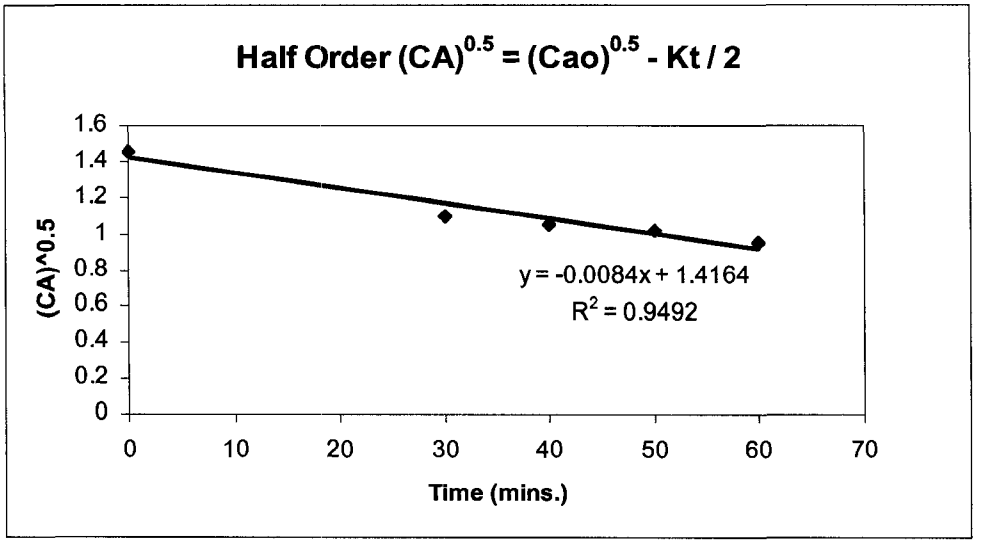

Figure D.01 Plot for Half Order Reaction

D.1.3 First Order Reaction Plot

A graph is plotted between ln (C_{Ao}/C_A) versus time't'. The slope is 'K' with no intercept.

Here slope K is 0.0141 and intercept is 0.0492

Figure D.02 shows the plot of first order reaction

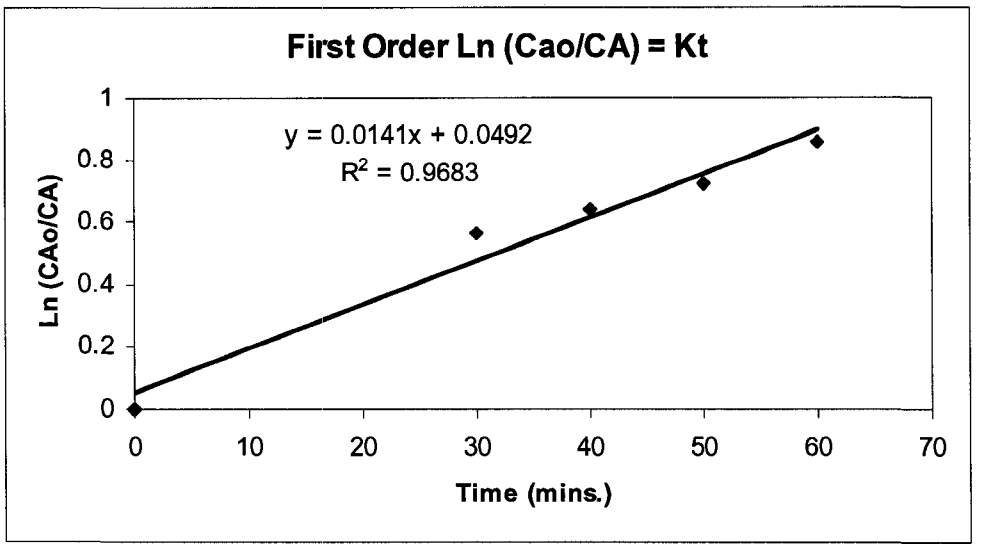

Figure D.02 Plot for First Order Reaction

D.1.4 One and Half Order Reaction Plot

A graph is plotted between 1 / $(CA)^{1/2}$ and time't'. The slope is K/2 i.e.0.006 with intercept $1/C_{Ao}^{1/2}$ i.e. 0.7014. R^2 value is 0.9826. Figure D.03 shows the plot of one and half order

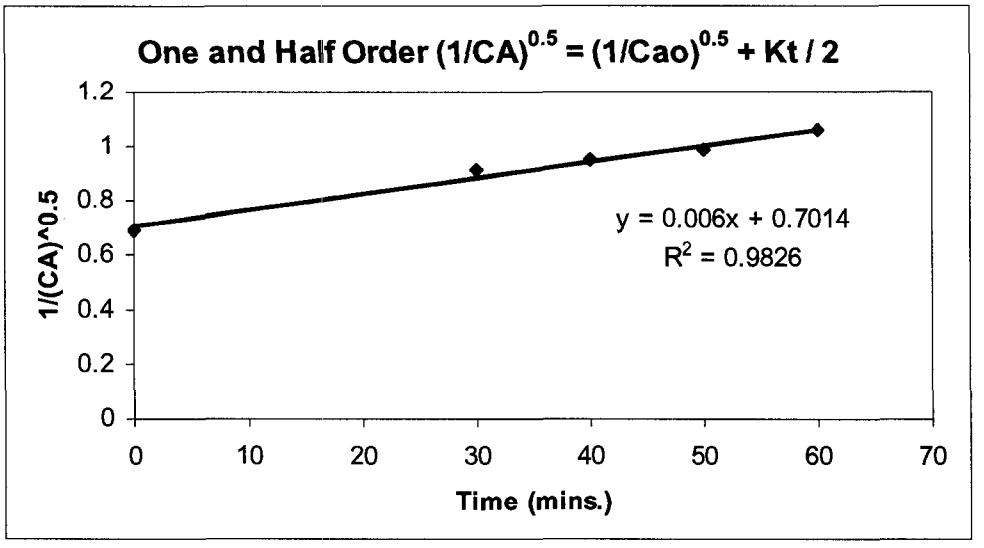

D.03 One and Half Order Reaction Plot

D.1.5 Second Order Reaction Plot

A graph is plotted between $1/C_A$ versus time't'. The slope is K i.e. 0.0104 with $1/C_{Ao}$ as intercept i.e. 0.4842. R2 is 0.9902. Figure D.04 shows the plot of $1/C_A$ versus time't'

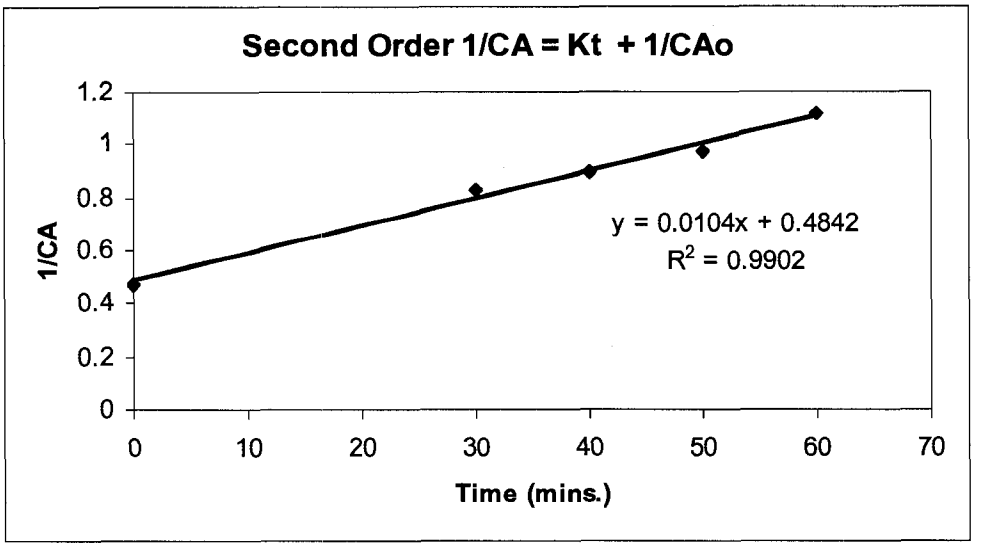

Figure D.04 Second Order Plot

D.2 Calculation of activation energy of the reaction with chabazite catalyst

Activation energy calculation of the reaction with chabazite catalyst is shown. Second order of reaction is considered in calculation of the rate constant K and includes the surface area of the catalyst. Surface area of the chabazite catalyst is 70 m^2/gram

Table D.04 shows the results of initial and final concentration of 0.25 mass % basic nitrogen solution of dihydroindole in 1-methylnaphthalene reacted with ammonium exchanged upgraded sodium chabazite catalyst. The reactions were carried out at 300°C, 325°C, 350°C, 375°C and 425°C

Table D.04 Dihydroindole Initial and Final Concentration

Serial No.	Temperature°C	Temperature°K (°C+273)	Time (Secs.)	Initial Concentration C_{Ao}	Final Concentration C_A
1	300	573	3600	2.1165	1.7358
2	325	598	3600	2.1165	1.6299
3	350	623	3600	2.1165	1.1412
4	375	648	3600	2.1165	0.5730
5	425	698	3600	2.1165	0

Table D.05 shows the calculations and Figure D.05 shows the Arrhenius Plot

Table D.05 Calculations of ln K and 1/T

Serial No.	$K= (1/ C_A - 1/ C_{Ao})/ t$	K * 70	ln K	1/T
1	5.98 e –05	0.00418	-5.4754	0.001745
2	8.78 e-05	0.00614	-5.0920	0.001672
3	1.78 e-04	0.01249	-4.3825	0.001605
4	5.43 e-04	0.03802	-3.2694	0.001543

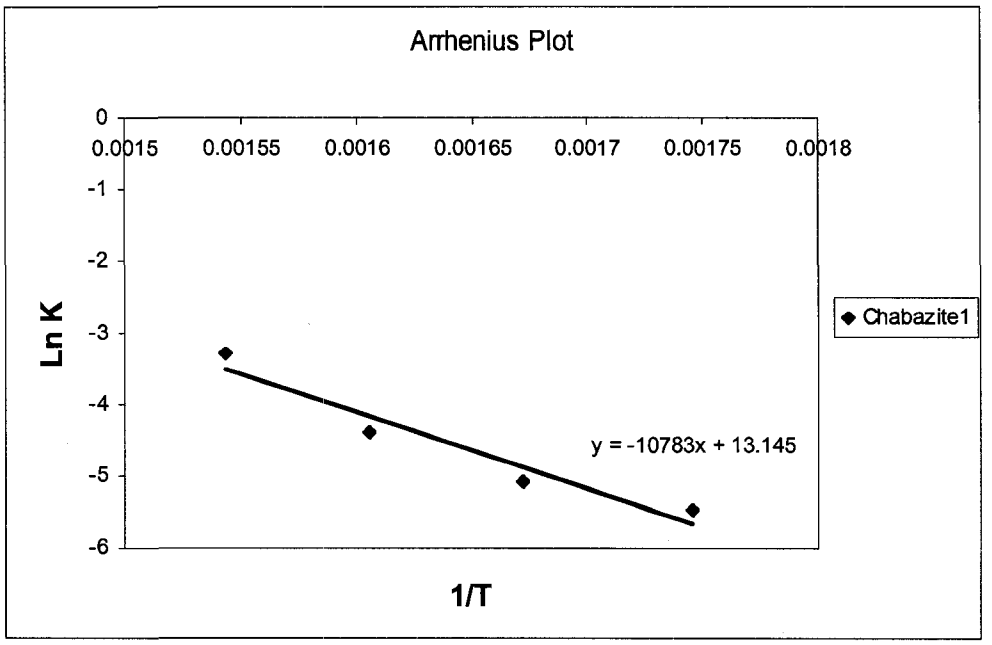

Figure D.05 Arrhenius plot of ln (K) versus 1/T

Activation energy is found using Arrhenius equation

$K = A\, e^{-Ea/RT}$

Where K is the rate constant, A is a pre-exponential factor, Ea is the energy of activation, R is the gas constant and the value is 8.31472 J/mol K and T is the temperature in degree Kelvin

Taking the natural log

$\ln(K) = -Ea/R * 1/T + \ln(A)$

From the Arrhenius plot of ln (K) and 1/T, the slope –Ea/R is -10783

1-Ea/8.31472 = -10783

Ea = 10783*8.31472

Or 89657.62576 J/ mol

Or 89.6576 kJ/mol

D.3 Binding Energy

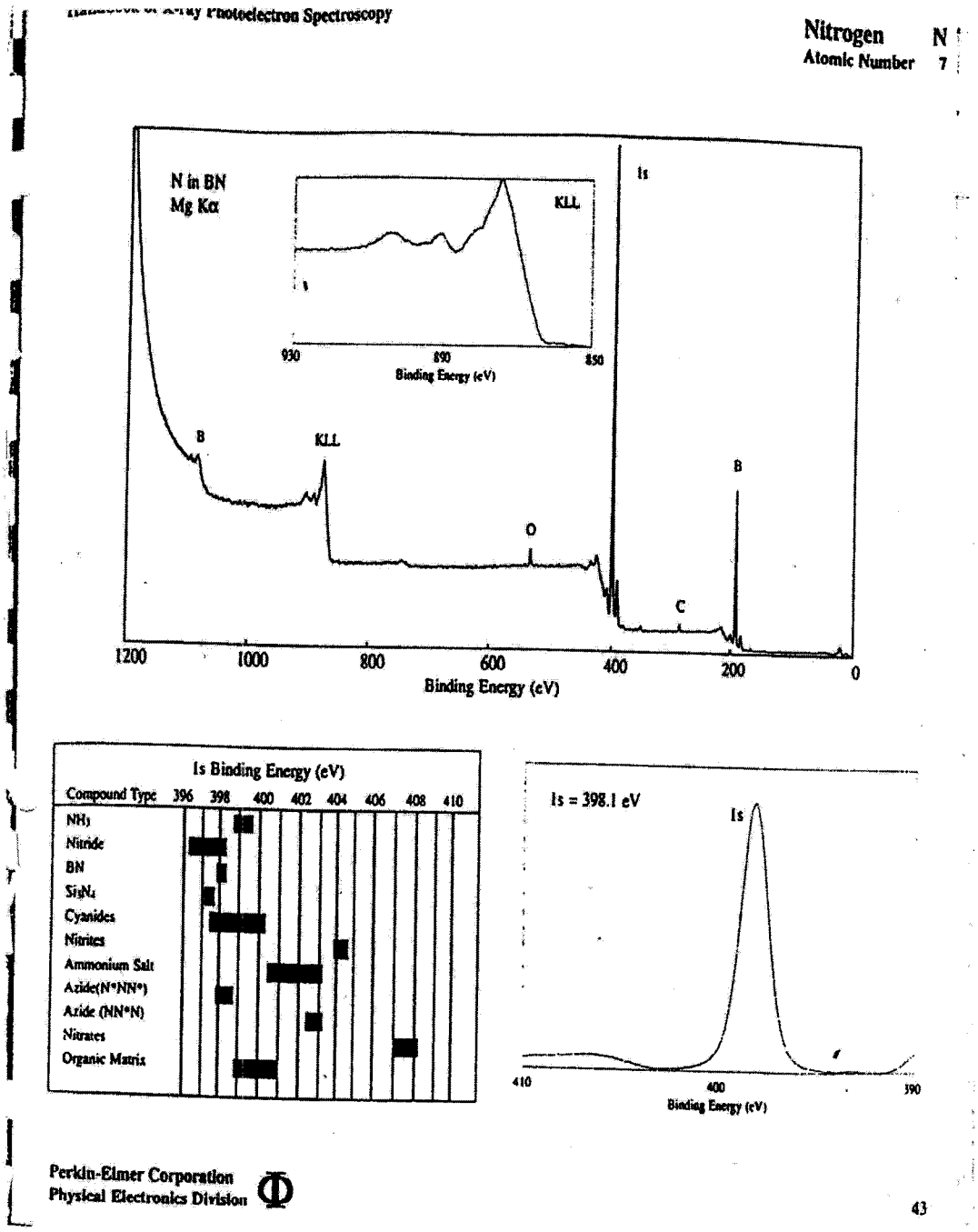

D.06 Binding Energies of Nitrogen Compounds